Supporting Information for:

Hydrazine Capture and N-N Bond Cleavage at Iron Enabled by Flexible Appended Lewis Acids

*John J. Kiernicki,[a] Matthias Zeller,[b] and Nathaniel K. Szymczak[a]**

[a]Department of Chemistry, University of Michigan, Ann Arbor, Michigan 48109, United States
[b]H.C. Brown Laboratory, Department of Chemistry, Purdue University, West Lafayette, Indiana 44555, United States

Table of Contents:

General Considerations. All air- and moisture-sensitive manipulations were performed using standard Schlenk techniques or in an inert atmosphere drybox with an atmosphere of purified nitrogen. The drybox was equipped with a cold well designed for freezing samples in liquid nitrogen as well as a −35 °C freezer for cooling samples and crystallizations. Solvents were purified using a Glass Contour solvent purification system through percolation through a Cu catalyst, molecular sieves, and alumina. Solvents were then stored over sodium and/or sieves. Benzene-d_6 and chloroform-*d* were purchased from Cambridge Isotope Laboratories. Benzene-d_6 was dried with molecular sieves and sodium, and degassed by three freeze–pump–thaw cycles. Chloroform-*d* was distilled from CaH_2 and stored over molecular sieves. Sodium hydride, allyl bromide, iodobutane, 9-borabicyclo(3.3.1)nonane, $FeBr_2$, $FeCl_2$, $ZnCl_2$, triethylammonium chloride, and phenol were purchased from commercial vendors and used as received. Hydrazine was degassed by three freeze-pump-thaw cycles and passed over activated alumina prior to use. $[^{15}N_2H_6][SO_4]$ was purchased from Cambridge Isotope Laboratories and deprotonated according to the procedure by Schrock et al[1] and was used as a DCM stock solution. 2,6-bis(5-*tert*-butyl-1*H*-pyrazol-3-yl)pyridine,[2] triethylammonium nitrate,[3] and potassium graphite[4] were synthesized according to literature procedures.

NMR spectra were recorded on Varian Vnmrs 700 or Varian MR400 spectrometers. ^{1}H, ^{13}C, and ^{11}B chemical shifts are reported in parts per million (ppm) relative to tetramethylsilane and referenced internally to the residual solvent peak. ^{11}B spectra were referenced on a unified scale, where the single primary reference is the frequency of the residual solvent peak in the ^{1}H NMR spectrum. ^{11}B is referenced vs. $BF_3(OEt_2)$. Multiplicities are reported as follows: singlet (s), doublet (d), triplet (t), quartet (q). The spectra for paramagnetic molecules were obtained by using an acquisition time of 0.5 s, thus the peak widths reported have an error of ±2 Hz. For paramagnetic molecules, the ^{1}H NMR data are reported with the chemical shift, followed by the peak width at half height in hertz, the integration value, and, where possible, the peak assignment. Infrared spectra were recorded using a Nicolet iS10 FT-IR spectrometer. Samples were diluted into dry KBr and recorded as pellets. Electronic absorption spectra were recorded at ambient temperature in sealed 1 cm quartz cuvettes with a Varian Cary-50 spectrophotometer. MALDI-TOF data were collected on a Bruker AutoFlex Speed with samples prepared under inert atmosphere in an anthracene matrix.

Single crystals of **1-Cl** and $(^{BBN}PDP^{tBu})ZnCl_2(N_2H_4)$ suitable for X-ray diffraction were coated with poly(isobutylene) oil in a drybox and mounted on a Rigaku AFC10K Saturn 944+ CCD-based X-ray diffractometer equipped with a low temperature device and Micromax-007HF Cu-target microfocus rotating anode (λ = 1.54187 Å). The data were collected using CrystalClear 2.011 and processed using *CrysAlis PRO* 1.171.38.41. Empirical absorption correction was applied using spherical harmonics, as implemented in the SCALE3 ABSPACK scaling algorithm. Single crystals of **2-Cl**, **3-Cl**, **5-Cl**, **5-ONO$_2$**, $(^{BBN}PDP^{tBu})ZnCl_2$, and **1-Bu** suitable for X-ray diffraction were coated with poly(isobutylene) oil in a drybox and quickly transferred to the goniometer head of a Bruker AXS D8 Quest diffractometer with kappa geometry, an I-μ-S microsource X-ray tube, laterally graded multilayer (Goebel) mirror for monochromatization, a Photon2 CMOS area detector and an Oxford Cryosystems low temperature device. Examination and data collection were performed with Cu Kα radiation (λ = 1.54184 Å). Single crystals of **2-Br**, **3-Br**, **4**, **5-OPh** suitable for X-ray diffraction, were coated with poly(isobutylene) oil in a drybox and quickly transferred to the goniometer head of a Bruker AXS D8 Quest diffractometer with a fixed chi angle, a sealed tube fine focus X-ray tube, single crystal curved graphite incident beam monochromator and a Photon100 CMOS area detector. Examination and data collection were

performed with Mo Kα radiation (λ = 0.71073 Å). For both Quest instruments, data were collected, reflections were indexed and processed, and the files scaled and corrected for absorption using APEX3.[5] For all samples, the space groups were assigned and the structures were solved by direct methods using XPREP within the SHELXTL suite of programs[6] and refined by full matrix least squares against F^2 with all reflections using Shelxl2016 or Shelxl2017[7] using the graphical interface Shelxle.[8] If not specified otherwise, H atoms attached to carbon atoms were positioned geometrically and constrained to ride on their parent atoms, with carbon hydrogen bond distances of 0.95 Å for and aromatic C-H, 1.00, 0.99 and 0.98 Å for aliphatic C-H, CH_2, and CH_3 moieties, respectively. Methyl H atoms were allowed to rotate but not to tip to best fit the experimental electron density. U_{iso}(H) values were set to a multiple of U_{eq}(C) with 1.5 for CH_3, and 1.2 for CH_2, and C-H units, respectively. Additional data collection and refinement details, including description of disorder (where present) can be found with the individual structure descriptions, below.

Synthesis of ^{allyl}PDP^{tBu}. A 500 mL Schlenk flask was charged with sodium hydride (1.143 g, 47.63 mmol) and 200 mL of THF and cooled to -78 °C. 2,6-bis(5-*tert*-butyl-1*H*-pyrazol-3-yl)pyridine (7.700 g, 23.80 mmol) was added as a solid against a flow of dinitrogen. The flask was then allowed to warm to room temperature resulting in the evolution of H_2. When H_2 evolution had ceased, allyl bromide (5.760 g, 47.60 mmol) was added via syringe. After stirring at room temperature for 16 hr volatiles were removed. The sample was extracted with 100 mL $CHCl_3$, filtered over Celite, and dried. The resulting viscous yellow oil was purified via column chromatography (ethyl acetate/hexane) to afford white solid (6.130 g, 15.19 mmol, 64%) assigned as 2,6-bis(1-allyl-5-*tert*-butyl-1*H*-pyrazol-3-yl)pyridine . ^{1}H NMR ($CDCl_3$, 25 °C): δ = 1.40 (s, 18H, C(C*H*$_3$)$_3$), 4.90 (d, *J* = 5.0, 4H, N-C*H*$_2$), 4.99 (d, *J* = 17.5, 2H, C=C*H*), 5.18 (d, *J* = 10.5, 2H, C=C*H*), 6.04 (m, 2H, CH_2-C*H*), 6.81 (s, 2H, pyrazole-C*H*), 7.67 (t, *J* = 7.50, 1H, *p*-pyridine-C*H*), 7.85 (d, *J* = 7.50, 2H, *m*-pyridine-C*H*). ^{13}C NMR ($CDCl_3$, 25 °C): δ = 30.25 (C(*C*H$_3$)$_3$), 31.42 (*C*(CH$_3$)$_3$), 53.60 (N-*C*H$_2$), 102.49 (pyrazole-*C*H), 116.86 (*C*H$_2$), 118.40 (*m*-pyridine *C*H), 134.24 (*C*HCH$_2$), 136.82 (*p*-pyridine-*C*H), 150.32 (Ar-*C*), 152.05 (Ar-*C*), 152.74 (Ar-*C*).

Synthesis of ^{BBN}PDP^{tBu}. A 20 mL scintillation vial was charged with 2,6-bis(1-allyl-5-*tert*-butyl-1*H*-pyrazol-3-yl)pyridine (3.000 g, 7.433 mmol), 9-borabicyclo[3.3.1]nonane (2.170 g, 17.783 mmol), and 20 mL of benzene. The mixture was heated to 45 °C for 2 hr, allowed to cool to room temperature, and volatiles were removed in vacuo. The off-white solid was washed with 20 mL of *n*-pentane and dried to afford ^{BBN}PDP^{tBu} (4.765 g, 7.358 mmol, 99%). ^{1}H NMR ($CDCl_3$, 25 °C) δ = 1.17-1.28 (m, 4H, 9-BBN-C*H*), 1.38-1.44 (m, 4H, B-C*H*$_2$), 1.59-1.69 (m, 12H, 9-BBN-C*H*), 1.74-1.88 (m, 12H, 9-BBN-C*H*), 2.16 (p, *J* = 7.5, 4H, CH$_2$C*H*$_2$CH$_2$), 4.25 (t, *J* = 7.5, 4H, N-C*H*$_2$), 6.73 (s, 2H, pyrazole-C*H*), 7.69 (t, *J* = 7.5, 1H, *p*-pyridine-C*H*), 7.80 (d, *J* = 7.5, 2H, *m*-pyridine-C*H*). ^{13}C NMR ($CDCl_3$, 25 °C): δ = 23.44 (9-BBN-*C*H$_2$), 24.06 (9-BBN-*C*H), 26.16 (CH$_2$*C*H$_2$CH$_2$), 30.34 (C(*C*H$_3$)$_3$), 30.89 (B-*C*H$_2$), 31.64 (*C*(CH$_3$)$_3$), 33.14 (9-BBN-*C*H$_2$), 53.61 (N-*C*H$_2$), 102.67 (pyrazole-C*H*), 119.16 (*m*-pyridine-*C*H), 136.71 (*p*-pyridine-*C*H), 150.29 (Ar-*C*), 152.29 (Ar-*C*), 152.66 (Ar-*C*).

Synthesis of ^{Bu}PDP^{tBu}. A 250 mL Schlenk flask was charged with sodium hydride (0.556 g, 23.34 mmol) and 100 mL of THF and cooled to -78 °C. 2,6-bis(5-*tert*-butyl-1*H*-pyrazol-3-yl)pyridine (3.000 g, 9.275 mmol) was added as a solid against a flow of dinitrogen. The flask was then allowed to warm to room temperature resulting in the evolution of H_2. When H_2 evolution had ceased, iodobutane (6.820 g, 37.06 mmol) was added via syringe. After stirring at room temperature for 16 hr volatiles were removed. The sample extracted with 60 mL $CHCl_3$, filtered over Celite, and dried. The resulting viscous yellow oil was

purified via column chromatography (ethyl acetate/hexane) to afford white solid (1.523 g, 3.496 mmol, 38%) assigned as 2,6-is(1-*n*-butyl-5-*tert*-butyl-1*H*-pyrazol-3-yl)pyridine . ^{1}H NMR ($CDCl_3$, 25 °C): δ = 1.00 (t, *J* = 7.5, 6H, CH_2CH_3), 1.44 (s, 18H, $C(CH_3)_3$), 1.46 (sextet, *J* = 7.5, 4H, CH_2CH_3), 1.98 (pentet, *J* = 8.0, 4H, NCH_2CH_2), 4.21 (t, *J* = 8.0, 4H, N-CH_2), 6.76 (s, 2H, pyrazole-C*H*), 7.70 (t, *J* = 8.0, 1H, *p*-pyridine-C*H*), 7.84 (d, *J* = 8.0, 2H, *m*-pyridine-C*H*). ^{13}C NMR ($CDCl_3$, 25 °C): δ = 14.01 (CH_2CH_3), 20.35 (CH_2CH_3), 30.36 ($C(CH_3)_3$), 31.56 ($C(CH_3)_3$), 33.21 (NCH_2CH_2), 51.32 (N-CH_2), 102.20 (pyrazole-*C*H), 118.30 (*m*-pyridine-*C*H), 136.94 (*p*-pyridine-*C*H), 150.10 (Ar-*C*), 152.29 (Ar-*C*), 152.46 (Ar-*C*).

Synthesis of (^{Bu}PDP^{tBu})FeBr$_2$. A 20 mL scintillation vial was charged with $FeBr_2$ (0.166 g, 0.770 mmol) and 20 mL DCM. While stirring, ^{Bu}PDP^{tBu} (0.336 g, 0.771 mmol) was added. After 12 hr, the solution was filtered and volatiles were removed in vacuo. The resulting orange material was washed with 20 mL of diethyl ether and dried to afford yellow powder (0.466 g, 0.715 mmol, 89%) assigned as (^{Bu}PDP^{tBu})$FeBr_2$. Single, X-ray quality crystals were obtained by slow diffusion of *n*-pentane into a DCM solution of (^{Bu}PDP^{tBu})$FeBr_2$ at room temperature. MALDI-TOF of $C_{27}H_{41}N_5Br_2Fe$ - Br: Calc. 570.189; Found 570.253. ^{1}H NMR ($CDCl_3$, 25 °C) δ = -31.75 (119, 1H, *p*-pyridine-C*H*), -2.02 (24, 6H, CH_2CH_3), 1.06 (42, 4H, CH_2CH_3), 5.85 (206, 4H, NCH_2CH_2), 9.22 (36, 18H, $C(CH_3)_3$), 29.44 (336, 4H, NCH_2), 44.27 (116, 2H, Ar-C*H*), 52.55 (105, 2H, Ar-C*H*). μ_{eff} ($CDCl_3$, 25 °C) = 4.98(1). UV-Vis (THF, ambient temperature; λ_{max}, molar absorptivity): 333 nm, 9700 $M^{-1}cm^{-1}$.

Synthesis of (^{BBN}PDP^{tBu})FeCl$_2$. A 20 mL scintillation vial was charged with $FeCl_2$ (0.165 g, 1.302 mmol) and 20 mL DCM. While stirring, ^{BBN}PDP^{tBu} (0.843 g, 1.302 mmol) was added. After 12 hr, the solution was filtered and volatiles were removed in vacuo. The resulting orange material was washed with 30 mL of pentane and dried to afford yellow powder (0.891 g, 1.151 mmol, 88%) assigned as (^{BBN}PDP^{tBu})$FeCl_2$. Single, X-ray quality crystals were obtained by slow diffusion of *n*-pentane into a fluorobenzene solution of (^{BBN}PDP^{tBu})$FeCl_2$ at room temperature. MALDI-TOF of $C_{41}H_{63}N_5B_2Cl_2Fe$: Calc. 773.399; Found 773.477. ^{1}H NMR ($CDCl_3$, 25 °C) δ = -30.30 (31, 1H, *p*-pyridine-C*H*), -0.56 (36, 4H, 9-BBN-C*H*), -0.10 (36, 8H, 9-BBN-C*H*), 0.12 (31, 4H, 9-BBN-C*H*), 0.54 (78, 4H, 9-BBN-C*H*), 0.66 (25, 8H, 9-BBN-C*H*), 1.05 (31, 4H, B-CH_2), 4.23 (260, 4H, NCH_2CH_2), 6.83 (19, 18H, $C(CH_3)_3$), 19.46 (377, 4H, NCH_2), 41.63 (45, 2H, Ar-C*H*), 50.98 (50, 2H, Ar-C*H*). μ_{eff} ($CDCl_3$, 25 °C) = 4.80(2). UV-Vis (C_6H_6, ambient temperature; λ_{max}, molar absorptivity): 333 nm, 7000 $M^{-1}cm^{-1}$.

Synthesis of (^{BBN}PDP^{tBu})FeBr$_2$. A 20 mL scintillation vial was charged with $FeBr_2$ (0.120 g, 0.556 mmol) and 20 mL DCM. While stirring, ^{BBN}PDP^{tBu} (0.360 g, 0.556 mmol) was added. After 12 hr, the solution was filtered and volatiles were removed in vacuo. The resulting orange material was washed with 20 mL of pentane and dried to afford orange powder (0.345 g, 0.400 mmol, 72%) assigned as (^{BBN}PDP^{tBu})$FeBr_2$. MALDI-TOF of $C_{41}H_{63}N_5B_2Br_2Fe$: Calc. 861.298; Found 861.223. ^{1}H NMR ($CDCl_3$, 25 °C) δ = -31.95 (24, 1H, *p*-pyridine-C*H*), -1.06 (21, 4H, 9-BBN-C*H*), -0.82 (34, 8H, 9-BBN-C*H*), -0.40 (23, 4H, 9-BBN-C*H*), 0.13 (26, 8H, 9-BBN-C*H*), 0.68 (31, 4H, 9-BBN-C*H*), 1.64 (42, 4H, B-CH_2), 7.91 (185, 4H, NCH_2CH_2), 9.38, (13, 18H, $C(CH_3)_3$), 29.12 (327, 4H, N-CH_2), 44.42 (40, 2H, Ar-C*H*), 51.93 (34, 2H, Ar-C*H*). μ_{eff} ($CDCl_3$, 25 °C) = 4.88(2). UV-Vis (C_6H_6, ambient temperature; λ_{max}, molar absorptivity): 334 nm, 11,200 $M^{-1}cm^{-1}$.

Synthesis of (^{BBN}PDP^{tBu})ZnCl$_2$. A 20 mL scintillation vial was charged with $ZnCl_2$ (0.305 g, 2.238 mmol) and 20 mL DCM. While stirring, ^{BBN}PDP^{tBu} (1.450 g, 2.239 mmol) was added. After 18 hr, the solution was filtered and volatiles were removed in vacuo. The resulting white material was washed with 20 mL of pentane and dried to afford white powder (1.505 g, 1.920 mmol, 86%) assigned as (^{BBN}PDP^{tBu})$ZnCl_2$. Single, X-ray quality crystals were obtained by slow diffusion of diethyl ether into a concentrated

fluorobenzene/hexamethyldisiloxane (10:1) solution of (^{BBN}PDP^{tBu})$ZnCl_2$ at room temperature. MALDI-TOF of $C_{41}H_{63}N_5B_2Cl_2Zn$ - Cl: Calc. 746.424; Found 746.442. ^{1}H NMR (C_6D_6, 25 °C) δ = 1.12 (s, 18H, C(C*H*$_3$)$_3$), 1.30-1.36 (m, 4H, 9-BBN-C*H*), 1.65 (t, *J* = 8.0, 4H, B-C*H*$_2$), 1.87-1.98 (m, 20H, 9-BBN-C*H*), 1.98-2.05 (m, 4H, 9-BBN-C*H*), 2.82 (pentet, *J* = 8.0, 4H, NCH$_2$C*H*$_2$), 4.76 (t, *J* = 8.0, 4H, NC*H*$_2$), 6.09 (s, 2H, pyrazole-C*H*), 6.73 (d, *J* = 8.0, 2H, *m*-pyridine-C*H*), 7.00 (t, *J* = 7.5, 1H, *p*-pyridine-C*H*). ^{13}C NMR (C_6D_6, 25 °C): δ = 14.57 (BCH$_2$), 23.82 (9-BBN-*C*H$_2$), 25.30 (9-BBN-*C*H$_2$), 27.21 (CH$_2$*C*H$_2$CH$_2$), 29.98 (C(*C*H$_3$)$_3$), 31.71 (*C*(CH$_3$)$_3$), 33.66 (9-BBN-*C*H$_2$), 54.97 (N-*C*H$_2$), 100.97 (pyrazole-C*H*), 118.43 (*m*-pyridine-*C*H), 140.29 (*p*-pyridine-*C*H), 143.70 (Ar-*C*), 148.45 (Ar-*C*), 154.31 (Ar-*C*). UV-Vis (C_6H_6, ambient temperature; λ_{max}, molar absorptivity): 331 nm, 11221 $M^{-1}cm^{-1}$.

Synthesis of (^{BBN}PDP^{tBu})$ZnCl_2(N_2H_4)$. A 20 mL scintillation vial was charged with (^{BBN}PDP^{tBu})$ZnCl_2$ (0.277 g, 0.353 mmol) and 8 mL THF. While stirring, hydrazine (0.0112 mL, 0.356 mmol) was added. After 10 min, volatiles were removed in vacuo. The resulting white material was washed with 10 mL of pentane and dried to afford white powder (0.276 g, 0.338 mmol, 96%) assigned as (^{BBN}PDP^{tBu})$ZnCl_2(N_2H_4)$. Single, X-ray quality crystals were obtained by layering a DCM solution of (^{BBN}PDP^{tBu})$ZnCl_2(N_2H_4)$ with *n*-pentane at room temperature. MALDI-TOF of $C_{41}H_{67}N_7B_2Cl_2Zn$ - (N_2H_4 + Cl): Calc. 746.42; Found 746.30. ^{1}H NMR ($CDCl_3$, 25 °C) δ = 0.64 (t, *J* = 8.0, 4H, B-C*H*$_2$), 0.89 (s, 4H, 9-BBN-C*H*), 1.45 (s, 18H, C(C*H*$_3$)$_3$), 1.52-1.59 (m, 4H, 9-BBN-C*H*), 1.67-1.76 (m, 16H, 9-BBN-C*H*), 1.81-1.97 (m, 8H, 9-BBN-C*H*), 2.57 (s, 4H, NCH$_2$C*H*$_2$), 4.44 (t, *J* = 8.0, 4H, NC*H*$_2$), 6.38 (s, 4H, N_2H_4), 6.47 (s, 2H, pyrazole-C*H*), 7.58 (d, *J* = 7.5, 2H, *m*-pyridine-C*H*), 7.98 (t, *J* = 7.5, 1H, *p*-pyridine-C*H*). ^{13}C NMR (C_6D_6, 25 °C): δ = 13.85 (BCH$_2$), 22.07 (9-BBN-*C*H$_2$), 24.41 (9-BBN-*C*H$_2$), 26.06 (CH$_2$*C*H$_2$CH$_2$), 29.99 (C(*C*H$_3$)$_3$), 31.55 (9-BBN-*C*H$_2$), 31.86 (*C*(CH$_3$)$_3$), 55.30 (N-*C*H$_2$), 100.48 (pyrazole-C*H*), 118.97 (*m*-pyridine-*C*H), 141.71 (*p*-pyridine-*C*H), 143.38 (Ar-*C*), 148.25 (Ar-*C*), 155.87 (Ar-*C*). ^{11}B NMR ($CDCl_3$, 25 °C) δ = -10.41. UV-Vis (THF, ambient temperature; λ_{max}, molar absorptivity): 335 nm, 6629 $M^{-1}cm^{-1}$. IR (KBr): $\nu_{(N-H)}$ = 3286, 3220, 3166, 3070 cm^{-1}.

Synthesis of (^{BBN}PDP^{tBu})$FeCl_2(N_2H_4)$. A 20 mL scintillation vial was charged with (^{BBN}PDP^{tBu})$FeCl_2$ (0.241 g, 0.311 mmol) and 6 mL THF. While stirring, hydrazine (0.0098 mL, 0.312 mmol) was added resulting in an immediate color change from orange to yellow. After 15 min, volatiles were removed in vacuo. The resulting yellow material was washed with 10 mL of pentane and dried to afford yellow powder (0.247 g, 0.306 mmol, 99%) assigned as (^{BBN}PDP^{tBu})$FeCl_2(N_2H_4)$. MALDI-TOF of $C_{41}H_{67}N_7B_2Cl_2Fe$ - N_2H_4: Calc. 773.399; Found 773.450. ^{1}H NMR ($CDCl_3$, 25 °C) δ = -35.13 (44, 1H, *p*-pyridine-C*H*), -9.61 (403, 4H, N_2H_4), -3.46 (100, 8H, 9-BBN-C*H*), -2.42 (45, 8H, 9-BBN-C*H*), -1.34 (42, 4H, 9-BBN-C*H*), -1.04 (37, 4H, 9-BBN-C*H*), 1.38 (76, 4H, 9-BBN-CH), 6.0-7.5 (147, 4H, NCH$_2$C*H*$_2$), 9.66 (27, 18H, C(C*H*$_3$)$_3$), 41.96 (72, 2H, Ar-C*H*), 49.26 (56, 2H, Ar-C*H*). The –NC*H*$_2$, and –BC*H*$_2$ resonances are not observed. UV-Vis (THF, ambient temperature; λ_{max}, molar absorptivity): 338 nm, 7700 $M^{-1}cm^{-1}$. IR (KBr): $\nu_{(N-H)}$ = 3286, 3217, 3168, 3080 cm^{-1}.

Synthesis of (^{BBN}PDP^{tBu})$FeBr_2(N_2H_4)$. A 20 mL scintillation vial was charged with (^{BBN}PDP^{tBu})$FeBr_2$ (0.256 g, 0.297 mmol) and 6 mL THF. While stirring, hydrazine (0.0093 mL, 0.296 mmol) was added resulting in an immediate color change from orange to yellow. After 20 min, volatiles were removed in vacuo. The resulting yellow material was washed with 10 mL of pentane and dried to afford yellow powder (0.262 g, 0.293 mmol, 99%) assigned as (^{BBN}PDP^{tBu})$FeBr_2(N_2H_4)$. Single, X-ray quality crystals were obtained by layering a DCM solution of (^{BBN}PDP^{tBu})$FeBr_2(N_2H_4)$ with *n*-pentane at room temperature. The ^{15}N labeled complex, (^{BBN}PDP^{tBu})$FeBr_2(^{15}N_2H_4)$, was synthesized analogously. MALDI-TOF of $C_{41}H_{67}N_7B_2Br_2Fe$ - N_2H_4: Calc. 861.298; Found 861.299. ^{1}H NMR ($CDCl_3$, 25 °C) δ = -34.28 (61, 1H, *p*-pyridine-C*H*), -9.94 (265, 4H, N_2H_4), -3.63 (92, 8H, 9-BBN-C*H*), -2.62 (55, 8H, 9-BBN-C*H*), -1.45 (48, 4H, 9-BBN-C*H*), -1.10 (43, 4H, 9-

BBN-C*H*), 9.37 (147, 4H, NCH_2CH_2), 9.98 (37, 18H, $C(CH_3)_3$), 42.15 (84, 2H, Ar-C*H*), 51.46 (66, 2H, Ar-C*H*). The –NCH_2, –BCH_2, and 9-BBN-C*H* resonances are not observed. UV-Vis (THF, ambient temperature; λ_{max}, molar absorptivity): 338 nm, 17,700 $M^{-1}cm^{-1}$. IR (KBr): $\nu_{(N-H)}$ = 3283, 3210, 3163, 3093 cm^{-1}. IR (KBr) for **2-Br-^{15}N**: $\nu_{(N-H)}$ = 3273, 3208, 3150, 3072 cm^{-1}.

Synthesis of (^{BBN}PDP^{tBu})$FeCl_2(N_2H_4)_2$. A 20 mL scintillation vial was charged with (^{BBN}PDP^{tBu})$FeCl_2$ (0.215 g, 0.278 mmol) and 10 mL THF. While stirring, hydrazine (0.018 mL, 0.573 mmol) was added resulting in an immediate color change from orange to yellow. After 30 min, volatiles were removed in vacuo. The resulting yellow material was washed with 10 mL of pentane and dried to afford yellow powder (0.209 g, 0.249 mmol, 90%) assigned as (^{BBN}PDP^{tBu})$FeCl_2(N_2H_4)_2$. Single, X-ray quality crystals were obtained by slow diffusion *n*-pentane into a DCM solution of (^{BBN}PDP^{tBu})$FeCl_2(N_2H_4)_2$ at room temperature. MALDI-TOF of $C_{41}H_{71}N_9B_2Cl_2Fe$ - 2(N_2H_4): Calc. 773.399; Found 773.441. ^{1}H NMR ($CDCl_3$, 25 °C) δ = -30.59 (33, 1H, *p*-pyridine-C*H*), -13.28 (71, 4H, NH_2), -12.54 (95, 4H, NH_2), -3.04 (20, 4H, 9-BBN-C*H*), -2.58 (38, 4H, NCH_2CH_2), -0.67 (32, 4H, 9-BBN-C*H*), -0.43 (29, 4H, 9-BBN-C*H*), 0.29 (40, 4H, B-CH_2), 0.82 (25, 8H, 9-BBN-CH), 1.59 (34, 8H, 9-BBN-CH), 8.80 (14, 18H, $C(CH_3)_3$), 28.70 (290, 4H, NCH_2), 43.23 (47, 2H, Ar-C*H*), 53.76 (41, 2H, Ar-C*H*). UV-Vis (THF, ambient temperature; λ_{max}, molar absorptivity): 338 nm, 9700 $M^{-1}cm^{-1}$. IR (KBr): $\nu_{(N-H)}$ = 3346, 3281, 3220, 3150 cm^{-1}.

Synthesis of (^{BBN}PDP^{tBu})$FeBr_2(N_2H_4)_2$. A 20 mL scintillation vial was charged with (^{BBN}PDP^{tBu})$FeBr_2$ (0.140 g, 0.162 mmol) and 8 mL toluene. While stirring, hydrazine (0.0102 mL, 0.325 mmol) was added resulting in an immediate color change from orange to yellow with precipitation of a yellow powder. After 20 min, volatiles were removed in vacuo. The resulting yellow material was washed with 20 mL of pentane and dried to afford yellow powder (0.128 g, 0.138 mmol, 85%) assigned as (^{BBN}PDP^{tBu})$FeBr_2(N_2H_4)_2$. Single, X-ray quality crystals were obtained by slow diffusion of *n*-pentane into a DCM solution of (^{BBN}PDP^{tBu})$FeBr_2(N_2H_4)_2$ at room temperature. MALDI-TOF of $C_{41}H_{71}N_9B_2Br_2Fe$ - 2(N_2H_4): Calc. 861.298; Found 861.366. ^{1}H NMR ($CDCl_3$, 25 °C) δ = -31.09 (26, 1H, *p*-pyridine-C*H*), -14.79 (98, 4H, NH_2), -14.60 (89, 4H, NH_2), -3.20 (38, 8H, 9-BBN-C*H*), -3.03 (20, 4H, 9-BBN-C*H*), -0.65 (30, 4H, 9-BBN-C*H*), 0.16 (41, 4H, BCH_2), 2.05 (34, 8H, 9-BBN-C*H*), 2.63 (40, 4H, 9-BBN-C*H*), 4.55 (215, 4H, NCH_2CH_2), 10.08 (13, 18H, $C(CH_3)_3$), 33.55 (241, 4H, NCH_2), 44.34 (36, 2H, Ar-C*H*), 54.87 (33, 2H, Ar-C*H*). UV-Vis (THF, ambient temperature; λ_{max}, molar absorptivity): 338 nm, 5200 $M^{-1}cm^{-1}$. IR (KBr): $\nu_{(N-H)}$ = 3356, 3319, 3304, 3268, 3212, 3165, 3104 cm^{-1}.

Synthesis of (^{BBN}PDP^{tBu})$Fe(NH_2)_2$. A 20 mL scintillation vial was charged with (^{BBN}PDP^{tBu})$FeBr_2(N_2H_4)$ (0.100 g, 0.112 mmol) and 8 mL THF and frozen. On thawing, potassium graphite (0.030 g, 0.222 mmol) was added resulting in an immediate color change from yellow to dark green. On warming to RT, the green color dissipated and the solution became brown. After 30 min, volatiles were removed in vacuo. The material was extracted into 10 mL DCM, filtered, and dried. The resulting material was washed with 10 mL of *n*-pentane and 20 mL diethyl ether and dried to afford salmon-colored powder (0.066 g, 0.090 mmol, 80%) assigned as (^{BBN}PDP^{tBu})$Fe(NH_2)_2$. Single, X-ray quality crystals were obtained by layering a concentrated DCM solution of (^{BBN}PDP^{tBu})$Fe(NH_2)_2$ with hexamethyldisiloxane at room temperature. MALDI-TOF of $C_{41}H_{67}N_7B_2Fe$: Calc. 735.499; Found 735.573. ^{1}H NMR ($CDCl_3$, 25 °C) δ = -45.57 (5000, 2H), -29.43 (44, 1H, *p*-pyridine-C*H*), -20.78 (525, 2H), -1.41 (460, 2H), -0.71 (70, 2H), -0.78 (62, 2H), 0.16 (28, 2H), 1.53 (38, 2H), 2.33 (33, 2H), 2.60 (157, 2H), 2.72 (53, 2H), 3.91 (16, 18H, $C(CH_3)_3$), 4.52 (51, 2H), 5.90 (38, 2H), 6.60 (39, 2H), 6.84 (283, 2H), 9.22 (268, 2H), 12.95 (188, 2H), 14.24 (29, 2H), 24.89 (113, 2H), 33.85 (63, 2H), 41.42 (259, 2H), 51.15 (68, 2H). Two 2H resonances were not observed and likely

originate from the N-*H* moieties. UV-Vis (THF, ambient temperature; λ_{max}, molar absorptivity): 332 nm, 4600 $M^{-1}cm^{-1}$. IR (KBr): $\nu_{(N-H)}$ = 3358, 3318, 3240, 3141 cm^{-1}.

Synthesis of (^{BBN}PDP^{tBu})FeCl$_2$(NH$_3$)$_2$. A 20 mL scintillation vial was charged with (^{BBN}PDP^{tBu})Fe(NH$_2$)$_2$ (0.058 g, 0.079 mmol) and 12 mL THF. While stirring, triethylammonium chloride (0.022 g, 0.160 mmol) was added and stirred at room temperature resulting to a gradual color change from salmon to light orange. After 4 hr, volatiles were removed in vacuo. The material was washed with *n*-pentane (2 x 10 mL) and dried to afford yellow powder (0.057 g, 0.071 mmol, 90%) assigned as (^{BBN}PDP^{tBu})FeCl$_2$(NH$_3$)$_2$. Single, X-ray quality crystals were obtained by slow diffusing *n*-pentane into a THF solution of (^{BBN}PDP^{tBu})FeCl$_2$(NH$_3$)$_2$ at room temperature. MALDI-TOF of $C_{41}H_{69}N_7B_2Cl_2Fe$ - 2(NH$_3$): Calc. 773.399; Found 773.487. ^{1}H NMR ($CDCl_3$, 25 °C) δ = -30.50 (34, 1H, *p*-pyridine-C*H*), -14.36 (84, 6H, N*H*$_3$), -3.99 (31, 4H), -2.95 (45, 4H), -0.76 (47, 8H, 9-BBN-C*H*), -0.07 (56, 4H), 0.37 (35, 4H), 0.52 (68, 4H), 1.02 (50, 8H, 9-BBN-C*H*), 8.81 (21, 18H, C(C*H*$_3$)$_3$), 28.51 (311, 4H, NC*H*$_2$), 43.57 (49, 2H, Ar-C*H*), 52.72 (43, 2H, Ar-C*H*). UV-Vis (THF, ambient temperature; λ_{max}, molar absorptivity): 337 nm, 8800 $M^{-1}cm^{-1}$. IR (KBr): $\nu_{(N-H)}$ = 3353, 3286, 3249, 3170 cm^{-1}.

Synthesis of (^{BBN}PDP^{tBu})Fe(OPh)$_2$(NH$_3$)$_2$. A 20 mL scintillation vial was charged with (^{BBN}PDP^{tBu})Fe(NH$_2$)$_2$ (0.053 g, 0.072 mmol) and 4 mL THF and chilled to -35 °C. A separate vial was charged with phenol (0.014 g, 0.149 mmol) and 2 mL THF and chilled to -35 °C. The solution of phenol was then added to the vial of (^{BBN}PDP^{tBu})Fe(NH$_2$) and warmed to room temperature resulting to a gradual color change from light orange to light red. After 45 min, volatiles were removed in vacuo. The material was washed with 10 mL *n*-pentane and dried to afford light red powder (0.054 g, 0.058 mmol, 82%) assigned as (^{BBN}PDP^{tBu})Fe(OPh)$_2$(NH$_3$)$_2$. Single, X-ray quality crystals were obtained by slow diffusing *n*-pentane into a benzene solution of (^{BBN}PDP^{tBu})Fe(OPh)$_2$(NH$_3$)$_2$ at room temperature. ^{1}H NMR (C_6D_6, 25 °C) δ = -28.13 (61, 1H, *p*-pyridine-C*H*), -18.99 (1300, 2H, *p*-Ph-C*H*), -14.31 (1900, 4H), -5.39 (1300, 4H), -2.92 (114, 4H), -1.66 (82, 4H), 0.73 (41, 4H), 1.09 (36, 8H, 9-BBN-C*H*), 1.40 (41, 8H, 9-BBN-C*H*), 1.60 (37, 4H), 1.74 (40, 4H), 3.04 (24, 18H, C(C*H*$_3$)$_3$), 32.04 (1700, 4H), 33.83 (83, 2H, Ar-C*H*), 47.20 (110, 2H, Ar-C*H*). A 6H resonance originating from the –N*H*$_3$ moieties was not observed. UV-Vis (THF, ambient temperature; λ_{max}, molar absorptivity): 334 nm, 7600 $M^{-1}cm^{-1}$. IR (KBr): $\nu_{(N-H)}$ = 3357, 3309, 3256, 3065 cm^{-1}.

Synthesis of (^{BBN}PDP^{tBu})Fe(ONO$_2$)$_2$(NH$_3$)$_2$. A 20 mL scintillation vial was charged with (^{BBN}PDP^{tBu})Fe(NH$_2$)$_2$ (0.050 g, 0.068 mmol) and 4 mL THF and chilled to -35 °C. While stirring, triethylammonium nitrate (0.022 g, 0.134 mmol) was added resulting in a gradual color change from light orange to yellow upon warming. After 45 min, volatiles were removed in vacuo. The material was washed with 20 mL *n*-pentane and dried to afford yellow powder (0.053 g, 0.062 mmol, 90%) assigned as (^{BBN}PDP^{tBu})Fe(ONO$_2$)$_2$(NH$_3$)$_2$. Single, X-ray quality crystals were obtained by slow diffusing *n*-pentane into a DCM solution of (^{BBN}PDP^{tBu})Fe(ONO$_2$)$_2$(NH$_3$)$_2$ at room temperature. MALDI-TOF of $C_{41}H_{69}N_9B_2O_6Fe$ - 2(NH$_3$) - NO$_3$: Calc. 765.449; Found 765.535. ^{1}H NMR (C_6D_6, 25 °C) δ = -17.91 (65, 1H, *p*-pyridine-C*H*), -0.34 (65, 6H, N*H*$_3$), 0.15 (45, 4H), 0.97 (36, 4H), 1.31 (63, 8H, 9-BBN-C*H*), 1.80 (46, 4H), 2.14 (71, 8H, 9-BBN-C*H*), 2.45 (60, 4H), 3.11 (51, 4H), 7.30 (65, 18H, C(C*H*$_3$)$_3$), 23.63 (320, 4H, NC*H*$_2$), 46.77 (86, 2H, Ar-C*H*), 62.16 (81, 2H, Ar-C*H*). UV-Vis (THF, ambient temperature; λ_{max}, molar absorptivity): 330 nm, 9700 $M^{-1}cm^{-1}$. IR (KBr): $\nu_{(N-H)}$ = 3355, 3319, 3262, 3192, 3148 cm^{-1}.

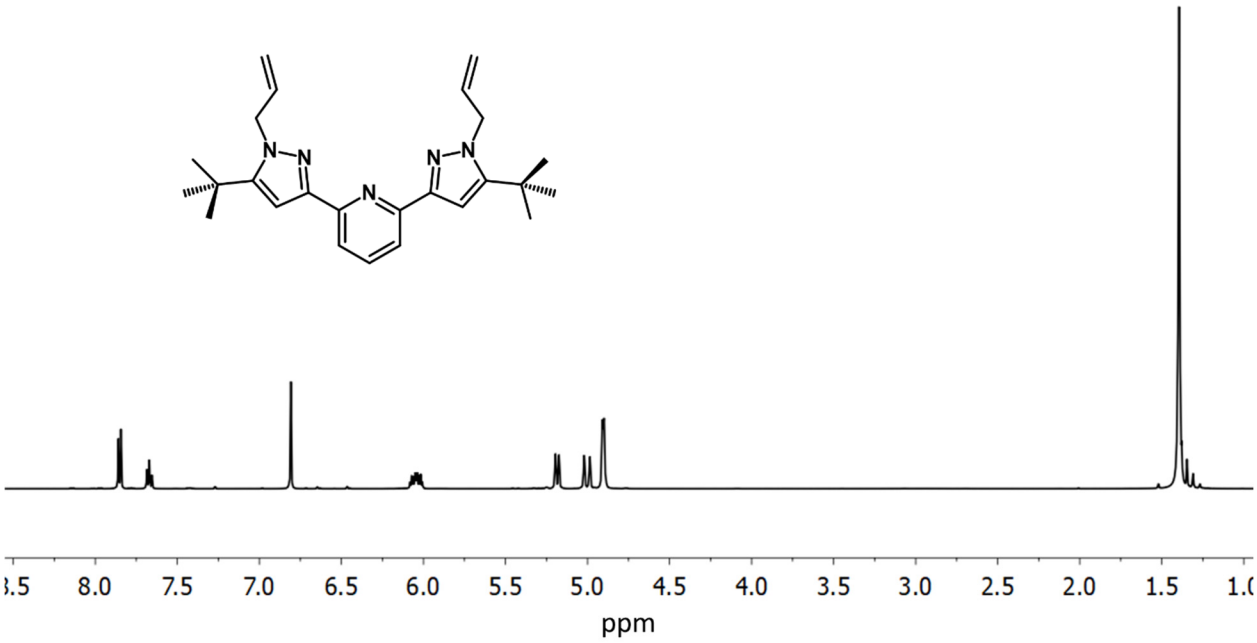

Figure S1 ^{1}H NMR spectrum ($CDCl_3$, 25 °C, 500.08 MHz) of ^{allyl}PDP^{tBu}.

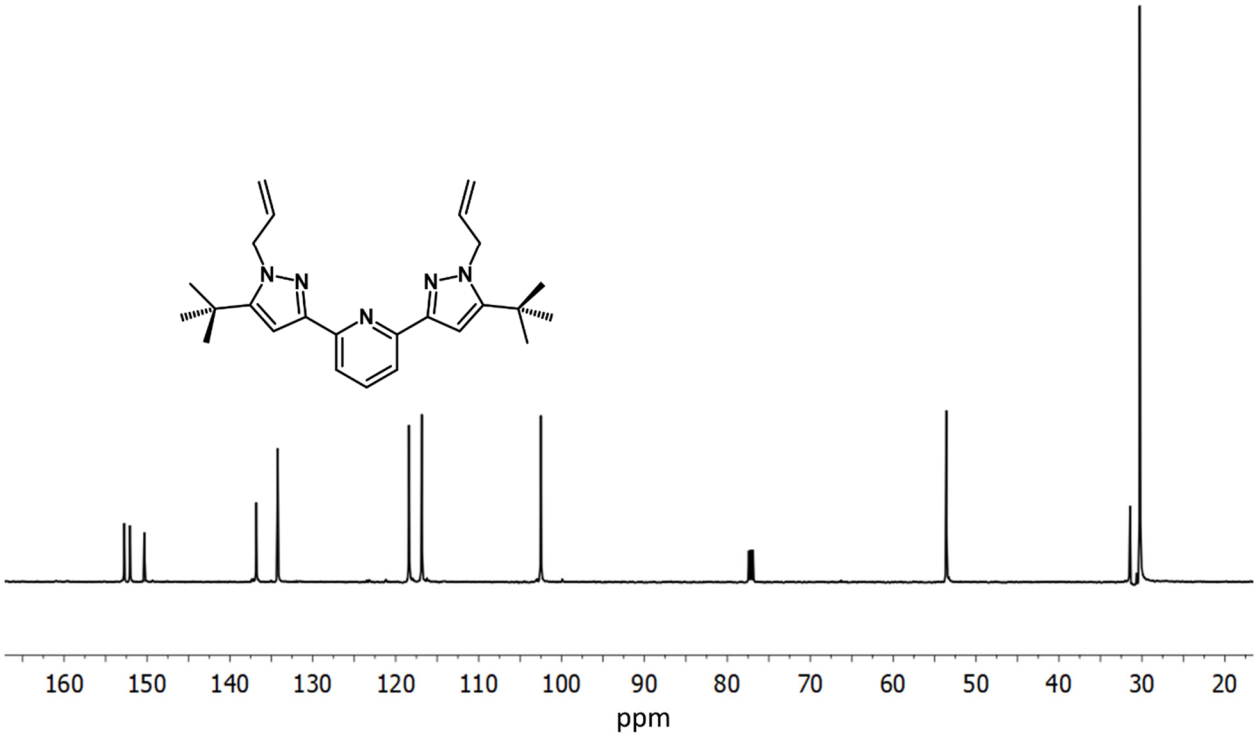

Figure S2 ^{13}C NMR spectrum ($CDCl_3$, 25 °C, 125.76 MHz) of ^{allyl}PDP^{tBu}.

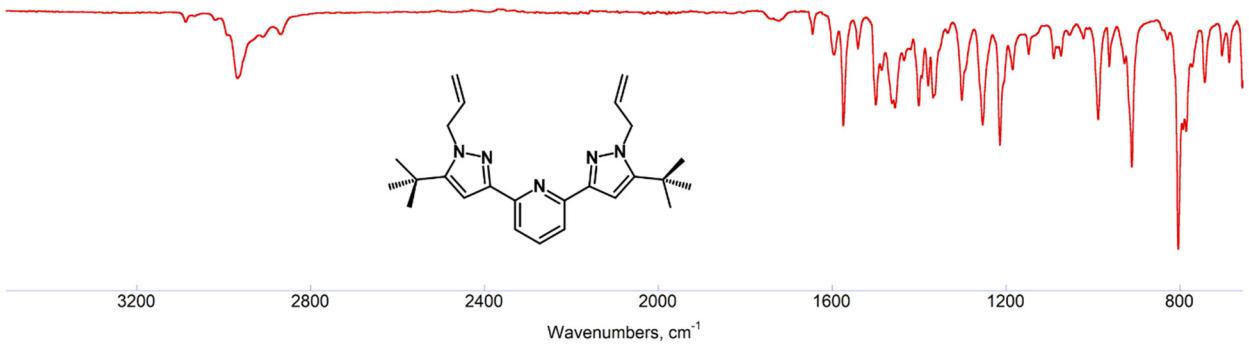

Figure S3 Infrared spectrum (Neat, ATR) of ^{allyl}PDP^{tBu}.

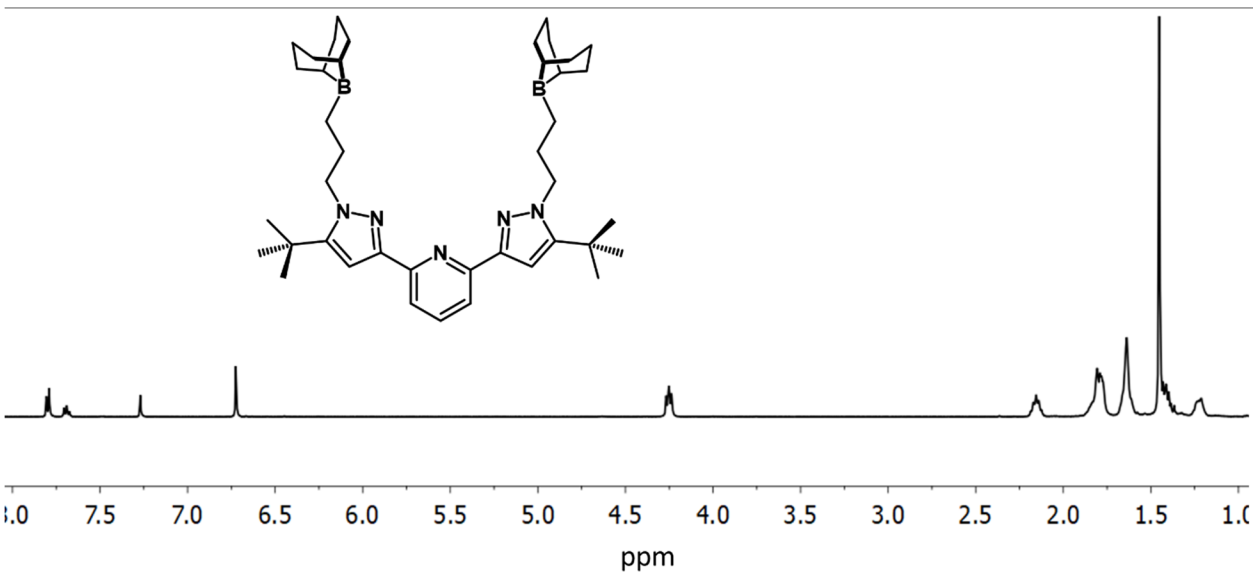

Figure S4 ^{1}H NMR spectrum ($CDCl_3$, 25 °C, 500.08 MHz) of ^{BBN}PDP^{tBu}.

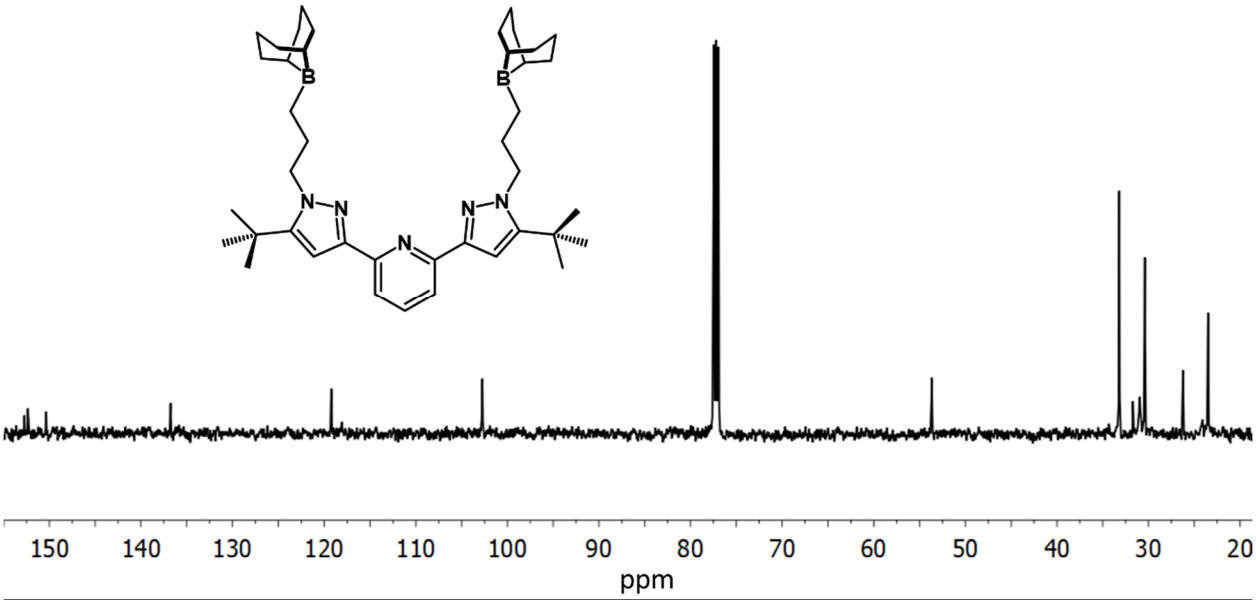

Figure S5 ^{13}C NMR spectrum ($CDCl_3$, 25 °C, 125.76 MHz) of $^{BBN}PDP^{tBu}$.

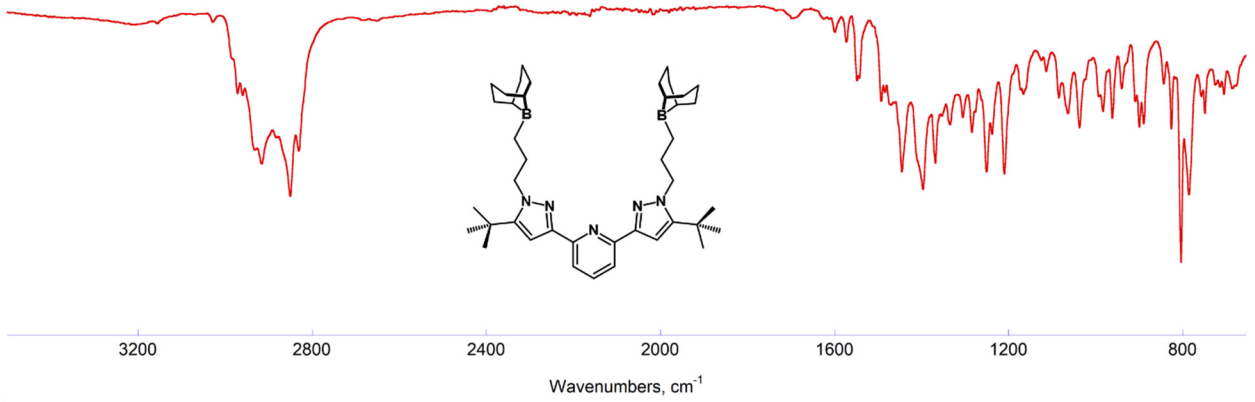

Figure S6 Infrared spectrum (Neat, ATR) of $^{BBN}PDP^{tBu}$.

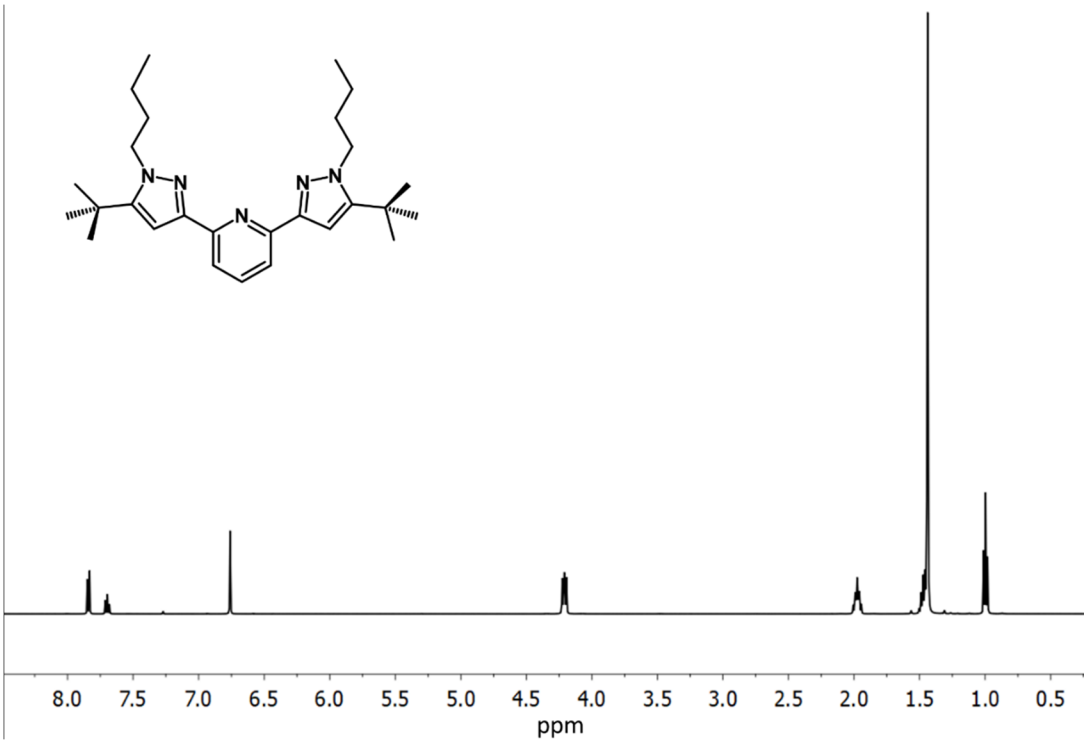

Figure S7 ^{1}H NMR spectrum ($CDCl_3$, 25 °C, 500.08 MHz) of $^{Bu}PDP^{tBu}$.

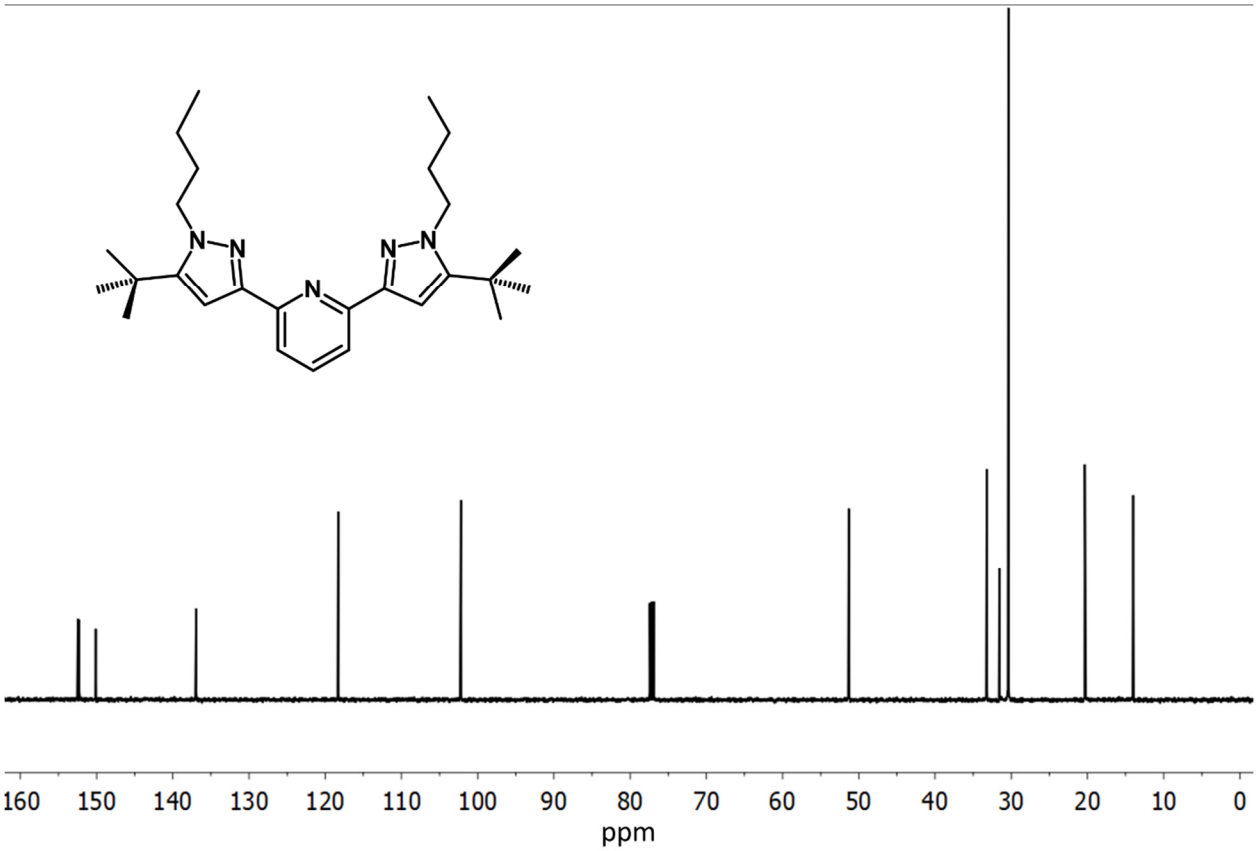

Figure S8 ^{13}C NMR spectrum ($CDCl_3$, 25 °C, 125.76 MHz) of $^{Bu}PDP^{tBu}$.

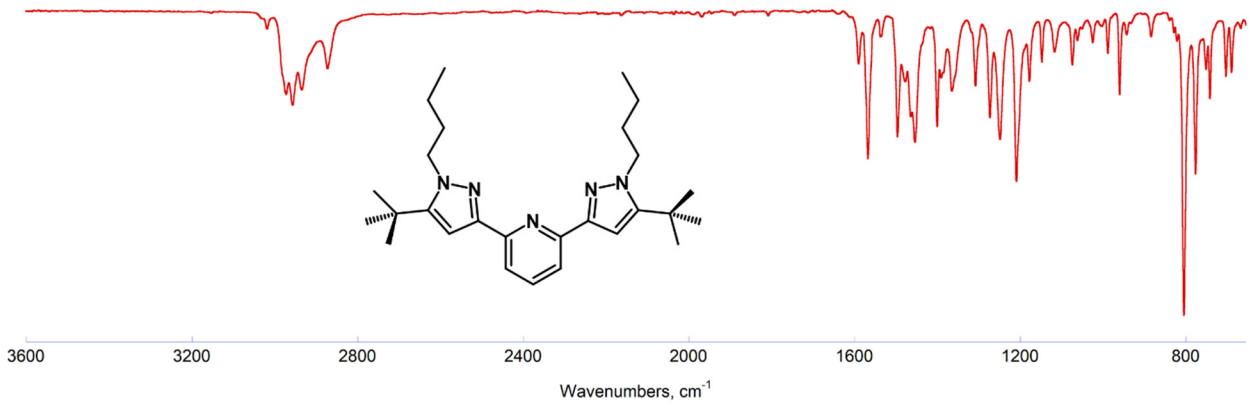

Figure S9 Infrared spectrum (Neat, ATR) of $^{BBN}PDP^{tBu}$.

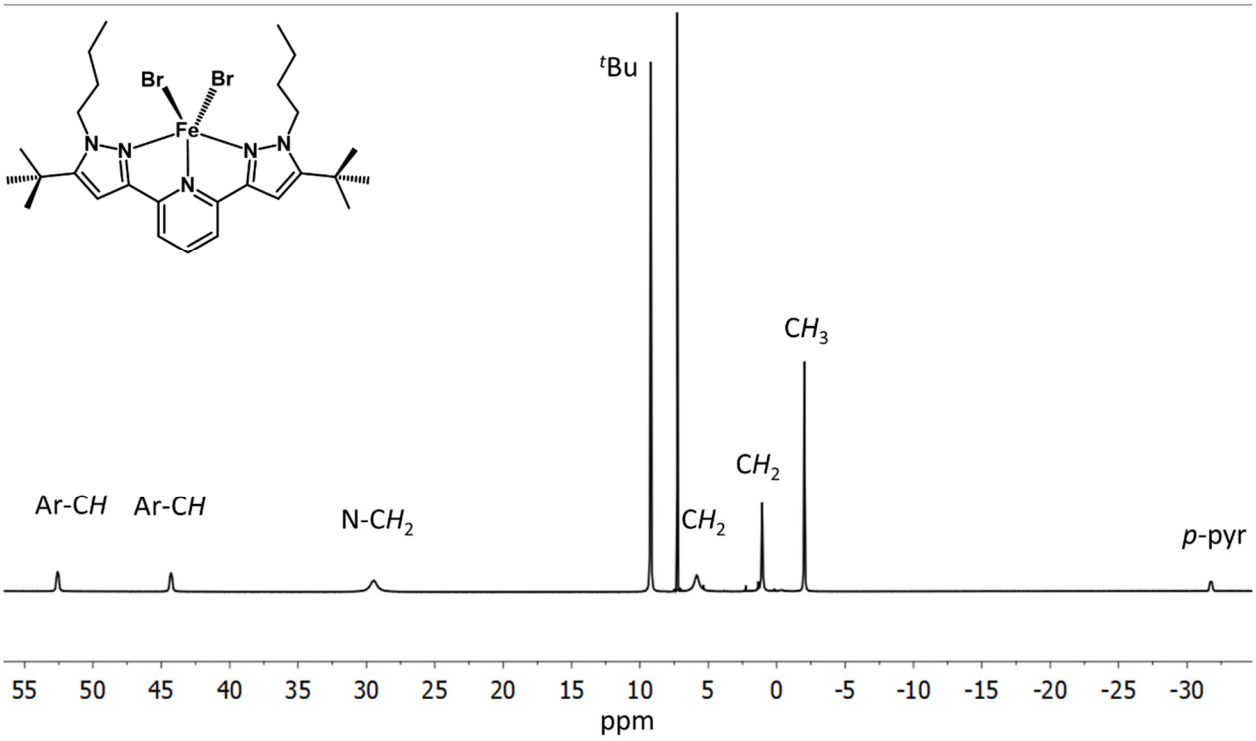

Figure S10 ^{1}H NMR spectrum ($CDCl_3$, 25 °C, 500.08 MHz) of ($^{Bu}PDP^{tBu}$)$FeBr_2$.

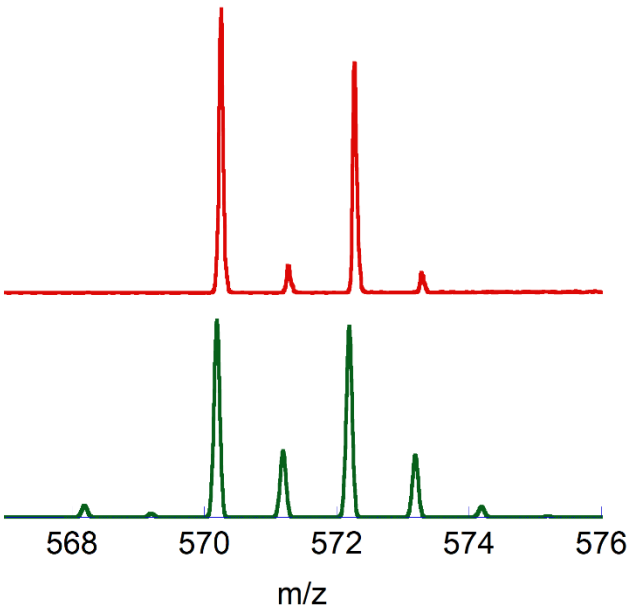

Figure S11 MALDI-TOF spectrum of (^{Bu}PDP^{tBu})FeBr$_2$ (top, red) obtained in an anthracene matrix and the predicted isotopic pattern (bottom, green). Monoisotopic mass for $C_{27}H_{41}N_5Br_2Fe$ - Br: Calculated 570.189; Found 570.253.

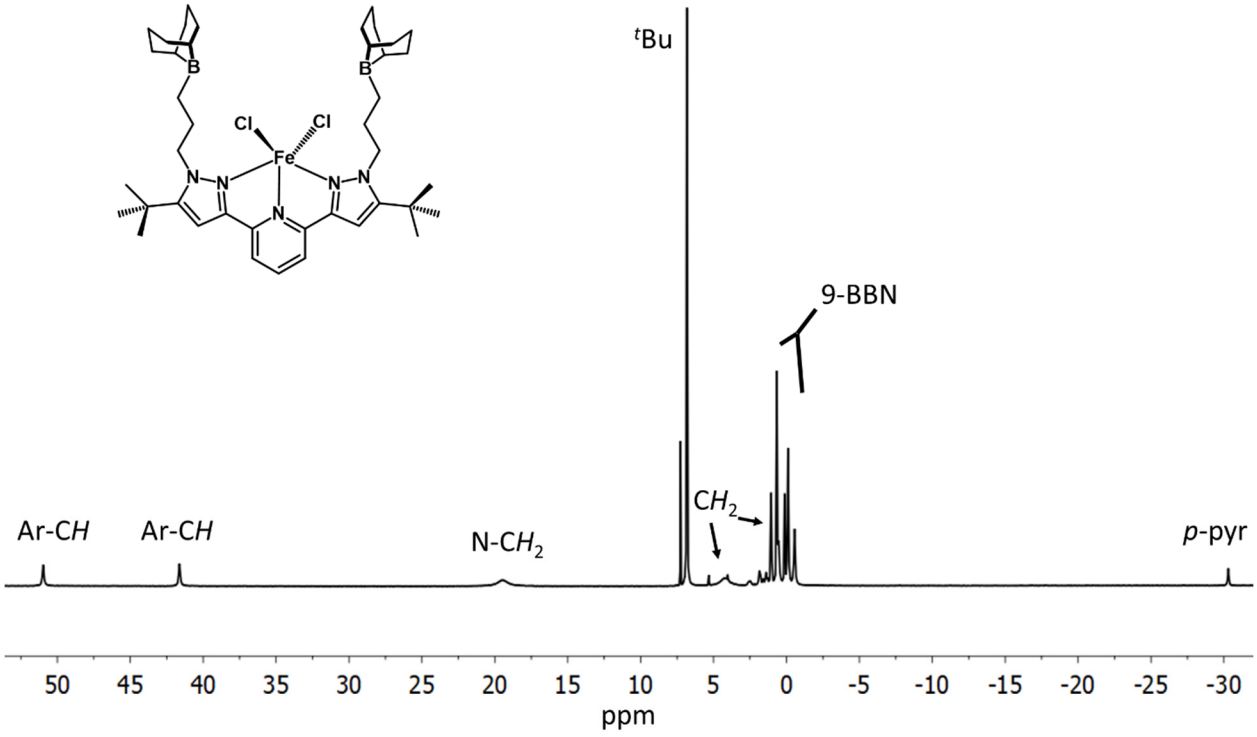

Figure S12 ^{1}H NMR spectrum ($CDCl_3$, 25 °C, 399.53 MHz) of (^{BBN}PDP^{tBu})FeCl$_2$.

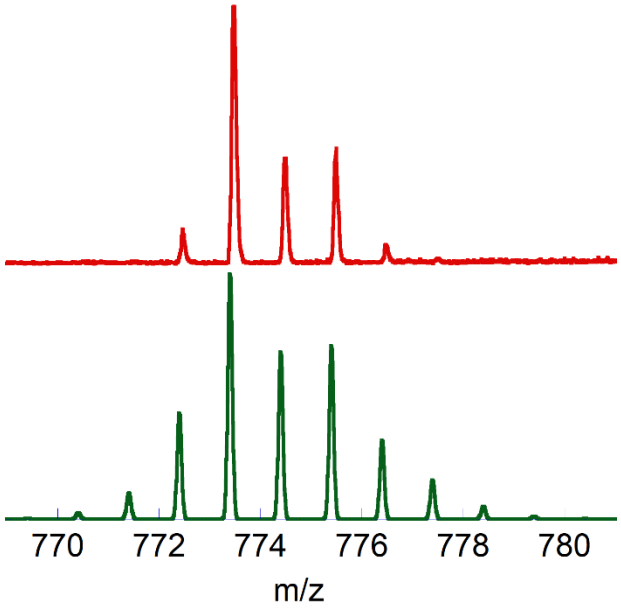

Figure S13 MALDI-TOF spectrum of (^{BBN}PDP^{tBu})$FeCl_2$ (top, red) obtained in an anthracene matrix and the predicted isotopic pattern (bottom, green). Monoisotopic mass for $C_{41}H_{63}N_5B_2Cl_2Fe$: Calculated 773.399; Found 773.477.

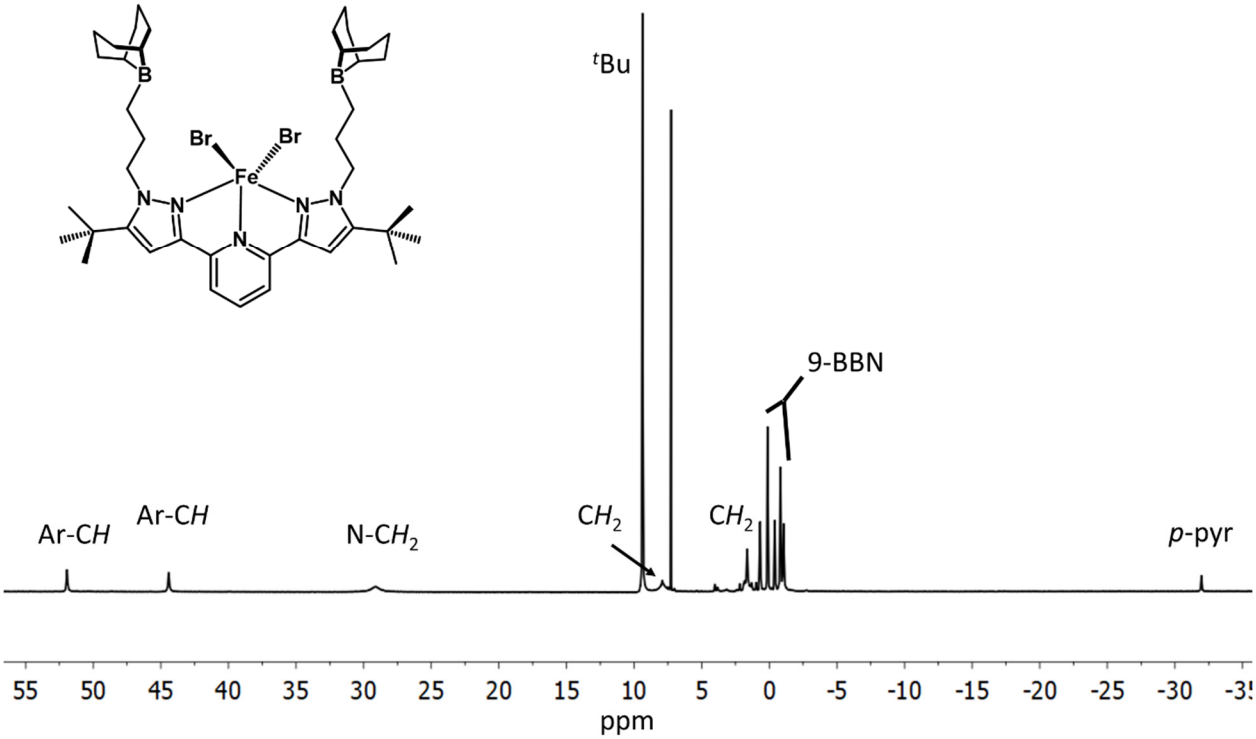

Figure S14 ^{1}H NMR spectrum ($CDCl_3$, 25 °C, 399.53 MHz) of (^{BBN}PDP^{tBu})$FeBr_2$.

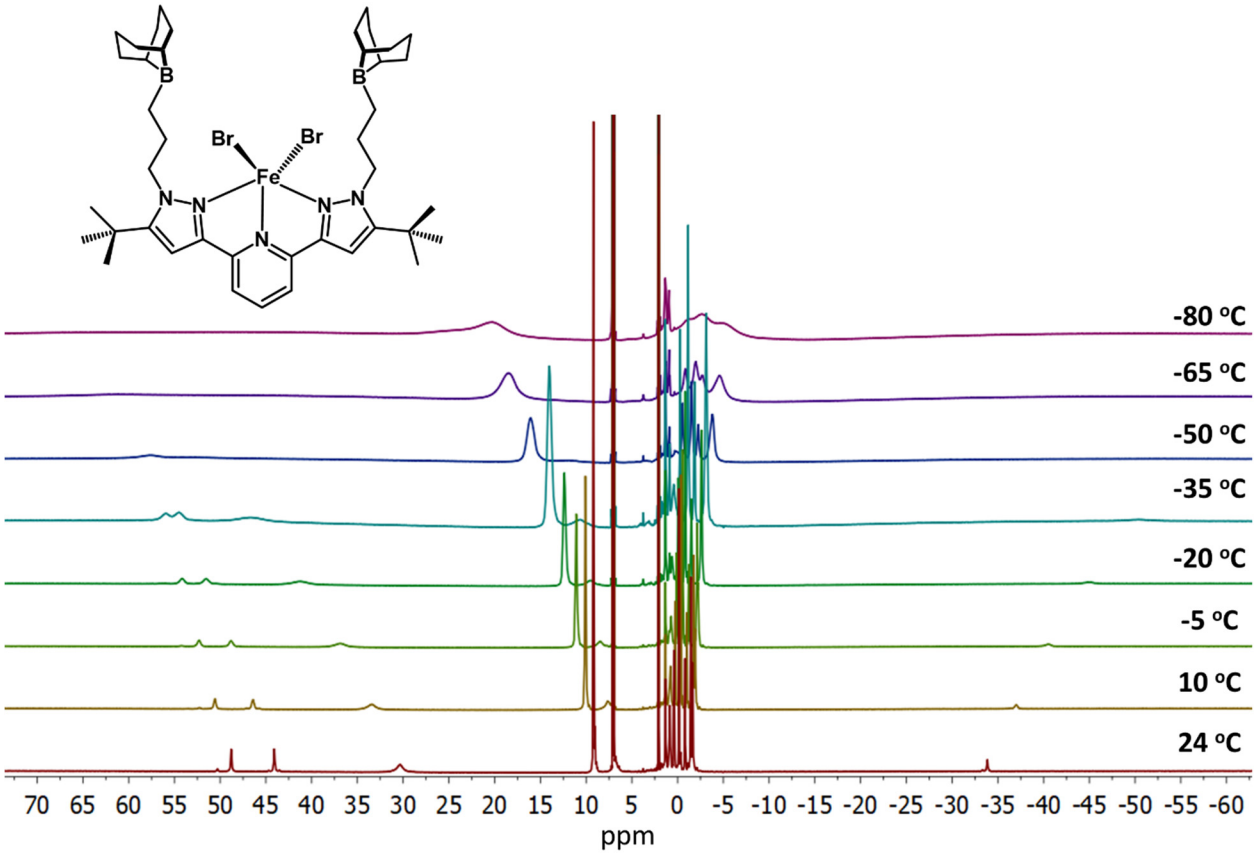

Figure S15 Variable temperature ^{1}H NMR spectrum (C_7D_8, 500.08 MHz) of (^{BBN}PDP^{tBu})$FeBr_2$.

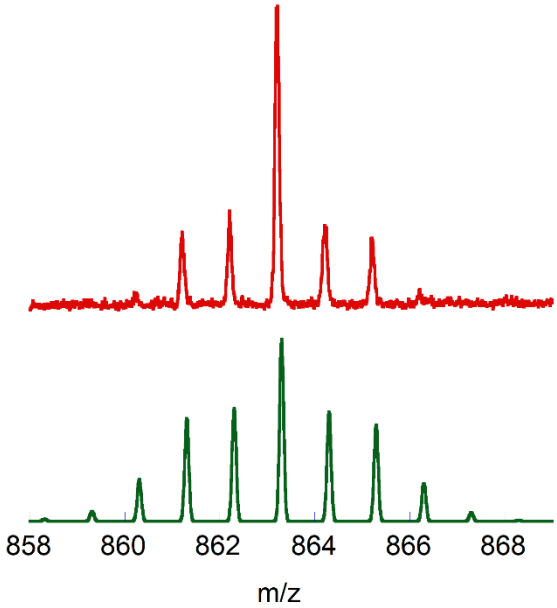

Figure S16 MALDI-TOF spectrum of (^{BBN}PDP^{tBu})$FeBr_2$ (top, red) obtained in an anthracene matrix and the predicted isotopic pattern (bottom, green). Monoisotopic mass for $C_{41}H_{63}N_5B_2Br_2Fe$: Calculated 861.298; Found 861.223.

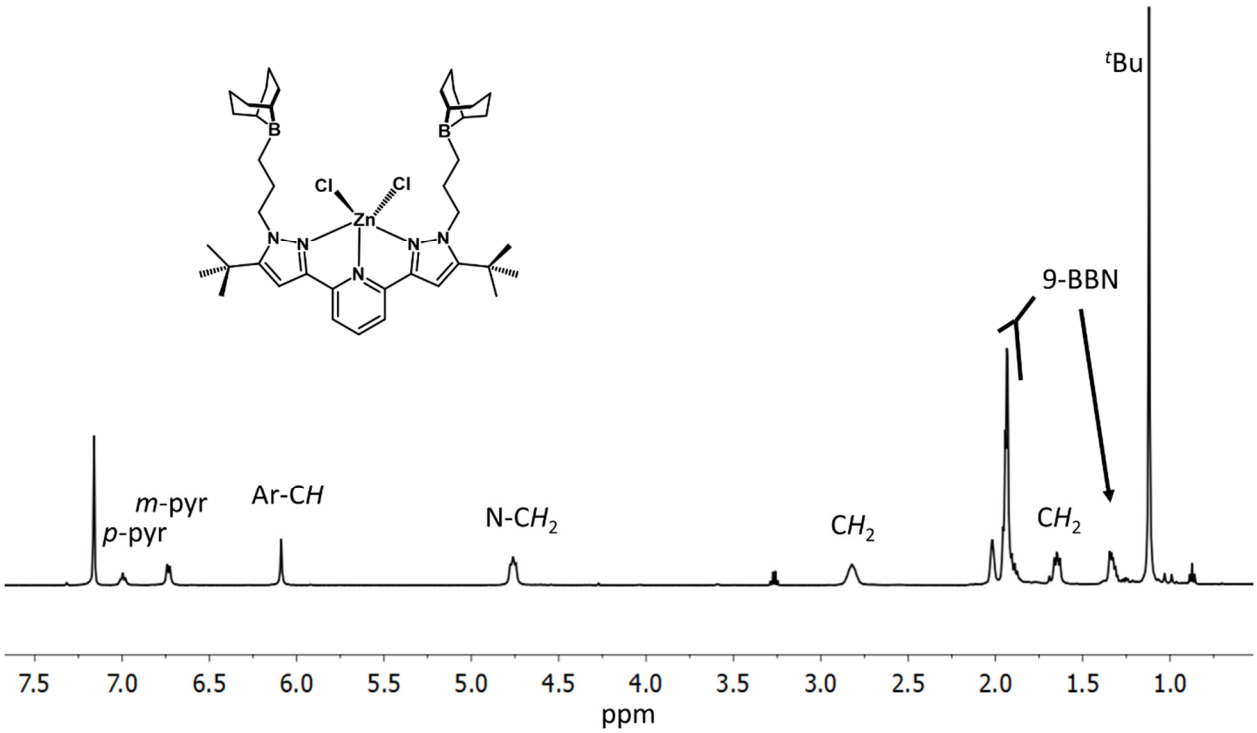

Figure S17 ^{1}H NMR spectrum (C_6D_6, 25 °C, 500.08 MHz) of (^{BBN}PDP^{tBu})$ZnCl_2$.

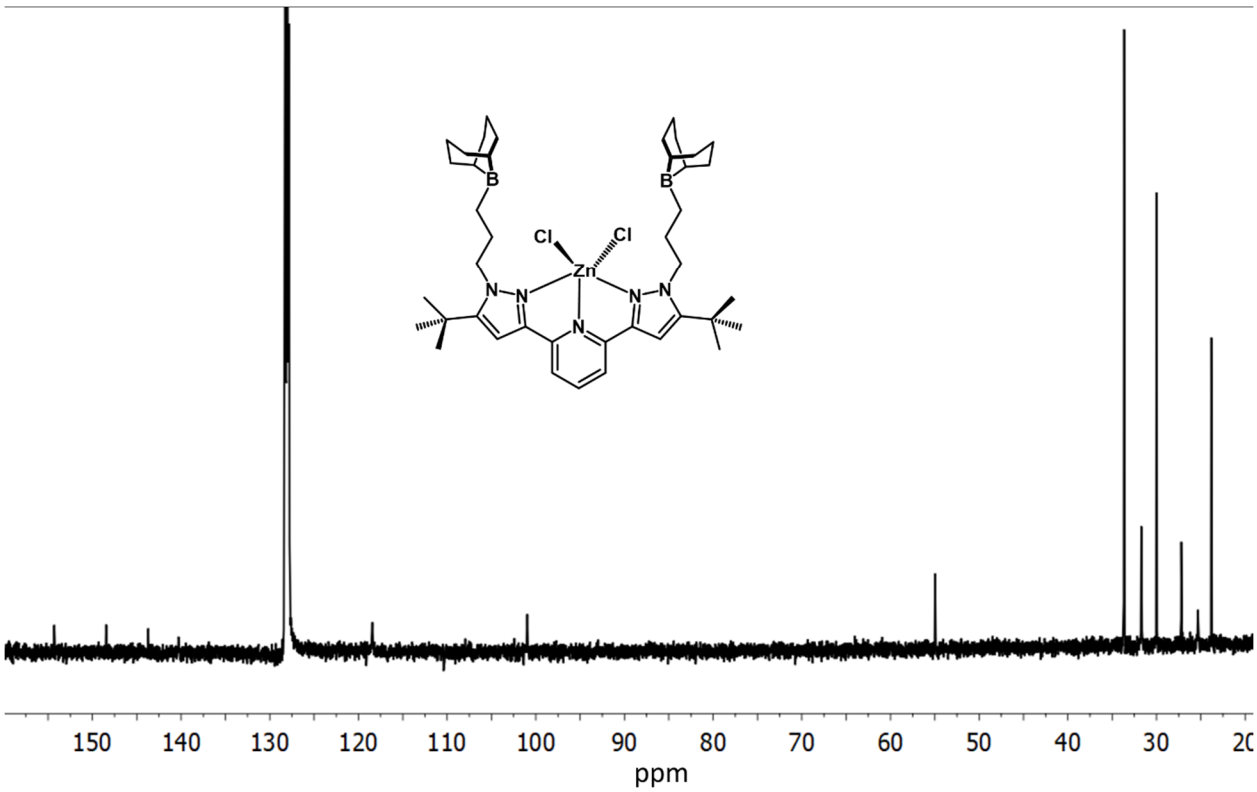

Figure S18 ^{13}C NMR spectrum (C_6D_6, 25 °C, 125.76 MHz) of (^{BBN}PDP^{tBu})$ZnCl_2$.

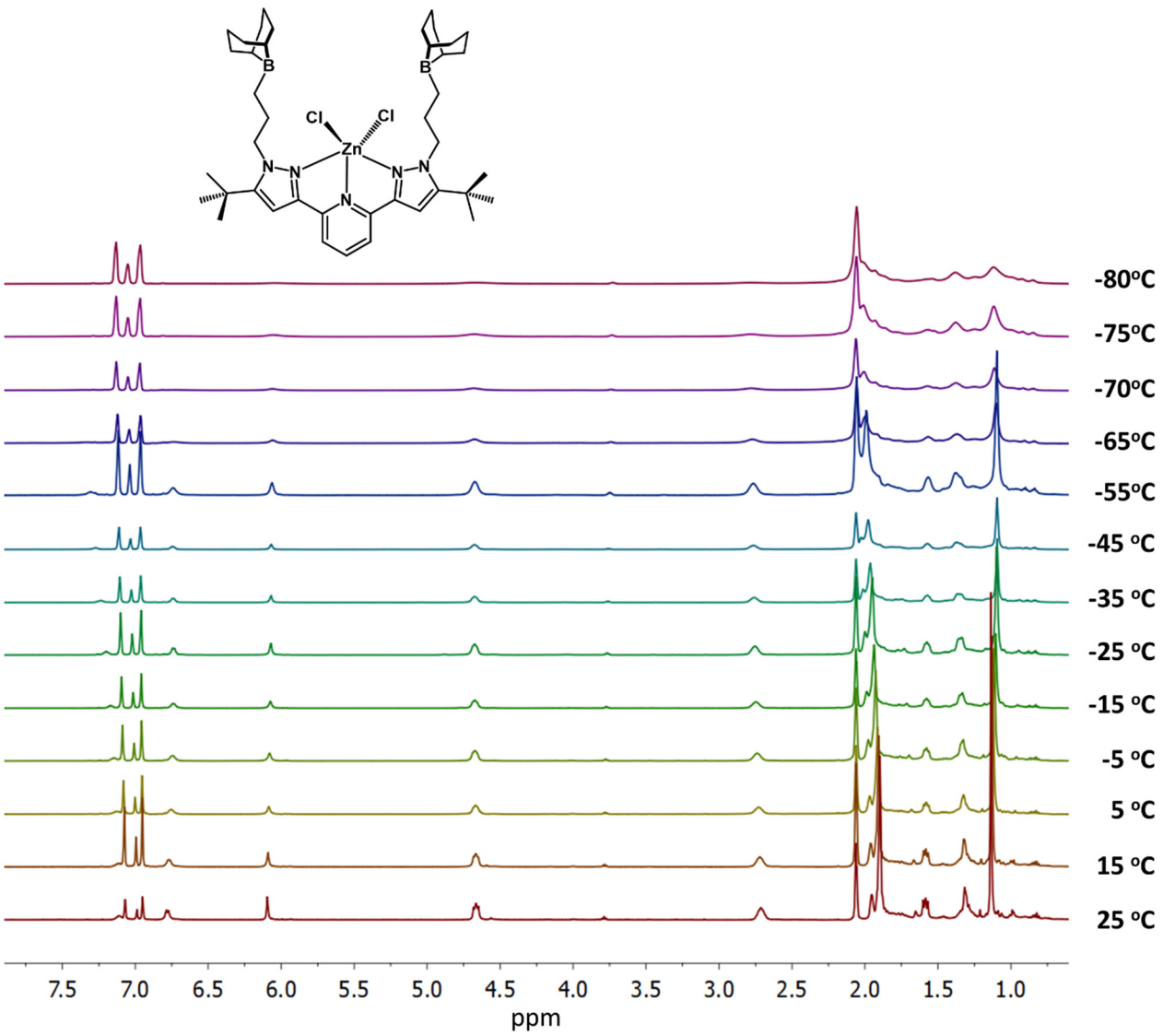

Figure S19 Variable temperature ^{1}H NMR spectrum (C_7D_8, 500.08 MHz) of (^{BBN}PDP^{tBu})$ZnCl_2$.

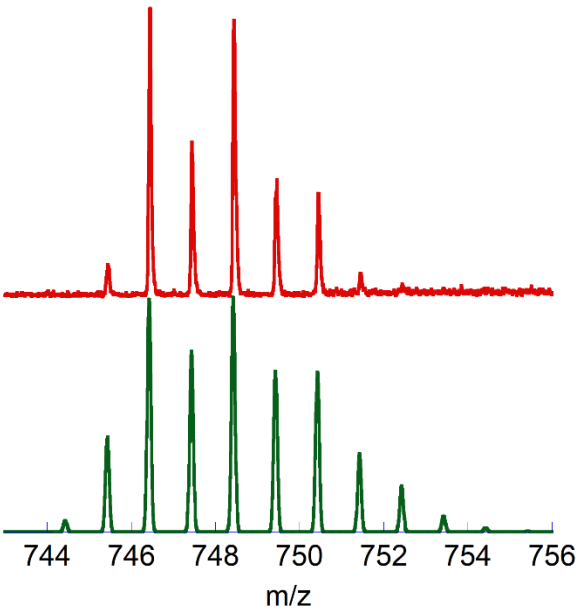

Figure S20 MALDI-TOF spectrum of (^{BBN}PDP^{tBu})$ZnCl_2$ (top, red) obtained in an anthracene matrix and the predicted isotopic pattern (bottom, green). Monoisotopic mass for $C_{41}H_{63}N_5B_2Cl_2Zn$ - Cl: Calculated 746.424; Found 746.442.

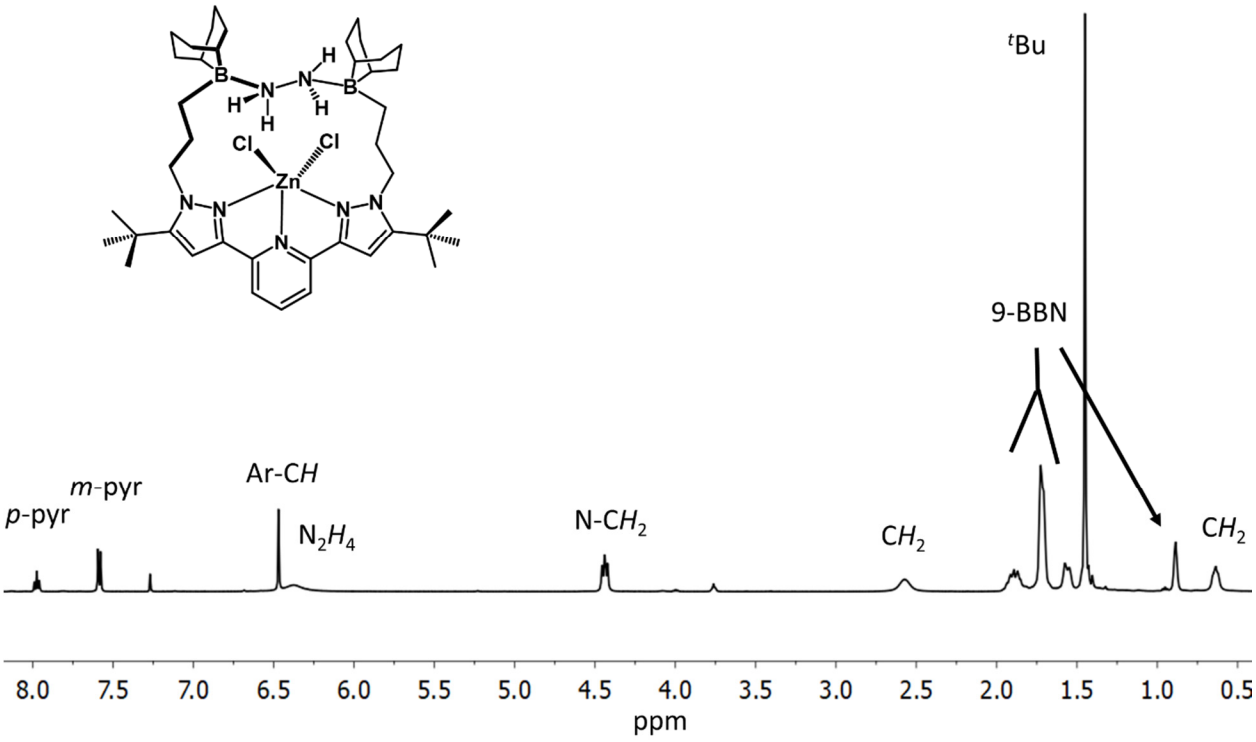

Figure S21 ^{1}H NMR spectrum ($CDCl_3$, 25 °C, 500.08 MHz) of (^{BBN}PDP^{tBu})$ZnCl_2(N_2H_4)$.

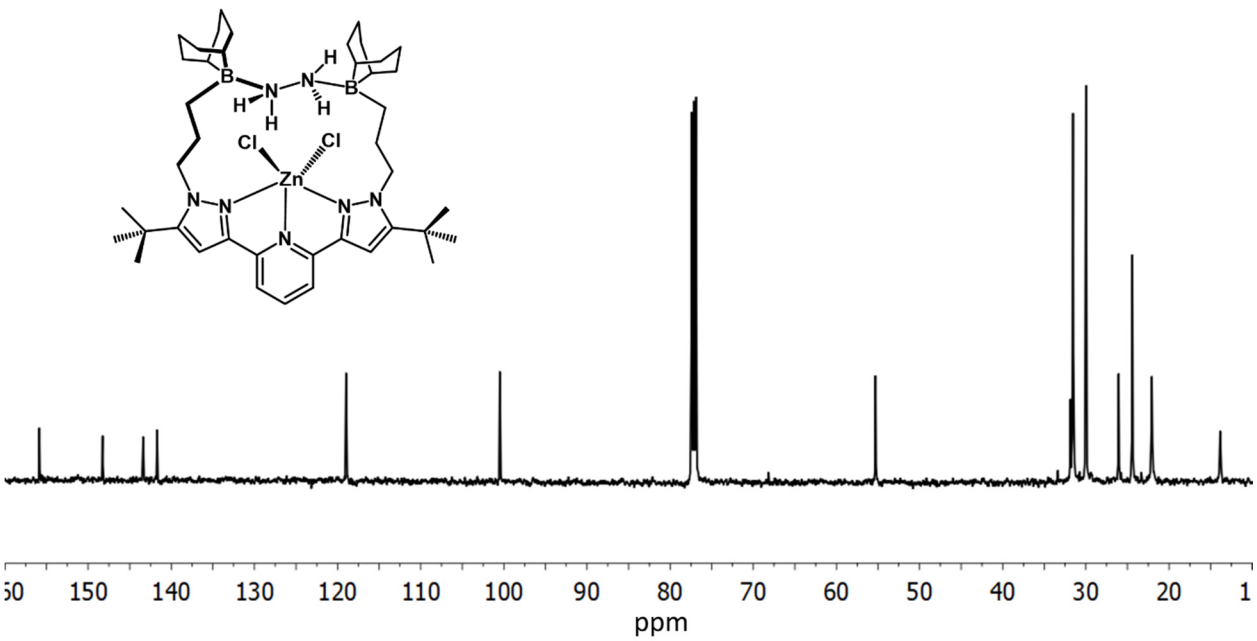

Figure S22 ^{13}C NMR spectrum ($CDCl_3$, 25 °C, 125.76 MHz) of ($^{BBN}PDP^{tBu}$)$ZnCl_2(N_2H_4)$.

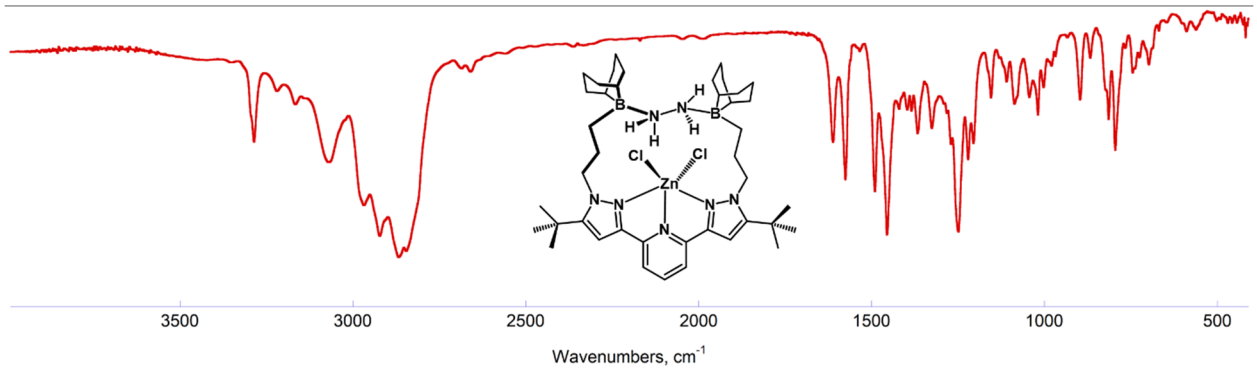

Figure S23 Infrared spectrum (KBr) of ($^{BBN}PDP^{tBu}$)$ZnCl_2(N_2H_4)$.

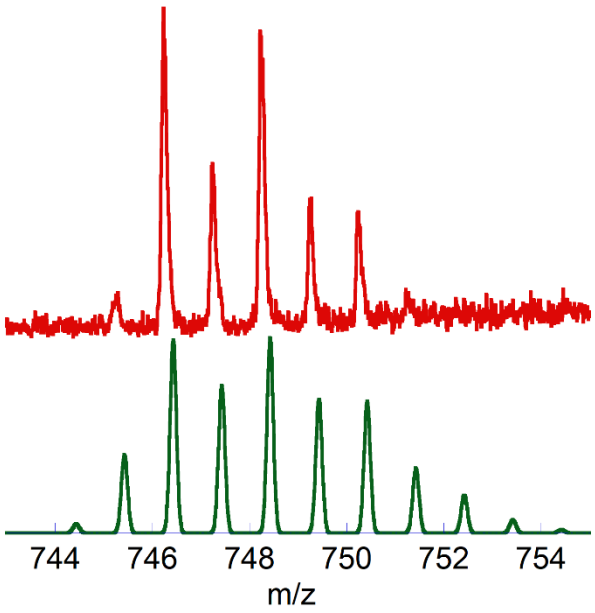

Figure S24 MALDI-TOF spectrum of (^{BBN}PDP^{tBu})ZnCl$_2$(N$_2$H$_4$) (top, red) obtained in an anthracene matrix and the predicted isotopic pattern (bottom, green). Monoisotopic mass for $C_{41}H_{67}N_7B_2Cl_2Zn$ – (N_2H_4 +Cl): Calculated 746.424; Found 746.300.

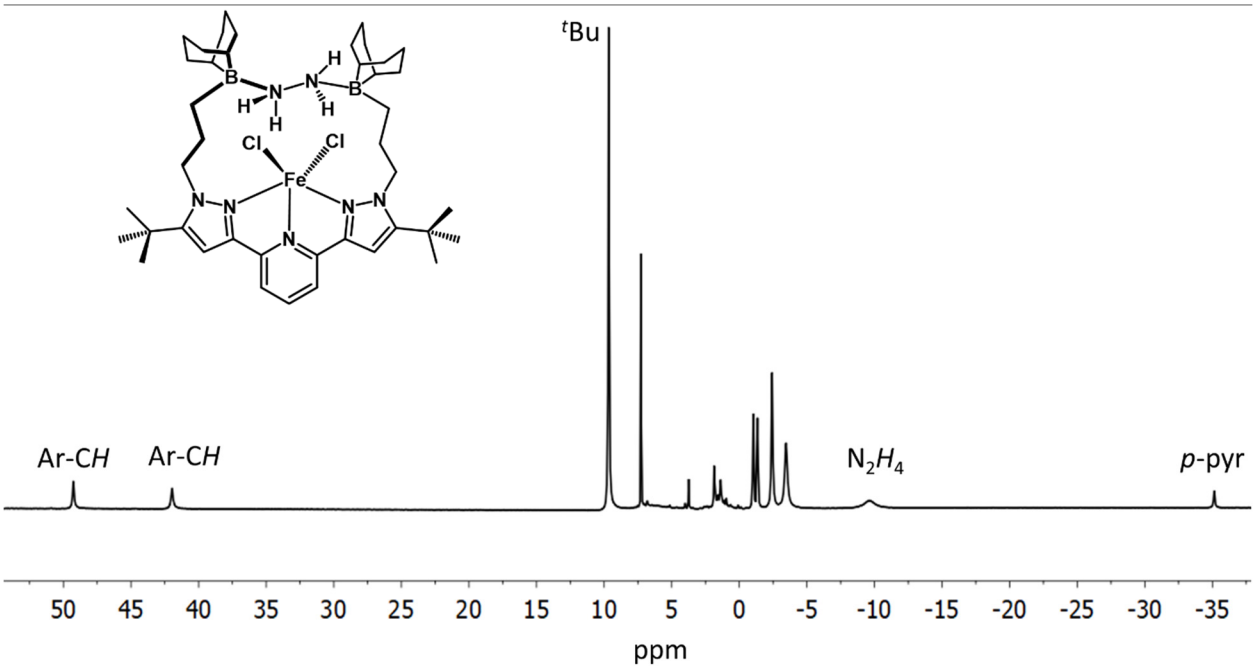

Figure S25 ^{1}H NMR spectrum ($CDCl_3$, 25 °C, 399.53 MHz) of (^{BBN}PDP^{tBu})FeCl$_2$(N$_2$H$_4$).

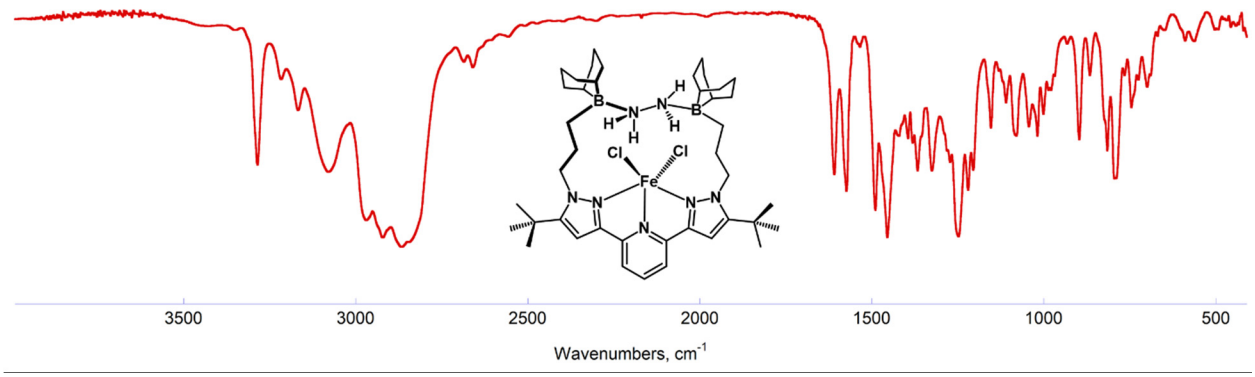

Figure S26 Infrared spectrum (KBr) of (^{BBN}PDP^{tBu})$FeCl_2(N_2H_4)$.

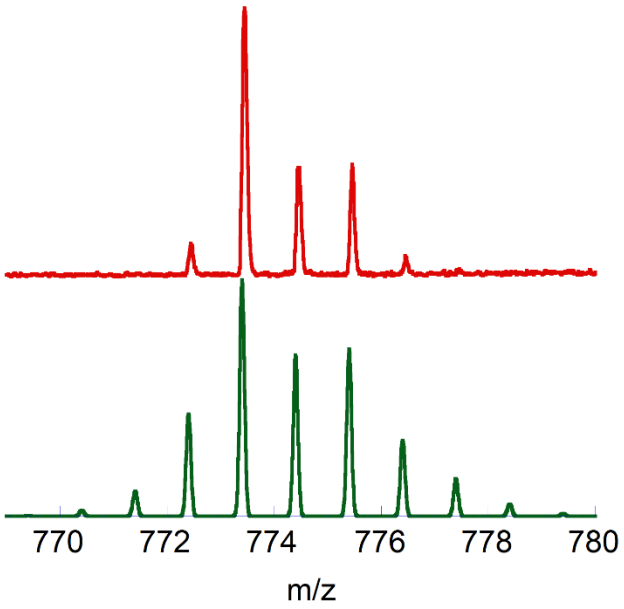

Figure S27 MALDI-TOF spectrum of (^{BBN}PDP^{tBu})$FeCl_2(N_2H_4)$ (top, red) obtained in an anthracene matrix and the predicted isotopic pattern (bottom, green). Monoisotopic mass for $C_{41}H_{67}N_7B_2Cl_2Fe - N_2H_4$: Calculated 773.399; Found 773.450.

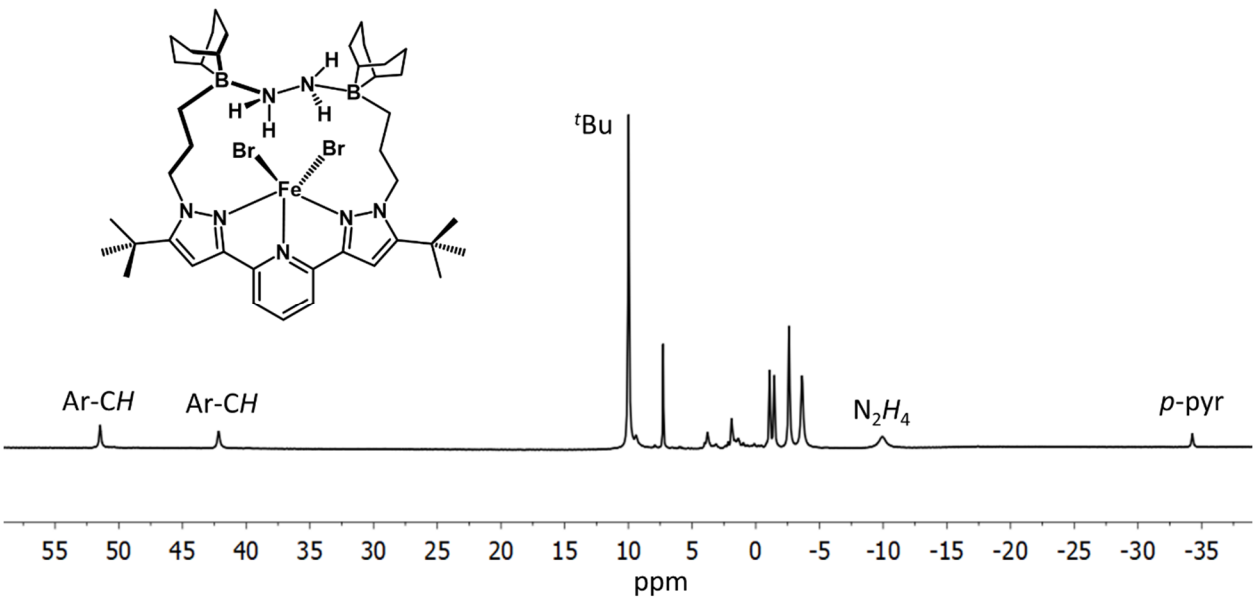

Figure S28 ^{1}H NMR spectrum ($CDCl_3$, 25 °C, 399.53 MHz) of ($^{BBN}PDP^{tBu}$)$FeBr_2(N_2H_4)$.

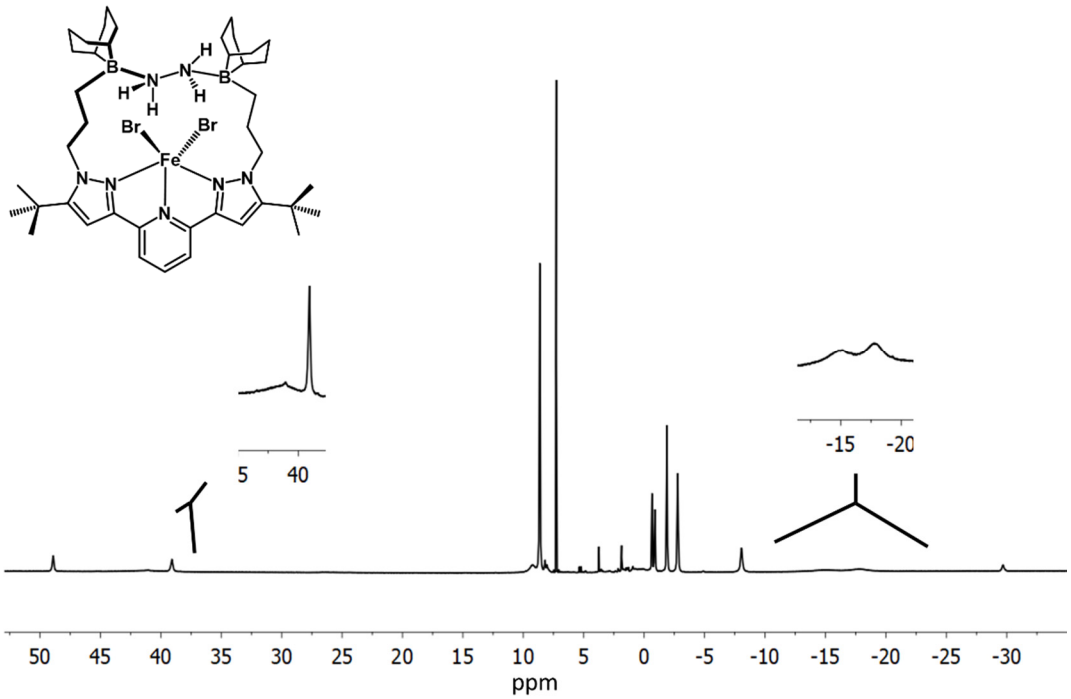

Figure S29 ^{1}H NMR spectrum ($CDCl_3$, 50 °C, 500.08 MHz) of ($^{BBN}PDP^{tBu}$)$FeBr_2(N_2H_4)$.

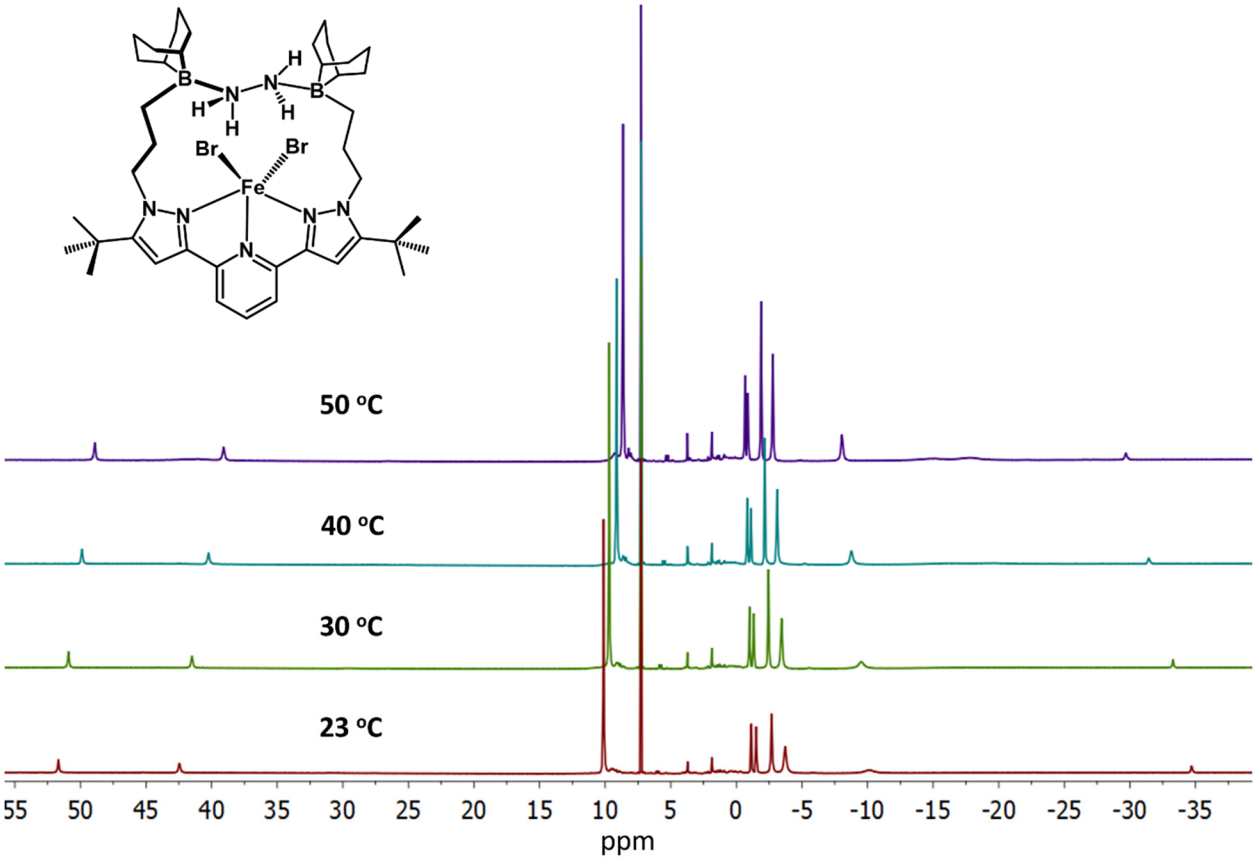

Figure S30 Variable temperature ^{1}H NMR spectrum ($CDCl_3$, 500.08 MHz) of ($^{BBN}PDP^{tBu}$)$FeBr_2(N_2H_4)$.

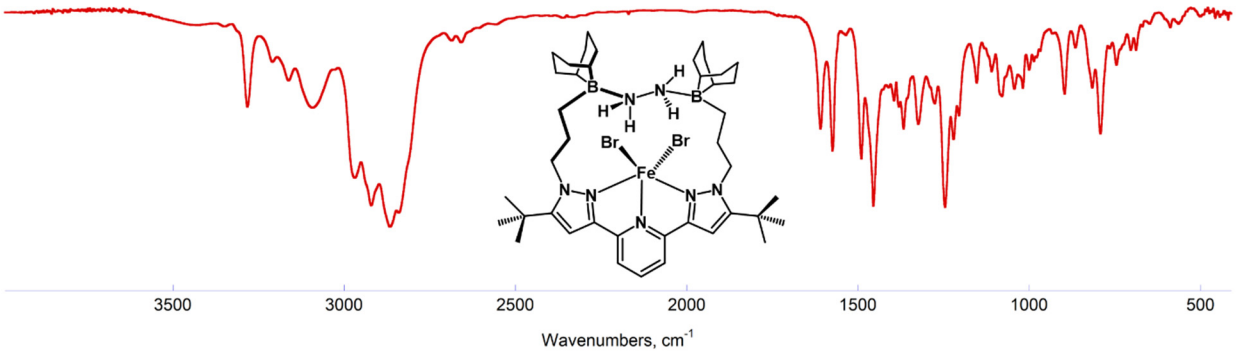

Figure S31 Infrared spectrum (KBr) of ($^{BBN}PDP^{tBu}$)$FeBr_2(N_2H_4)$.

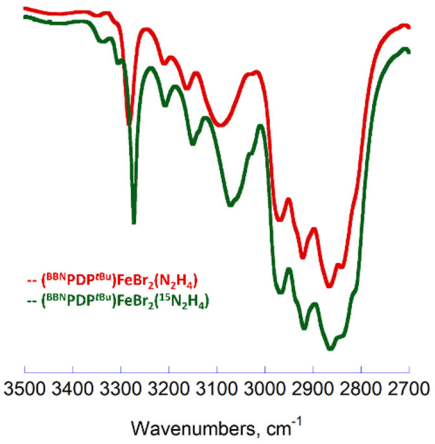

Figure S32 Overlay of N-H region of infrared spectrum (KBr) of (^{BBN}PDP^{tBu})FeBr$_2$(N$_2$H$_4$) (red) and (^{BBN}PDP^{tBu})FeBr$_2$(^{15}N$_2$H$_4$) (green)

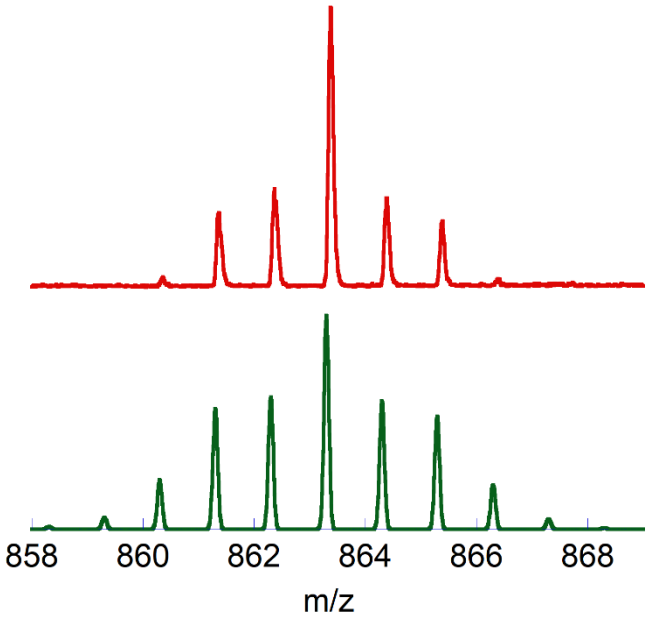

Figure S33 MALDI-TOF spectrum of (^{BBN}PDP^{tBu})FeBr$_2$(N$_2$H$_4$) (top, red) obtained in an anthracene matrix and the predicted isotopic pattern (bottom, green). Monoisotopic mass for $C_{41}H_{67}N_7B_2Br_2Fe$ – N_2H_4: Calculated 861.298; Found 861.299.

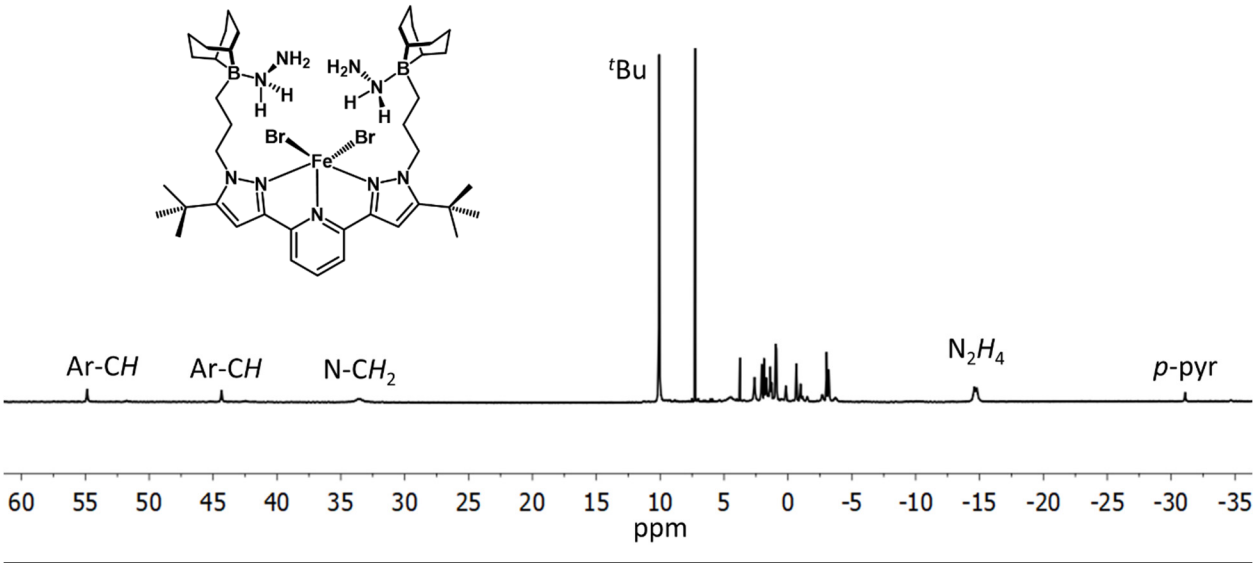

Figure S34 ^{1}H NMR spectrum ($CDCl_3$, 25 °C, 399.53 MHz) of ($^{BBN}PDP^{tBu}$)$FeBr_2(N_2H_4)_2$.

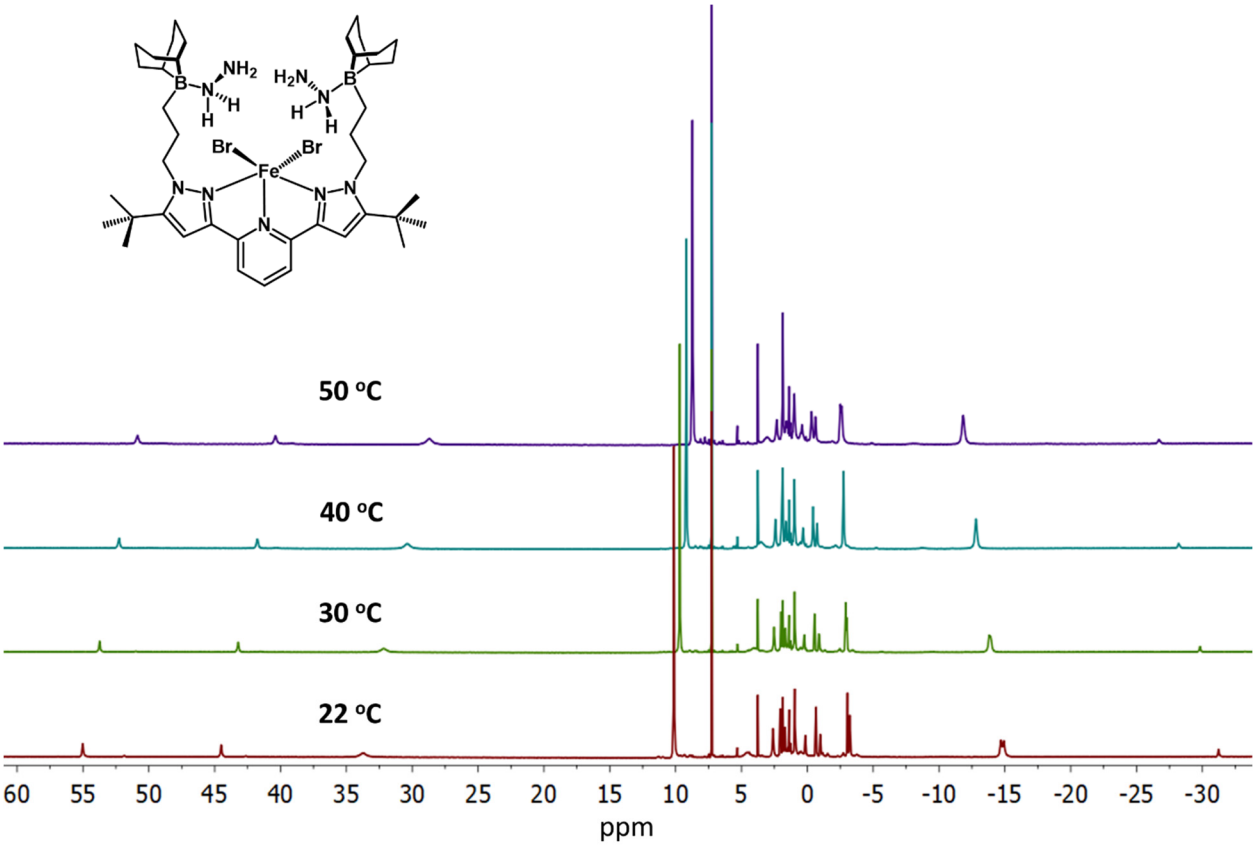

Figure S35 Variable temperature ^{1}H NMR spectrum ($CDCl_3$, 500.08 MHz) of ($^{BBN}PDP^{tBu}$)$FeBr_2(N_2H_4)_2$.

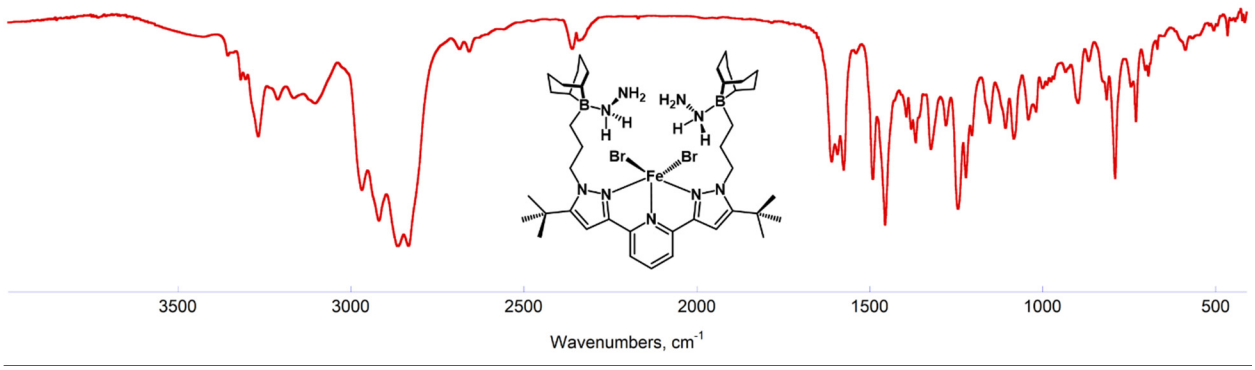

Figure S36 Infrared spectrum (KBr) of (^{BBN}PDP^{tBu})FeBr$_2$(N$_2$H$_4$)$_2$.

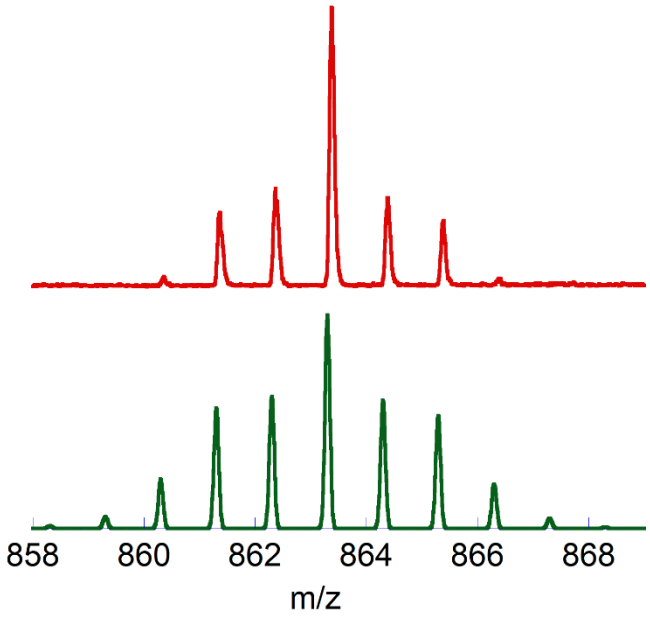

Figure S37 MALDI-TOF spectrum of (^{BBN}PDP^{tBu})FeBr$_2$(N$_2$H$_4$)$_2$ (top, red) obtained in an anthracene matrix and the predicted isotopic pattern (bottom, green). Monoisotopic mass for $C_{41}H_{71}N_9B_2Br_2Fe$ – $2N_2H_4$: Calculated 861.298; Found 861.366.

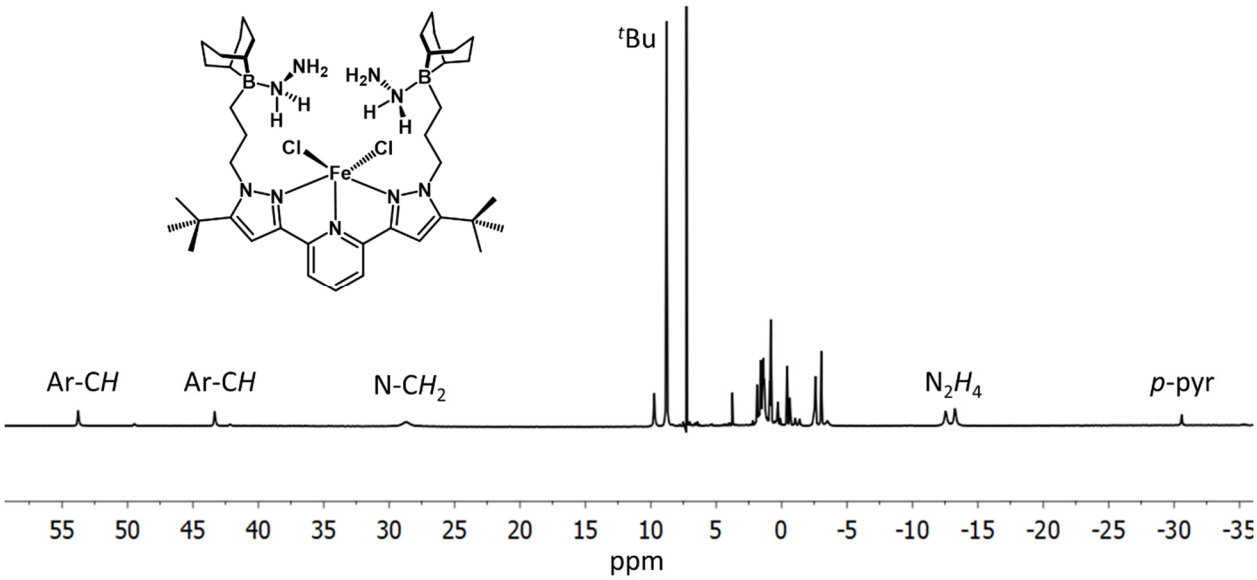

Figure S38 ^{1}H NMR spectrum ($CDCl_3$, 25 °C, 399.53 MHz) of ($^{BBN}PDP^{tBu}$)$FeCl_2(N_2H_4)_2$.

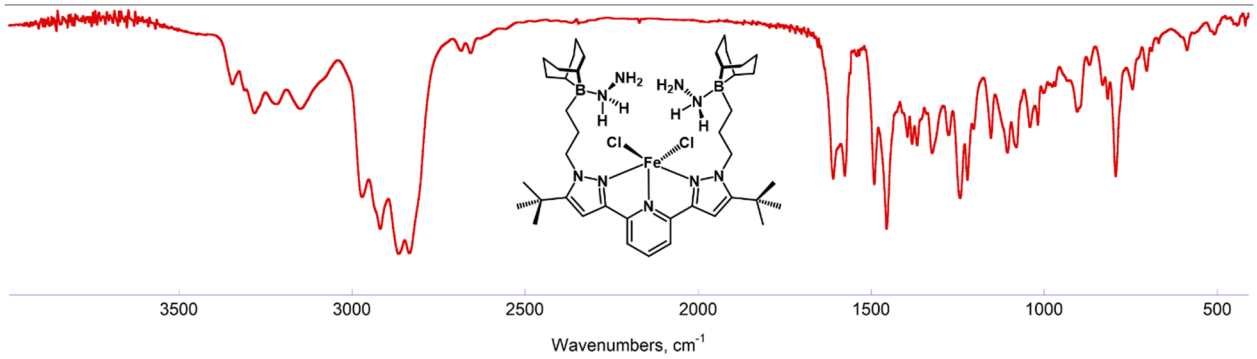

Figure S39 Infrared spectrum (KBr) of ($^{BBN}PDP^{tBu}$)$FeCl_2(N_2H_4)_2$.

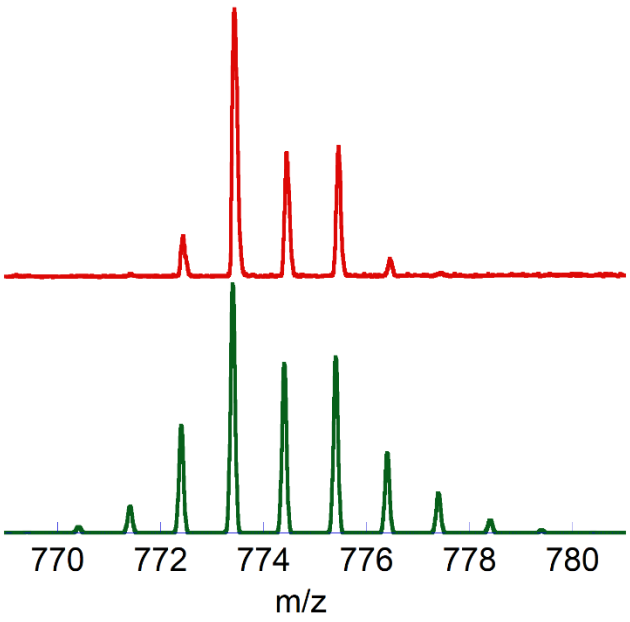

Figure S40 MALDI-TOF spectrum of (^{BBN}PDP^{tBu})FeCl$_2$(N$_2$H$_4$)$_2$ (top, red) obtained in an anthracene matrix and the predicted isotopic pattern (bottom, green). Monoisotopic mass for $C_{41}H_{71}N_9B_2Cl_2Fe$ – $2N_2H_4$: Calculated 773.399; Found 773.441.

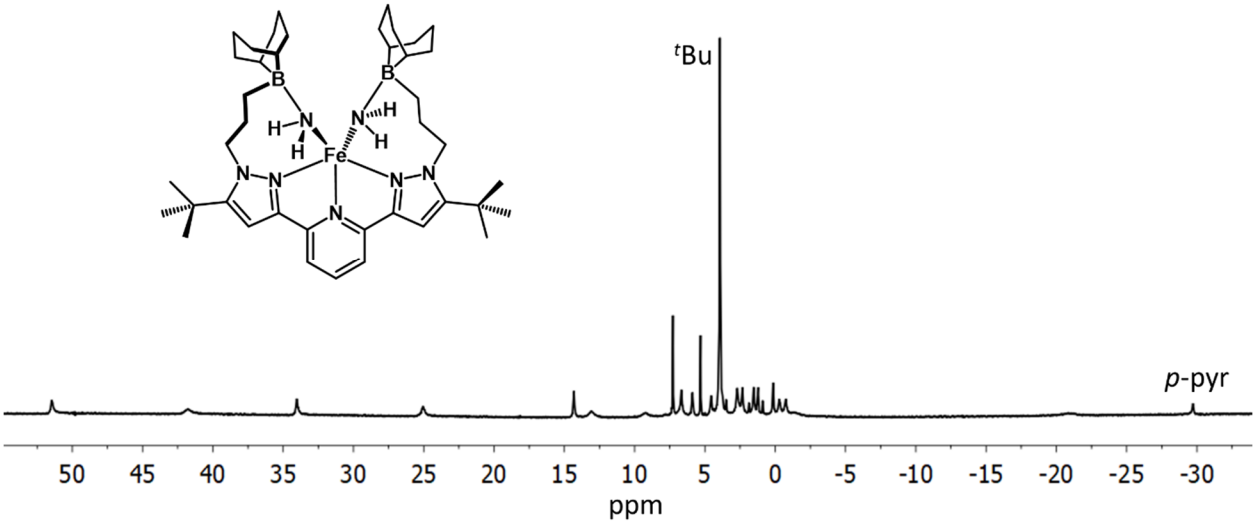

Figure S41 ^{1}H NMR spectrum ($CDCl_3$, 25 °C, 399.53 MHz) of (^{BBN}PDP^{tBu})Fe(NH$_2$)$_2$.

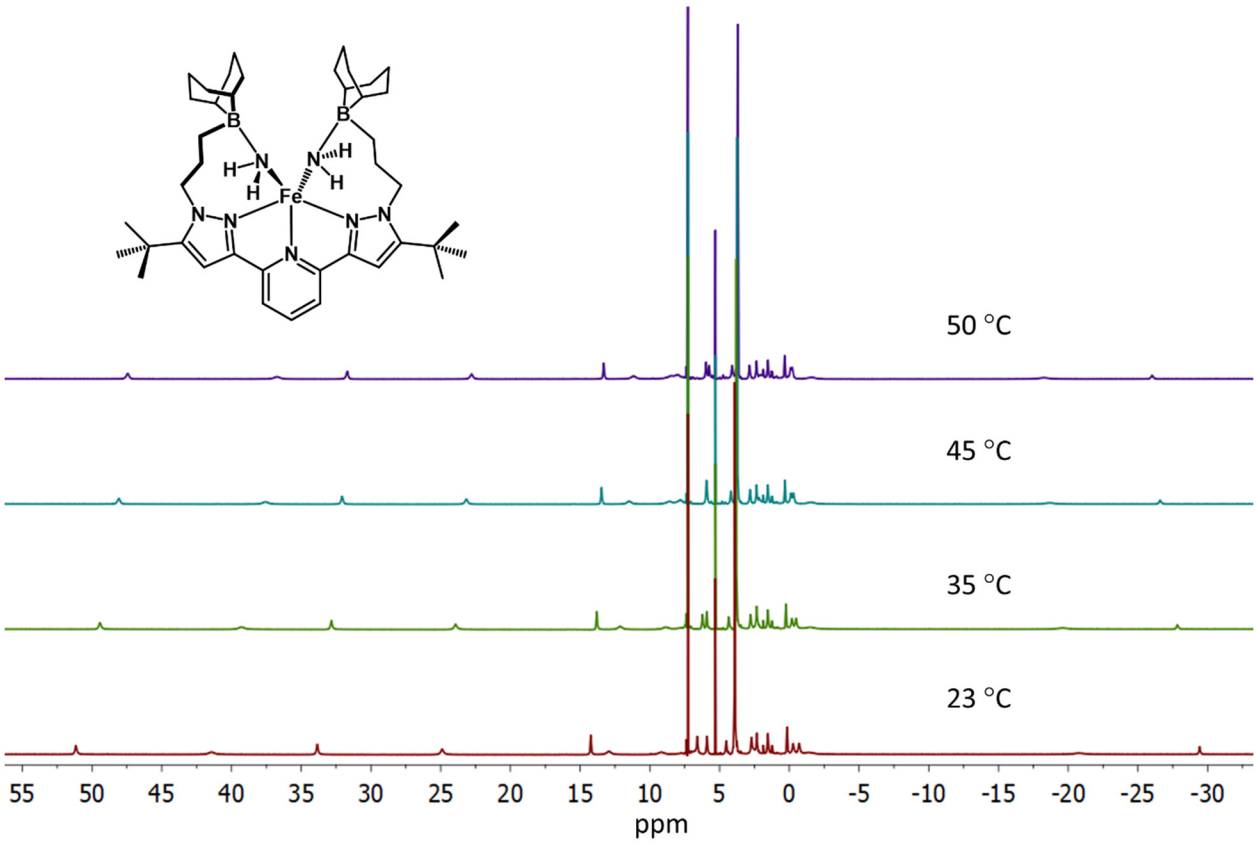

Figure S42 Variable temperature ^{1}H NMR spectrum ($CDCl_3$, 500.08 MHz) of ($^{BBN}PDP^{tBu}$)Fe(NH_2)$_2$.

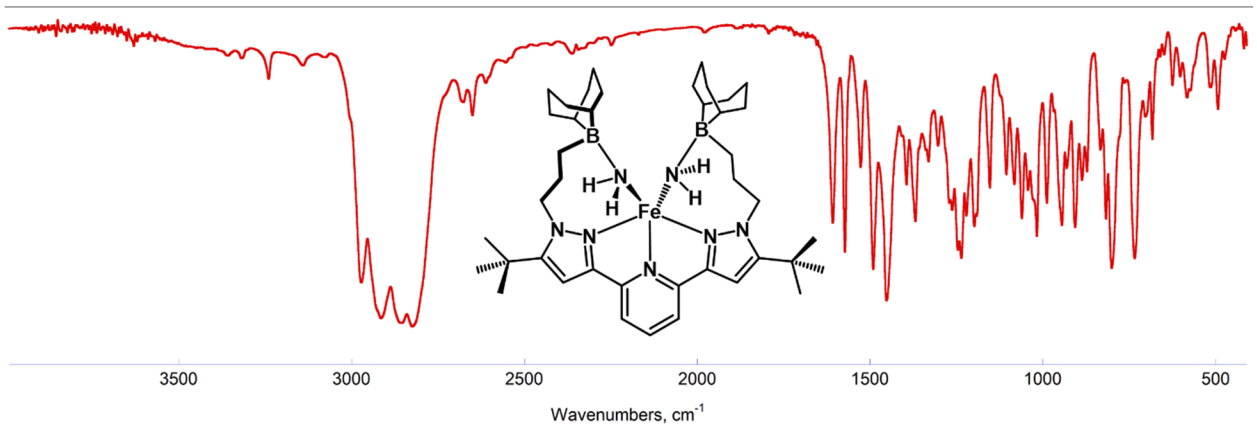

Figure S43 Infrared spectrum (KBr) of ($^{BBN}PDP^{tBu}$)Fe(NH_2)$_2$.

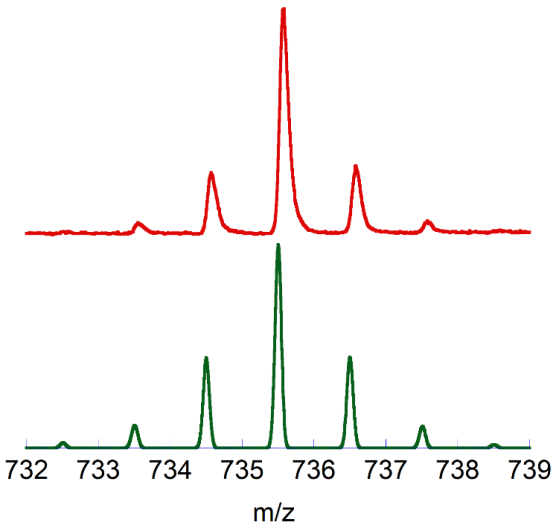

Figure S44 MALDI-TOF spectrum of (^{BBN}PDP^{tBu})Fe(NH_2)$_2$ (top, red) obtained in an anthracene matrix and the predicted isotopic pattern (bottom, green). Monoisotopic mass for $C_{41}H_{67}N_7B_2Fe$: Calculated 735.499; Found 735.573.

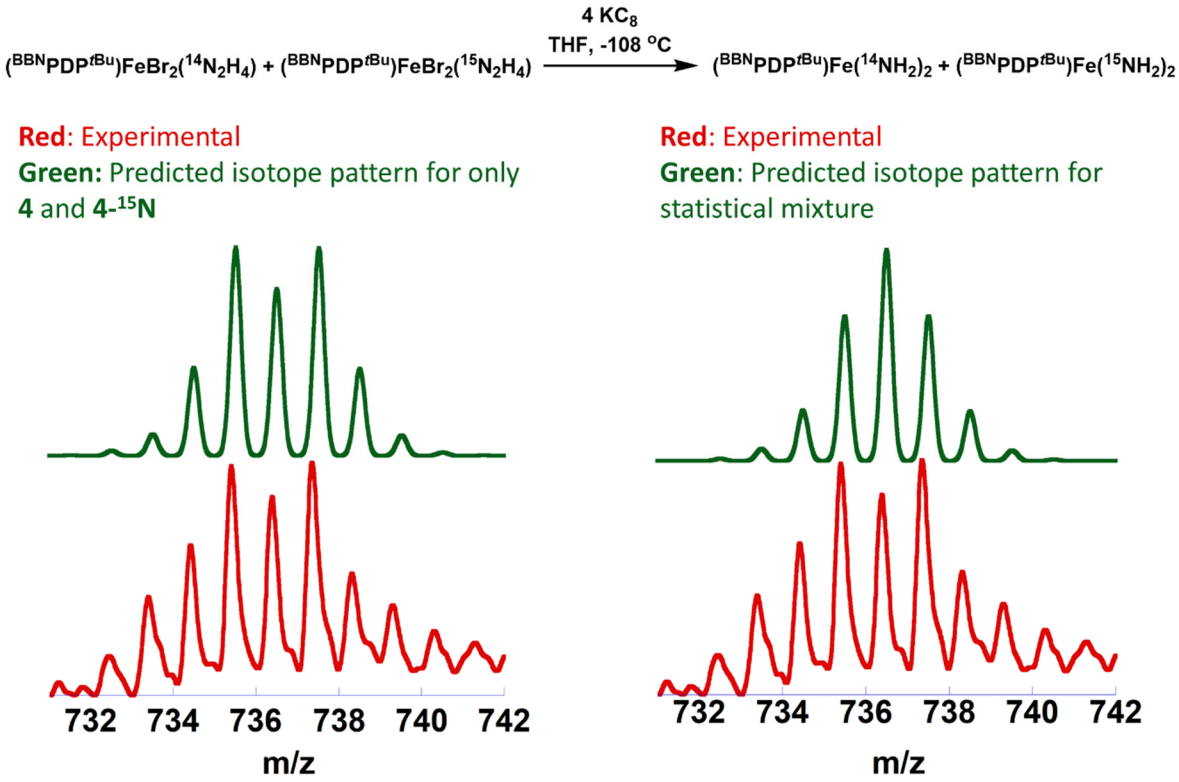

Figure S45 Top: Crossover experiment. Bottom left: MALDI-TOF spectrum of crude reaction mixture (bottom, red) obtained in an anthracene matrix and the predicted isotopic pattern for formation of only (^{BBN}PDP^{tBu})Fe($^{14}NH_2$)$_2$ and (^{BBN}PDP^{tBu})Fe($^{15}NH_2$)$_2$ (top, green). Bottom right: MALDI-TOF spectrum of crude reaction mixture (bottom, red) and the predicted isotopic pattern for formation of a statistical mixture of (^{BBN}PDP^{tBu})Fe($^{14}NH_2$)$_2$, (^{BBN}PDP^{tBu})Fe($^{14}NH_2$)($^{15}NH_2$), and (^{BBN}PDP^{tBu})Fe($^{15}NH_2$)$_2$ (top, green).

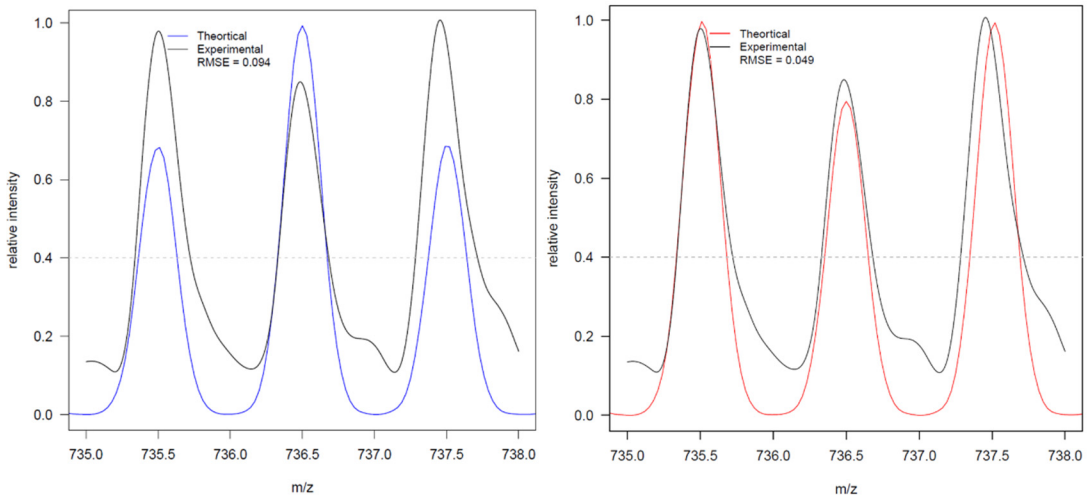

Figure S46 Statistical fitting of experimental MALDI-TOF data with theoretical spectra. Left: comparison of experimental (black) vs. theoretical statistical mixture (blue) of (^{BBN}PDP^{tBu})Fe($^{14}NH_2$)$_2$, (^{BBN}PDP^{tBu})Fe($^{14}NH_2$)($^{15}NH_2$), and (^{BBN}PDP^{tBu})Fe($^{15}NH_2$)$_2$. Root-mean-square error = 0.094. Right: comparison of experimental (black) vs. theoretical (red) formation of only (^{BBN}PDP^{tBu})Fe($^{14}NH_2$)$_2$ and (^{BBN}PDP^{tBu})Fe($^{15}NH_2$)$_2$. Root-mean-square error = 0.049. Statistical modeling was obtained by taking into account only the three largest peaks with a threshold (denoted by dashed line in figure) applied to remove baseline deviation.

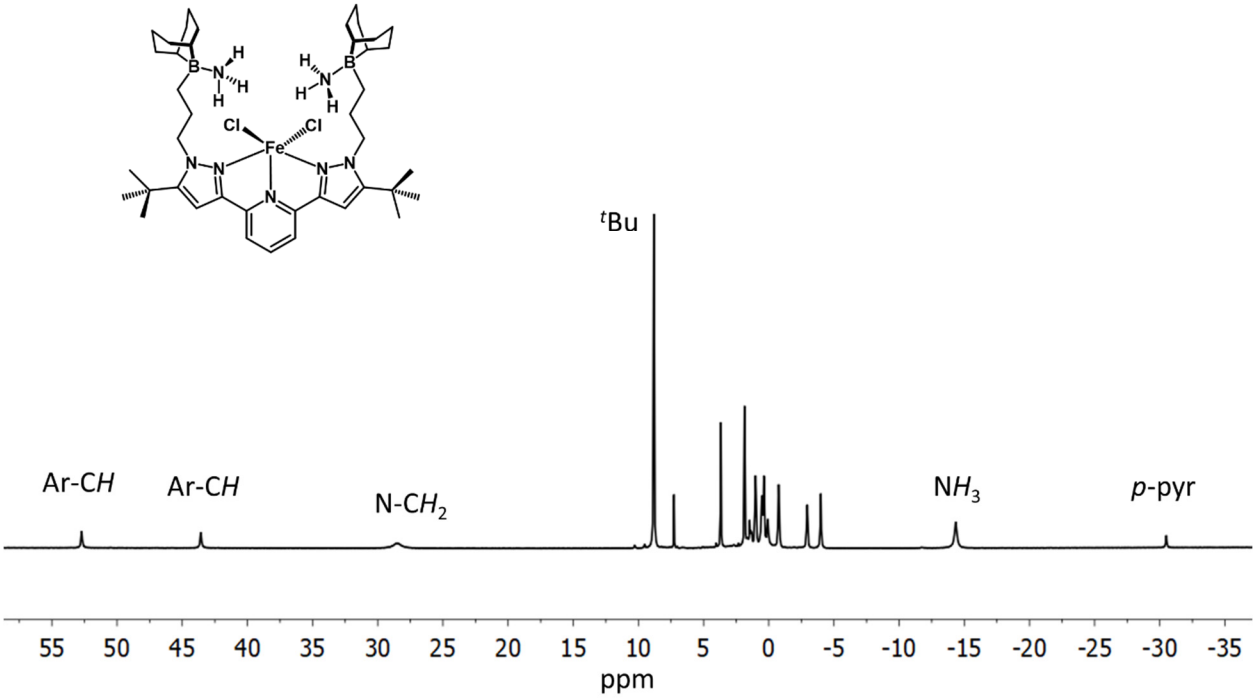

Figure S47 ^{1}H NMR spectrum ($CDCl_3$, 25 °C, 399.53 MHz) of (^{BBN}PDP^{tBu})$FeCl_2(NH_3)_2$.

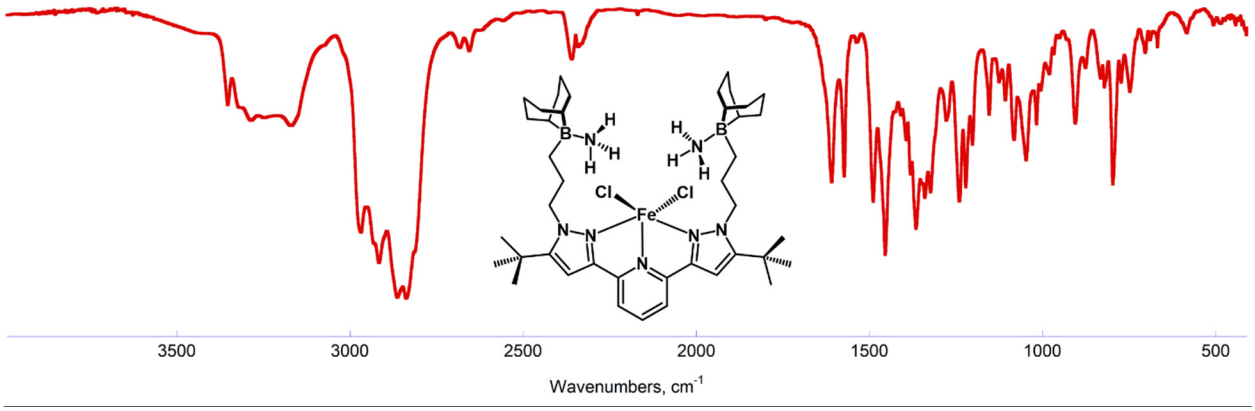

Figure S48 Infrared spectrum (KBr) of (^{BBN}PDP^{tBu})FeCl$_2$(NH$_3$)$_2$.

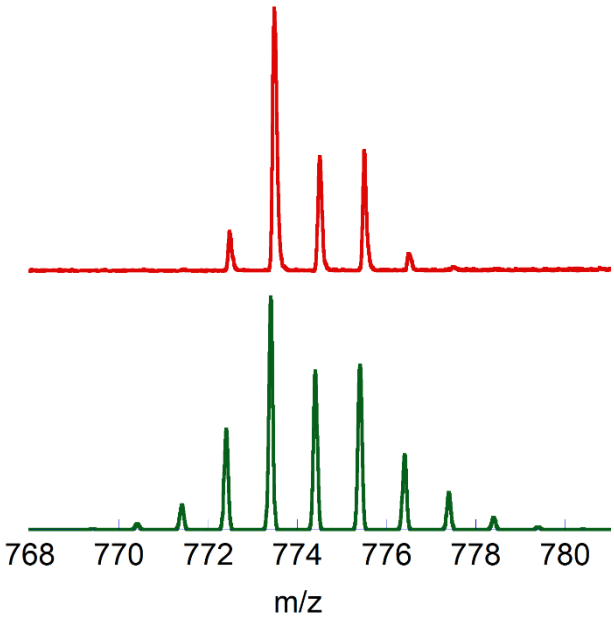

Figure S49 MALDI-TOF spectrum of (^{BBN}PDP^{tBu})FeCl$_2$(NH$_3$)$_2$ (top, red) obtained in an anthracene matrix and the predicted isotopic pattern (bottom, green). Monoisotopic mass for $C_{41}H_{69}N_7B_2Cl_2Fe$ - 2(NH$_3$): Calculated 773.399; Found 773.487.

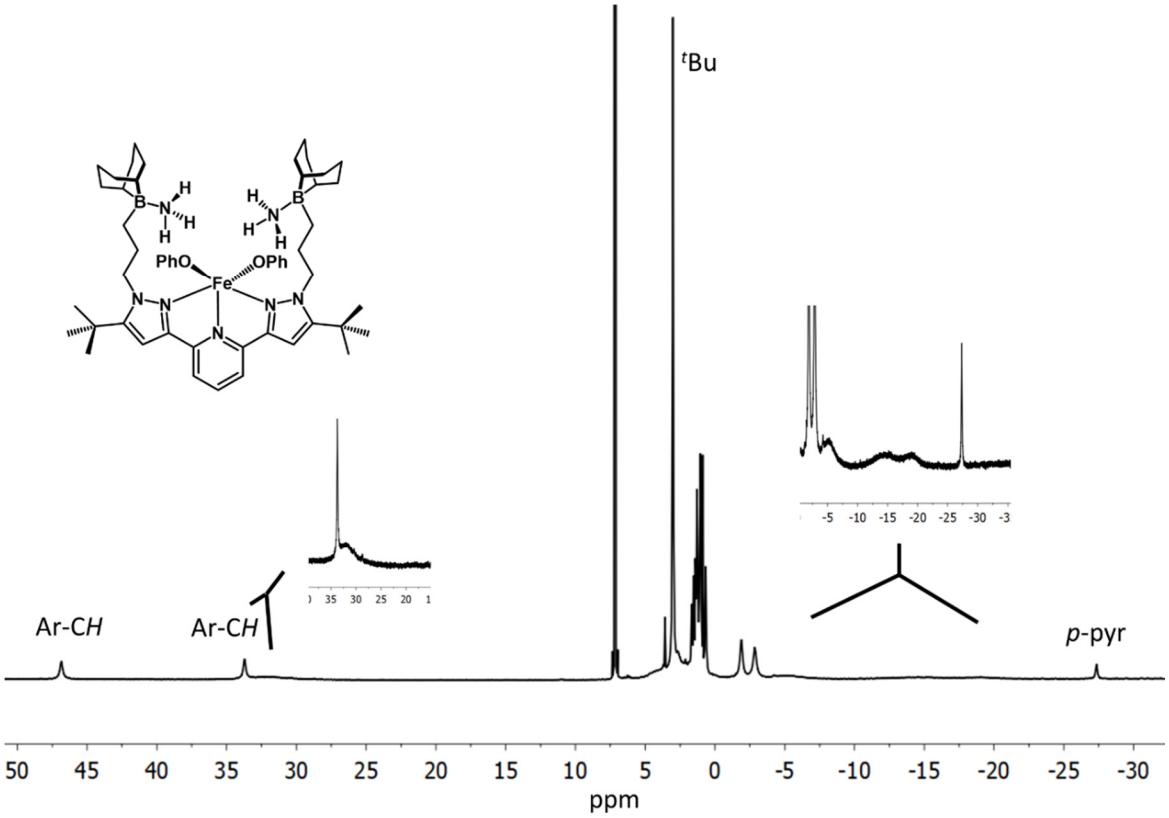

Figure S50 ^{1}H NMR spectrum (C_6D_6, 25 °C, 399.53 MHz) of (^{BBN}PDP^{tBu})Fe(OPh)$_2$(NH_3)$_2$.

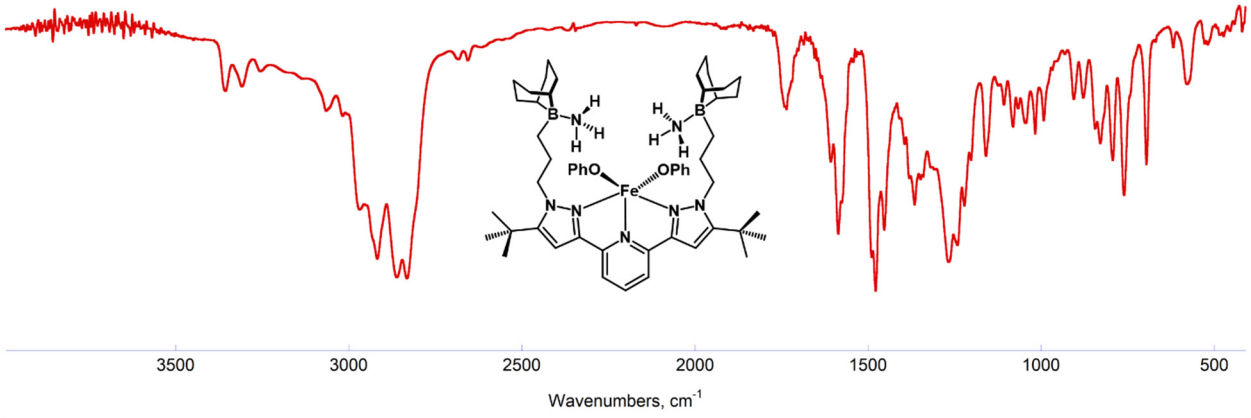

Figure S51 Infrared spectrum (KBr) of (^{BBN}PDP^{tBu})Fe(OPh)$_2$(NH_3)$_2$.

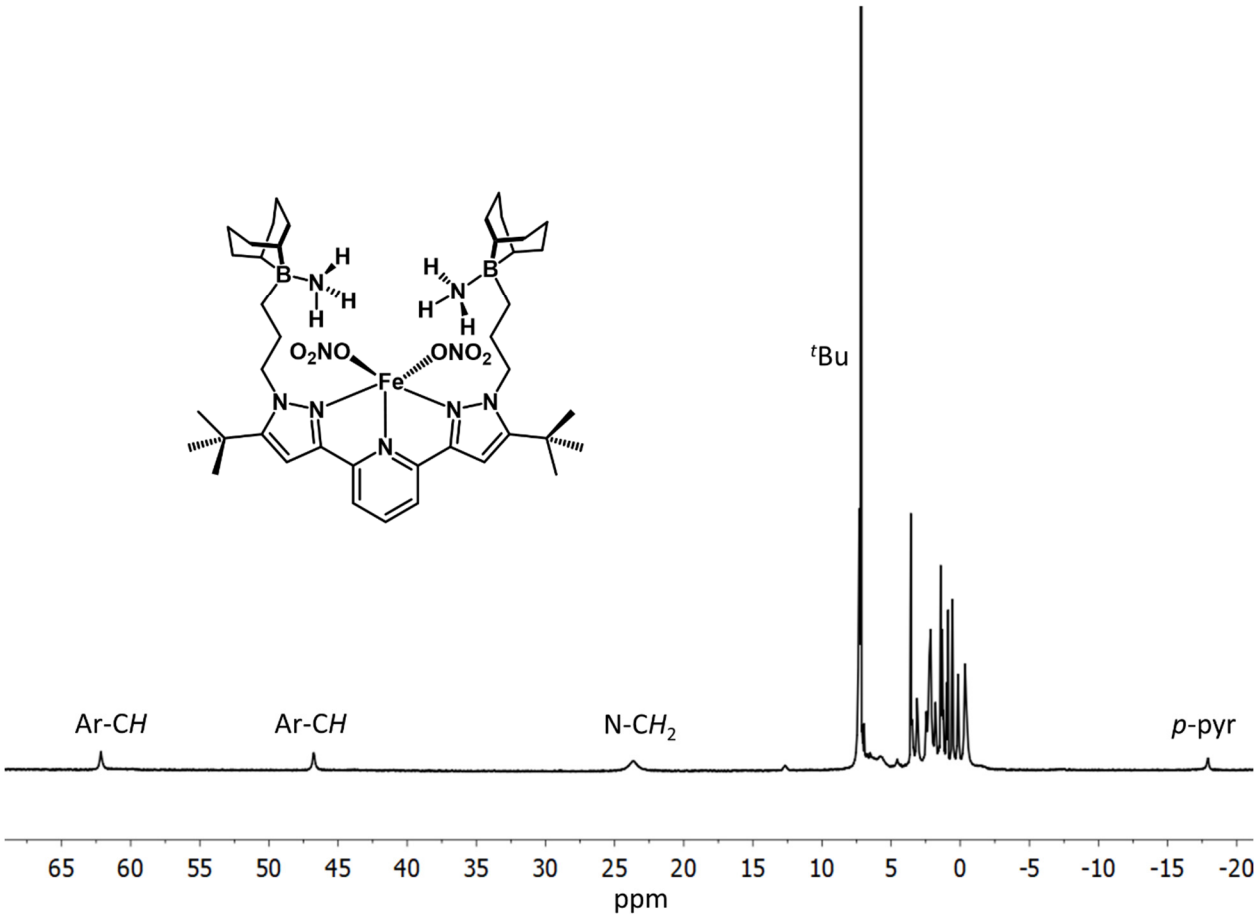

Figure S52 ^{1}H NMR spectrum (C_6D_6, 25 °C, 399.53 MHz) of (^{BBN}PDP^{tBu})Fe(ONO_2)$_2$(NH_3)$_2$.

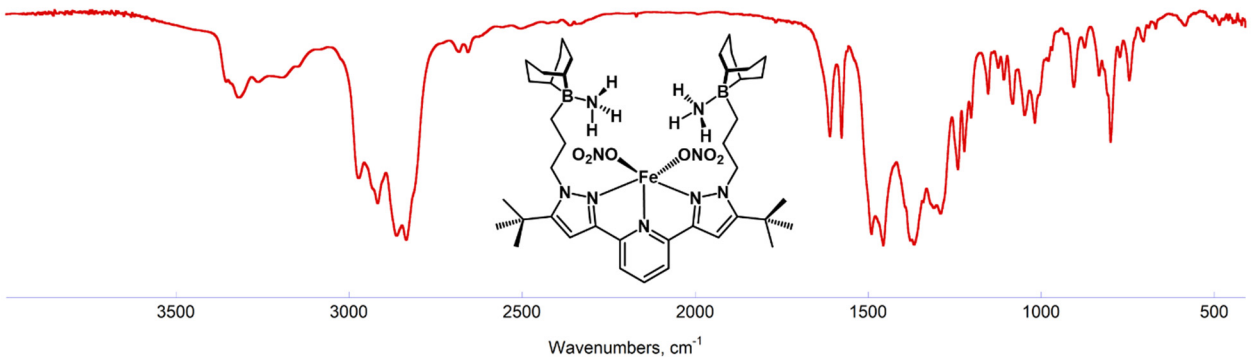

Figure S53 Infrared spectrum (KBr) of (^{BBN}PDP^{tBu})Fe(ONO_2)$_2$(NH_3)$_2$.

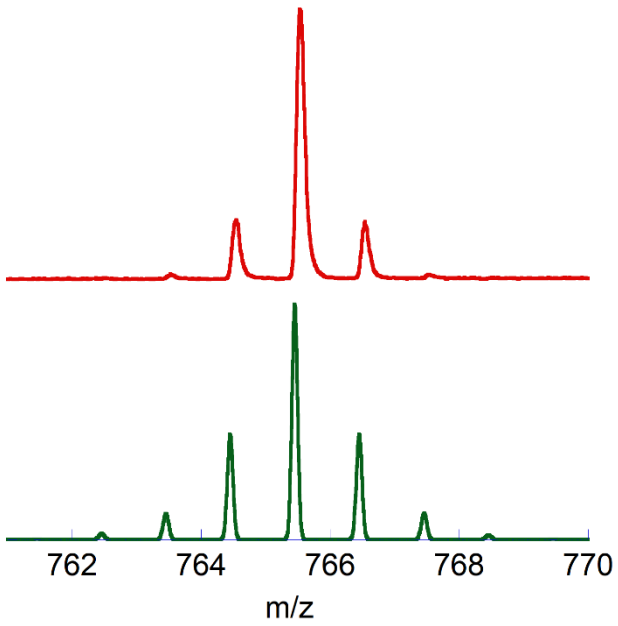

Figure S54 MALDI-TOF spectrum of (^{BBN}PDP^{tBu})Fe(ONO$_2$)$_2$(NH$_3$)$_2$ (top, red) obtained in an anthracene matrix and the predicted isotopic pattern (bottom, green). Monoisotopic mass for $C_{41}H_{69}N_9B_2O_6Fe$ - 2(NH$_3$) - NO$_3$: Calculated 765.449; Found 765.535.

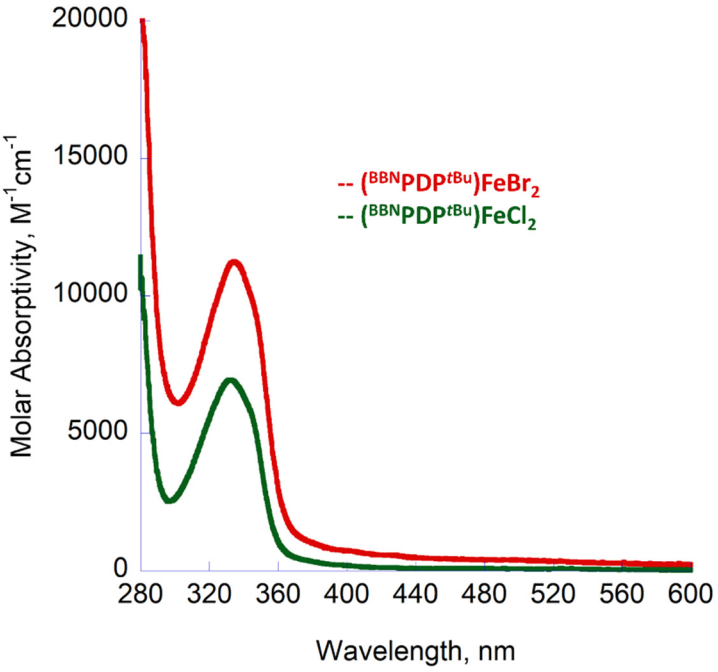

Figure S55 Electronic absorption spectra (C_6H_6, ambient temperature) of (^{BBN}PDP^{tBu})FeBr$_2$ (red) and (^{BBN}PDP^{tBu})FeCl$_2$ (green).

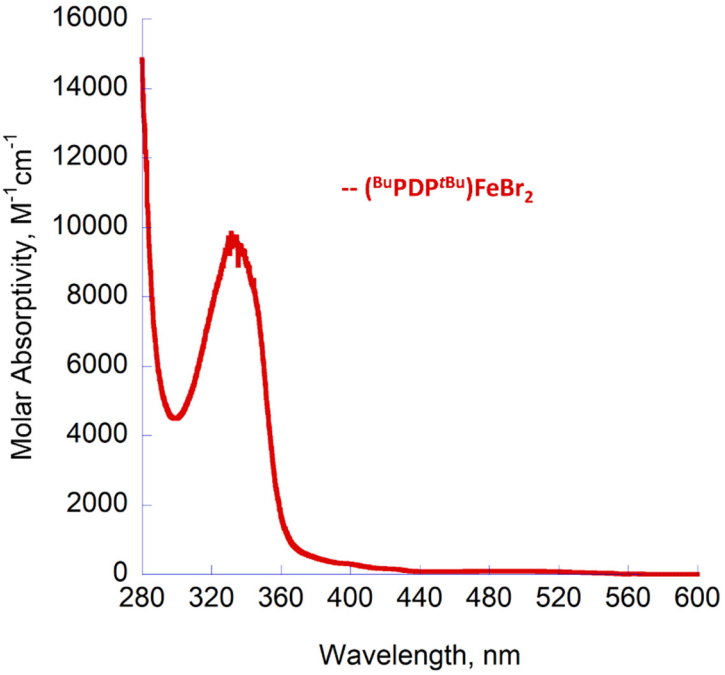

Figure S56 Electronic absorption spectrum (THF, ambient temperature) of (^{Bu}PDP^{tBu})FeBr$_2$.

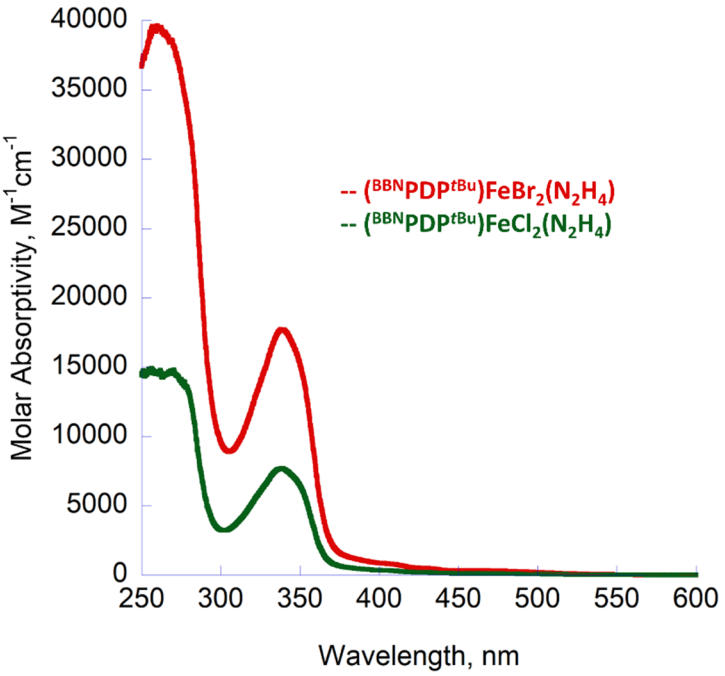

Figure S57 Electronic absorption spectra (THF, ambient temperature) of (^{BBN}PDP^{tBu})FeBr$_2$(N$_2$H$_4$) (red) and (^{BBN}PDP^{tBu})FeCl$_2$(N$_2$H$_4$) (green).

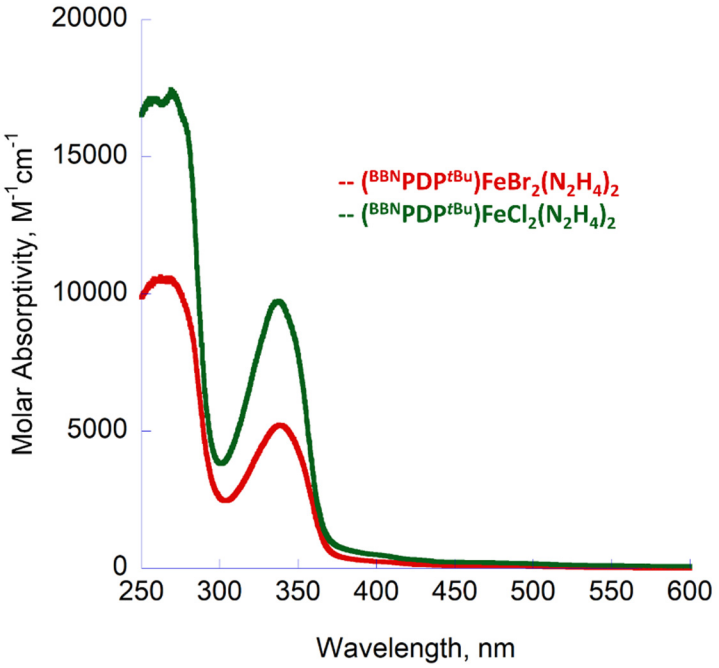

Figure S58 Electronic absorption spectra (THF, ambient temperature) of (^{BBN}PDP^{tBu})FeBr$_2$(N$_2$H$_4$)$_2$ (red) and (^{BBN}PDP^{tBu})FeCl$_2$(N$_2$H$_4$)$_2$ (green).

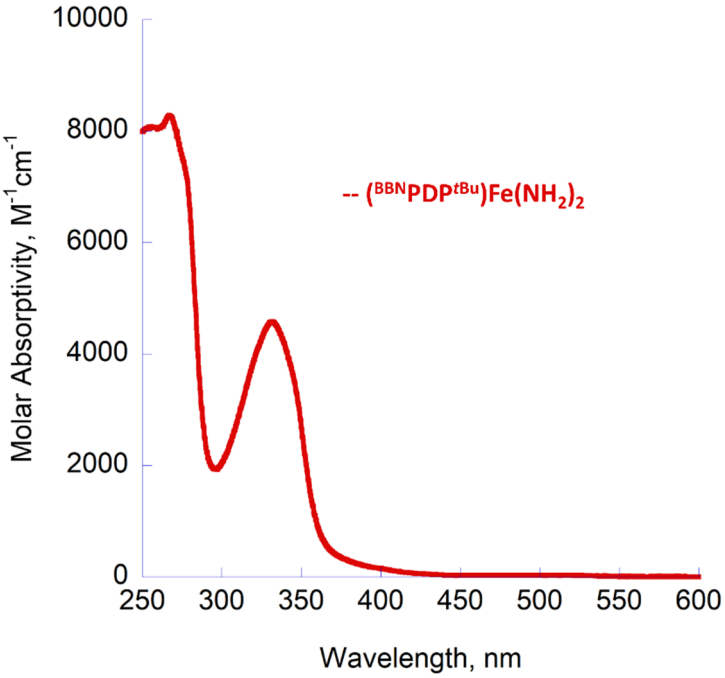

Figure S59 Electronic absorption spectra (THF, ambient temperature) of (^{BBN}PDP^{tBu})Fe(NH$_2$)$_2$.

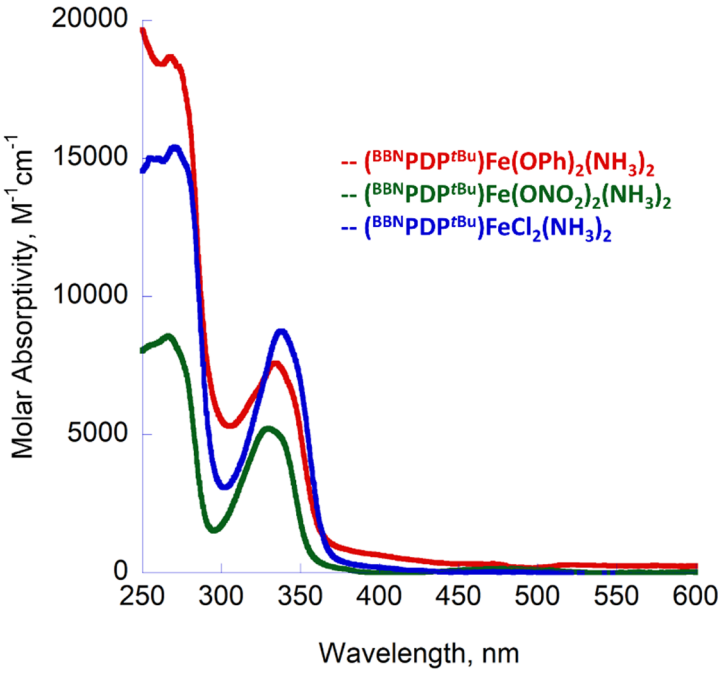

Figure S60 Electronic absorption spectra (THF, ambient temperature) of ($^{BBN}PDP^{tBu}$)$Fe(OPh)_2(NH_3)_2$ (red), ($^{BBN}PDP^{tBu}$)$Fe(ONO_2)_2(NH_3)_2$ (green), and ($^{BBN}PDP^{tBu}$)$FeCl_2(NH_3)_2$ (blue).

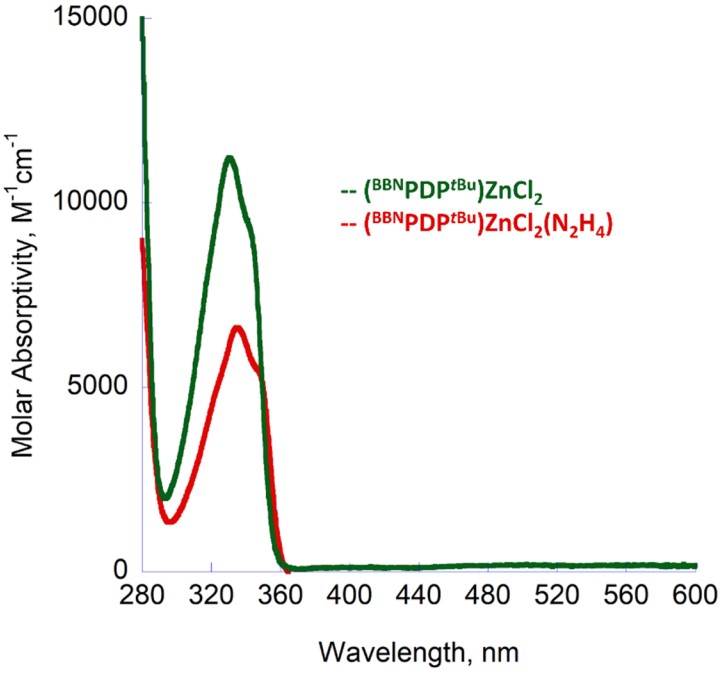

Figure S61 Electronic absorption spectra (ambient temperature) of ($^{BBN}PDP^{tBu}$)$ZnCl_2$ (green, THF) and ($^{BBN}PDP^{tBu}$)$ZnCl_2(N_2H_4)$ (red).

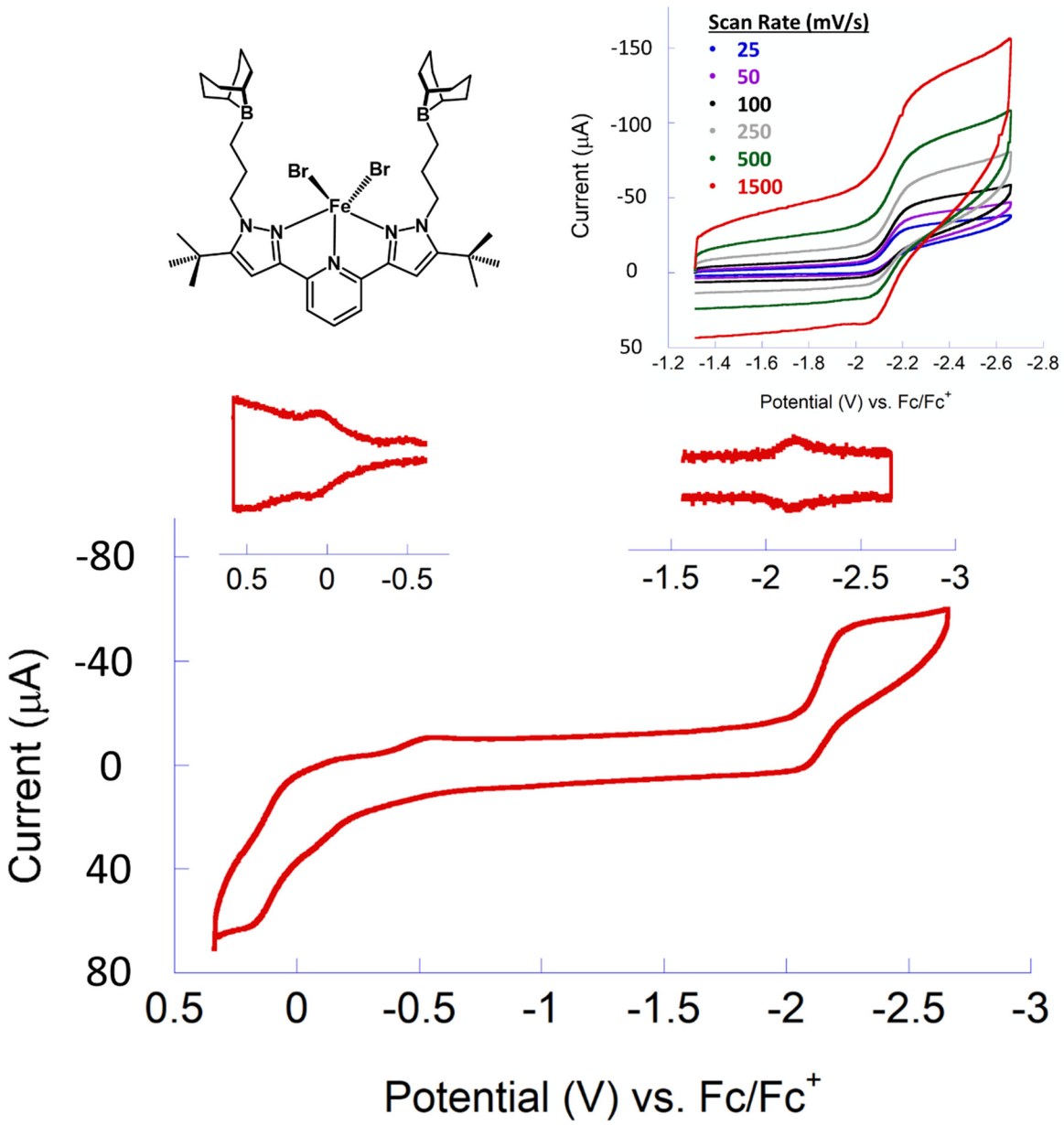

Figure S62 Cyclic Voltammogram (100 mV/s) of (^{BBN}PDP^{tBu})FeBr$_2$ (2.32 mmol) recorded in THF with 0.2 M [Bu$_4$N][PF$_6$] at ambient temperature. Insets display the square wave voltammograms of the oxidative (left) and reductive (right) portion as well as scan rate dependence of the reductive wave. Square wave parameters: amplitude = 20 mV; period = 0.02 seconds; increment = 2 mV; sampling width = 0.001 seconds.

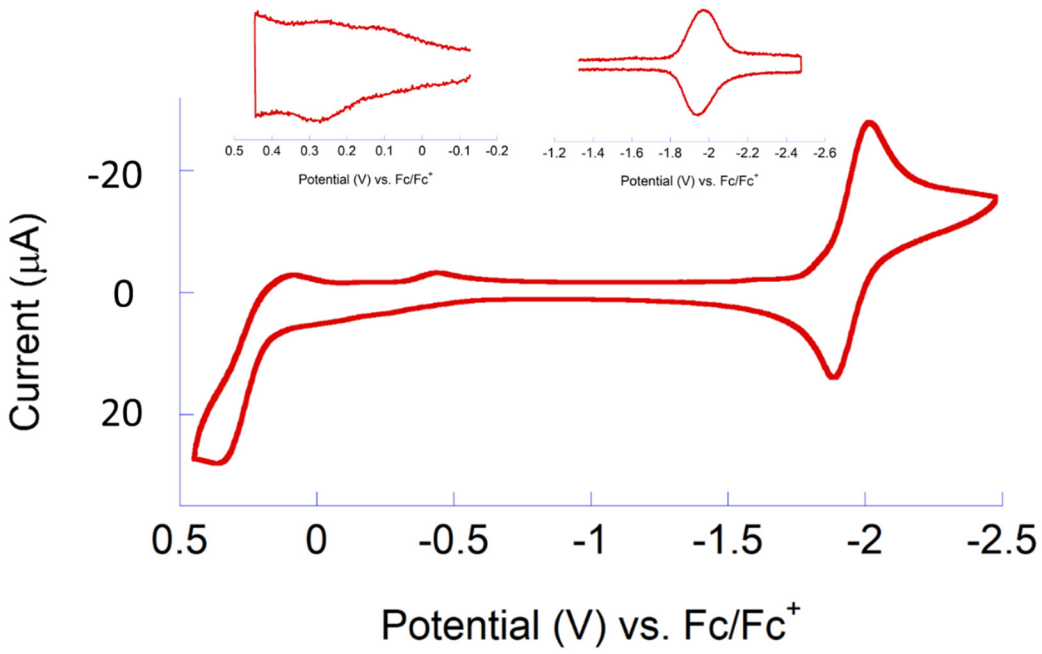

Figure S63 Cyclic Voltammogram (100 mV/s) of (^{BBN}PDP^{tBu})FeBr$_2$(N_2H_4) (2.23 mmol) recorded in THF with 0.2 M [Bu_4N][PF_6] at ambient temperature. Insets display the square wave voltammograms of the oxidative (left) and reductive (right) portion. Square wave parameters: amplitude = 20 mV; period = 0.02 seconds; increment = 2 mV; sampling width = 0.001 seconds.

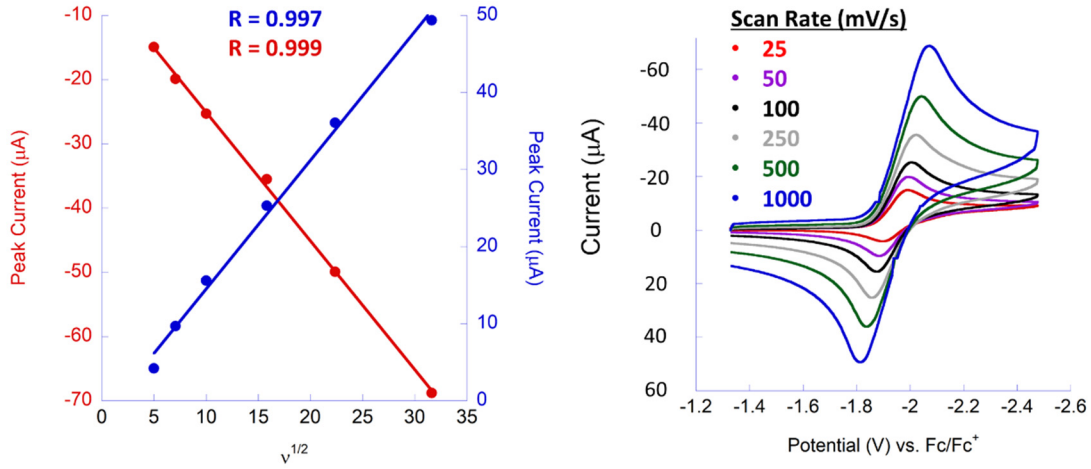

Figure S64 Scan rate dependence of the reductive wave of **2-Br** (2.23 mmol) recorded in THF with 0.2 M [Bu_4N][PF_6] at ambient temperature.

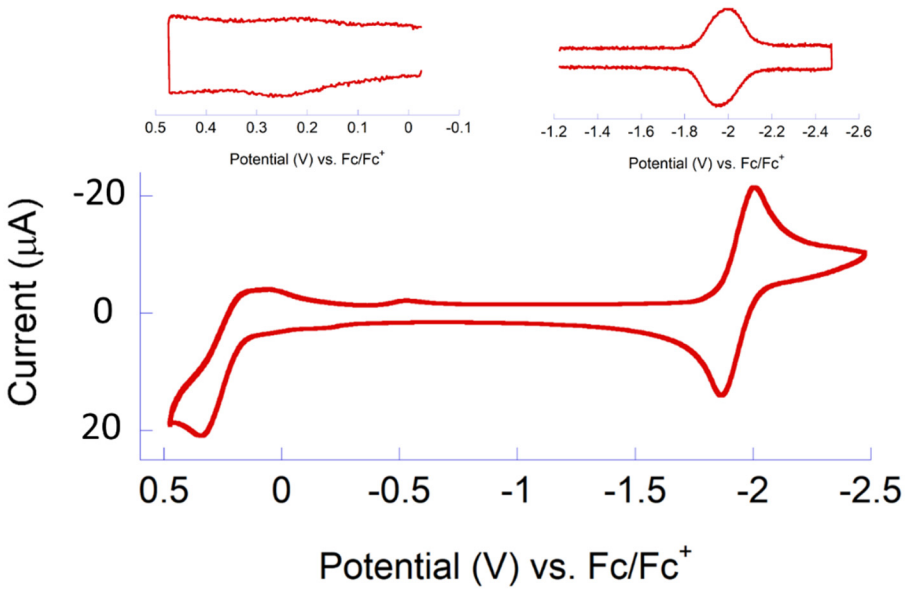

Figure S65 Cyclic Voltammogram (100 mV/s) of (^{BBN}PDP^{tBu})$FeCl_2(N_2H_4)$ (2.48 mmol) recorded in THF with 0.2 M [Bu_4N][PF_6] at ambient temperature. Insets display the square wave voltammograms of the oxidative (left) and reductive (right) portion. Square wave parameters: amplitude = 20 mV; period = 0.02 seconds; increment = 2 mV; sampling width = 0.001 seconds.

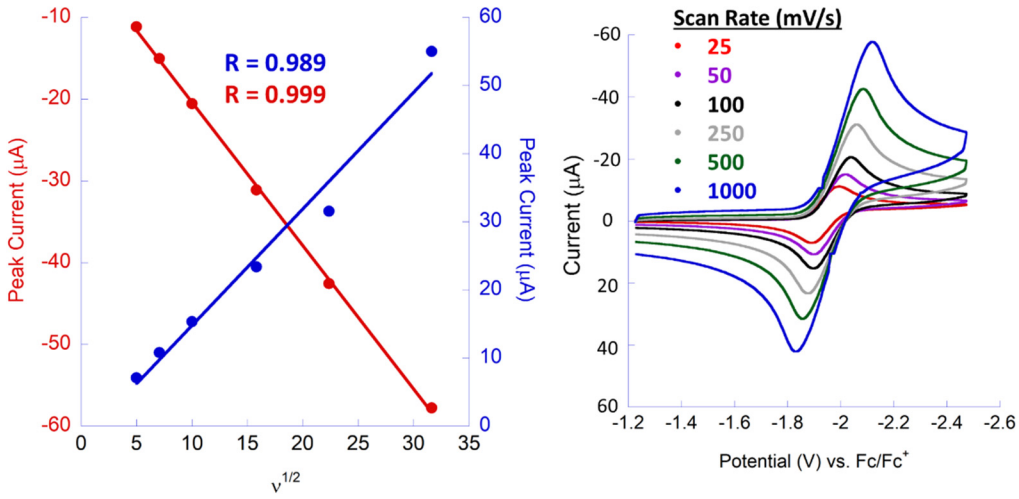

Figure S66 Scan rate dependence of the reductive wave of **2-Cl** (2.48 mmol) recorded in THF with 0.2 M [Bu_4N][PF_6] at ambient temperature.

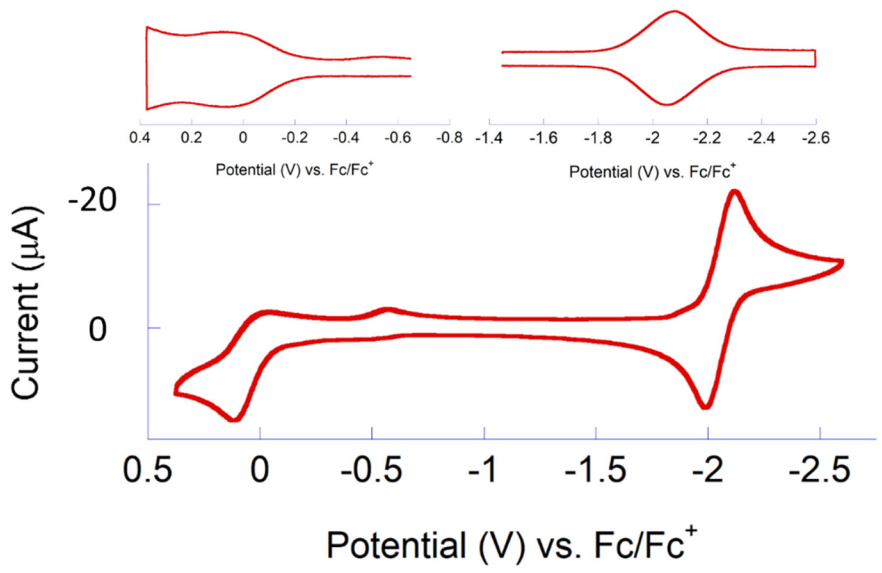

Figure S67 Cyclic Voltammogram (100 mV/s) of (^{BBN}PDP^{tBu})$FeCl_2$ (2.58 mmol) recorded in THF with 0.2 M $[Bu_4N][PF_6]$ at ambient temperature. Insets display the square wave voltammograms of the oxidative (left) and reductive (right) portion. Square wave parameters: amplitude = 160 mV; period = 0.02 seconds; increment = 2 mV; sampling width = 0.001 seconds.

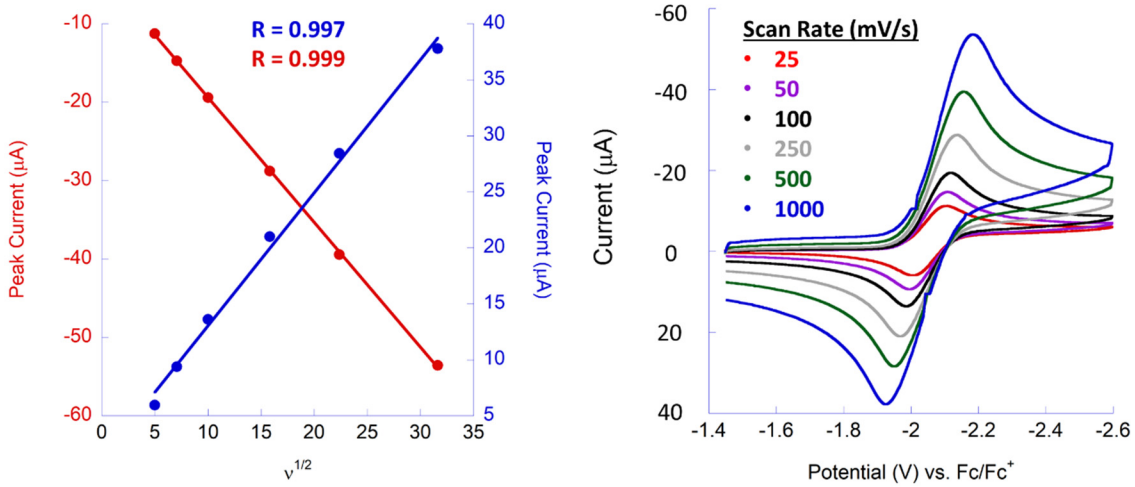

Figure S68 Scan rate dependence of the reductive wave of **1-Cl** (2.58 mmol) recorded in THF with 0.2 M $[Bu_4N][PF_6]$ at ambient temperature.

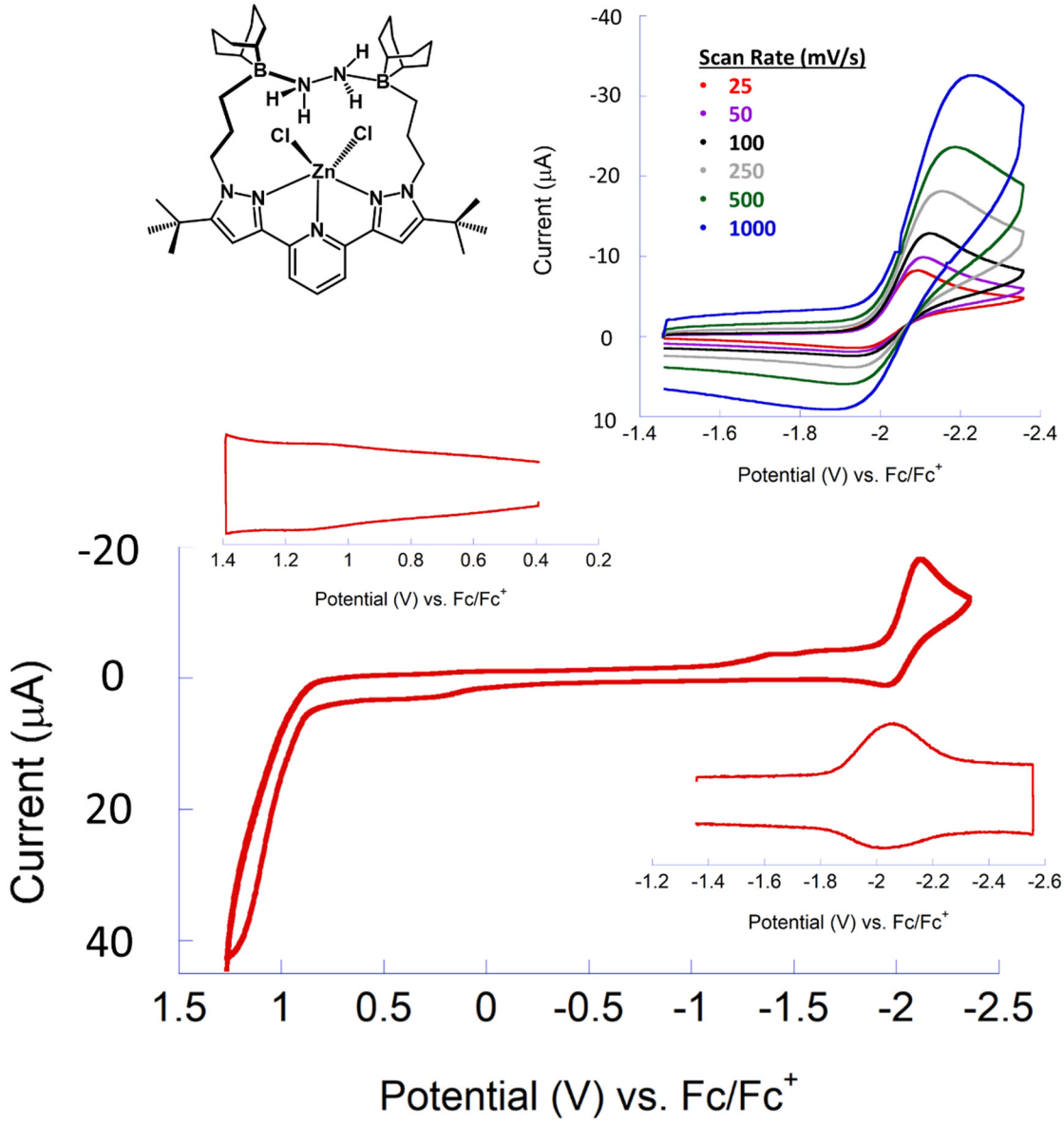

Figure S69 Cyclic Voltammogram (100 mV/s) of (^{BBN}PDP^{tBu})$ZnCl_2(N_2H_4)$ (2.45 mmol) recorded in THF with 0.2 M $[Bu_4N][PF_6]$ at ambient temperature. Insets display the square wave voltammograms of the oxidative (left) and reductive (right) portion as well as scan rate dependence of the reductive wave. Square wave parameters: amplitude = 160 mV; period = 0.02 seconds; increment = 2 mV; sampling width = 0.001 seconds.

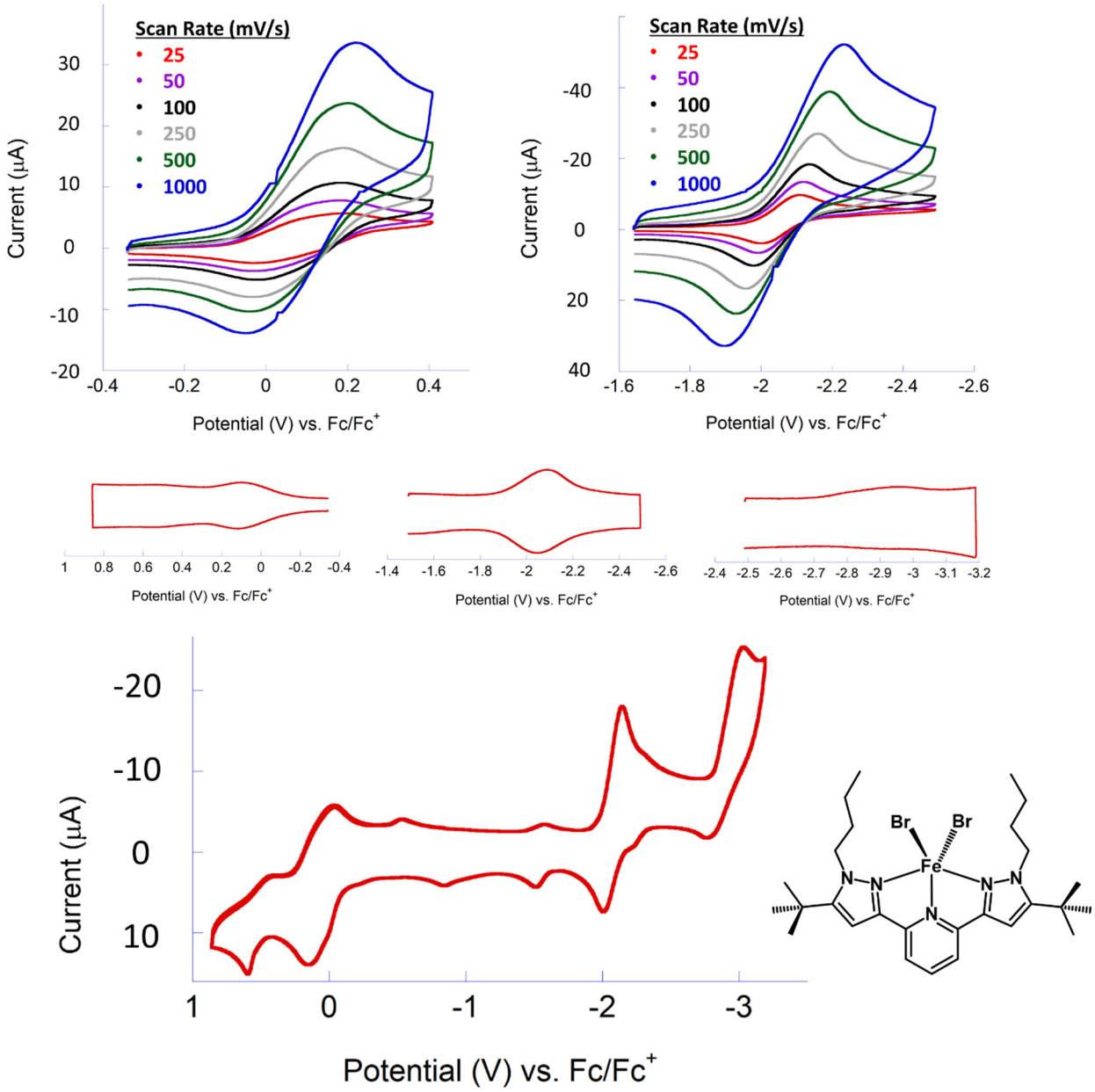

Figure S70 Cyclic Voltammogram (100 mV/s) of (^{Bu}PDP^{tBu})$FeBr_2$ (3.07 mmol) recorded in THF with 0.2 M $[Bu_4N][PF_6]$ at ambient temperature. Insets display the square wave voltammograms of the oxidative (left) and reductive (middle, right) portion as well as scan rate dependence of the oxidative (left) and reductive (right) waves. Square wave parameters: amplitude = 160 mV; period = 0.02 seconds; increment = 2 mV; sampling width = 0.001 seconds.

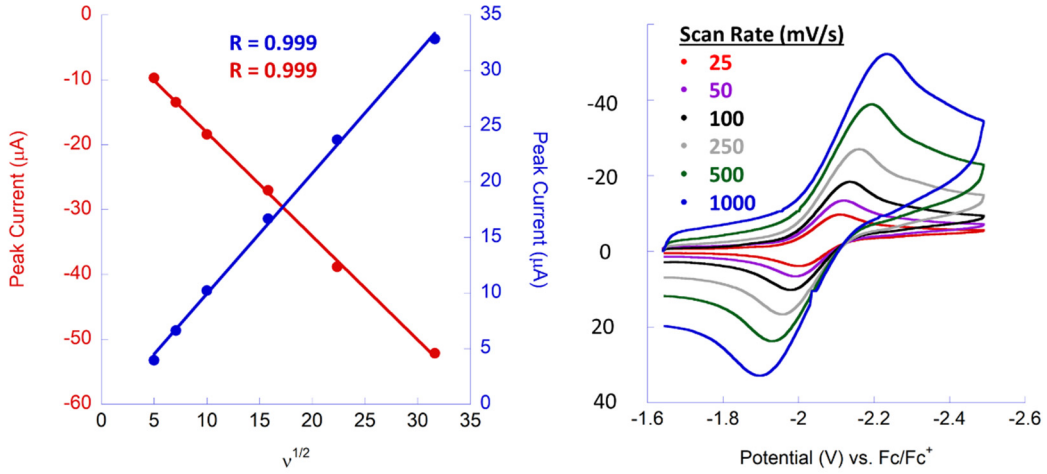

Figure S71 Scan rate dependence of the reductive wave of **1-Bu** (3.07 mmol) recorded in THF with 0.2 M $[Bu_4N][PF_6]$ at ambient temperature.

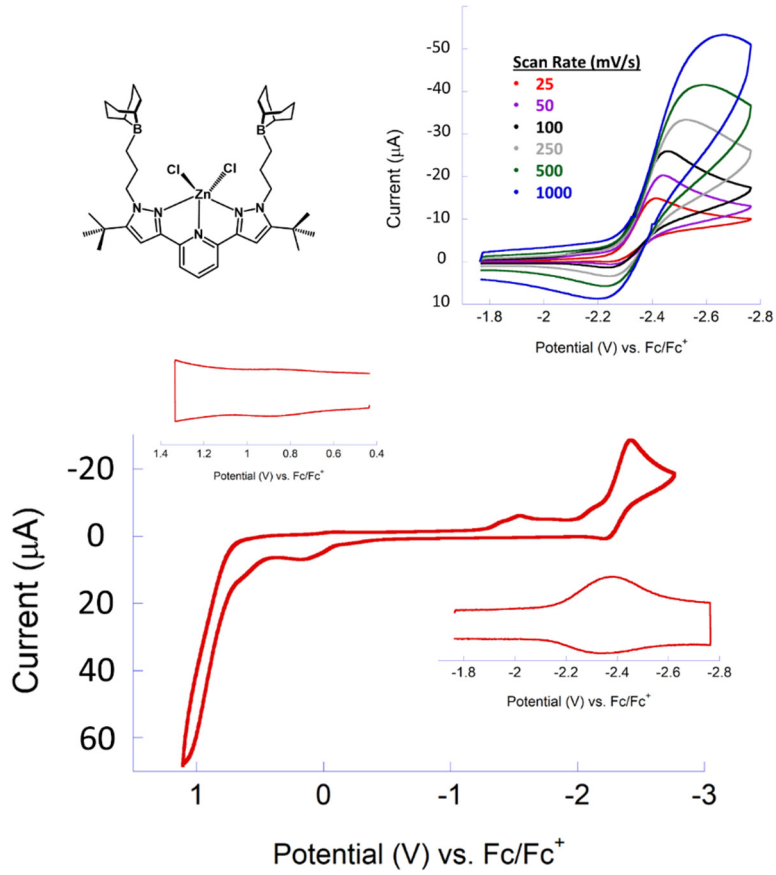

Figure S72 Cyclic Voltammogram (100 mV/s) of (^{BBN}PDP^{tBu})$ZnCl_2$ (2.55 mmol) recorded in THF with 0.2 M $[Bu_4N][PF_6]$ at ambient temperature. Insets display the square wave voltammograms of the oxidative (left) and reductive (right) portion as well as scan rate dependence of the reductive wave. Square wave parameters: amplitude = 160 mV; period = 0.02 seconds; increment = 2 mV; sampling width = 0.001 seconds.

Table S1 Tabulated redox potentials for complexes **1** and **2**.

Complex[a]	E_{red} (V, vs Fc/Fc^+)[b]	E_{ox} (V, vs Fc/Fc^+)[b]
($^{BBN}PDP^{tBu}$)$FeCl_2$ (**1-Cl**)	-2.070	0.084
($^{BBN}PDP^{tBu}$)$FeBr_2$ (**1-Br**)	-2.139	0.088
($^{Bu}PDP^{tBu}$)$FeBr_2$ (**1-Bu**)	-2.089	0.109
($^{BBN}PDP^{tBu}$)$ZnCl_2$	-2.359	0.915
($^{BBN}PDP^{tBu}$)$FeCl_2(N_2H_4)$ (**2-Cl**)	-1.981	0.246
($^{BBN}PDP^{tBu}$)$FeBr_2(N_2H_4)$ (**2-Br**)	-1.955	0.276
($^{BBN}PDP^{tBu}$)$ZnCl_2(N_2H_4)$	-2.041	1.160

[a] Conditions: 0.2 M $[Bu_4N][PF_6]$ in THF. Working electrode: glassy carbon; counter electrode: platinum wire; reference electrode: silver wire.

[b] Potentials determined by square wave voltammetry. Square wave parameters: amplitude = 160 mV; period = 0.02 seconds; increment = 2 mV; sampling width = 0.001 seconds.

Crystallographic Details **1-Bu**

Complex: (^{Bu}PDP^{tBu})$FeBr_2$

Local name: jk1260

Table S2 Experimental parameters of **1-Bu**.

Crystal data	
Chemical formula	$C_{27}H_{41}Br_2FeN_5$
M_r	651.32
Crystal system, space group	Monoclinic, $P2_1/c$
Temperature (K)	150
a, b, c (Å)	15.5028 (3), 39.8514 (7), 9.9718 (2)
β (°)	104.4502 (8)
V (Å^3)	5965.8 (2)
Z	8
Radiation type	Cu $K\alpha$
μ (mm^{-1})	7.37
Crystal size (mm)	0.32 × 0.21 × 0.13
Data collection	
Diffractometer	Bruker AXS D8 Quest CMOS diffractometer
Absorption correction	Multi-scan *SADABS* 2016/2: Krause, L., Herbst-Irmer, R., Sheldrick G.M. & Stalke D. J. Appl. Cryst. 48 (2015) 3-10
T_{min}, T_{max}	0.454, 0.754
No. of measured, independent and observed [$I > 2\sigma(I)$] reflections	34400, 12191, 11147
R_{int}	0.053
(sin θ/λ)$_{max}$ (Å^{-1})	0.638
Refinement	
$R[F^2 > 2\sigma(F^2)]$, $wR(F^2)$, S	0.037, 0.094, 1.04
No. of reflections	12191
No. of parameters	648
H-atom treatment	H-atom parameters constrained
$\Delta\rho_{max}$, $\Delta\rho_{min}$ (e Å^{-3})	0.78, -0.76

Computer programs: Apex3 v2016.9-0 (Bruker, 2016), *SAINT* V8.37A (Bruker, 2016), *SHELXS97* (Sheldrick, 2008), *SHELXL2016*/6 (Sheldrick, 2015, 2016), SHELXLE Rev714 (Hübschle *et al.*, 2011).

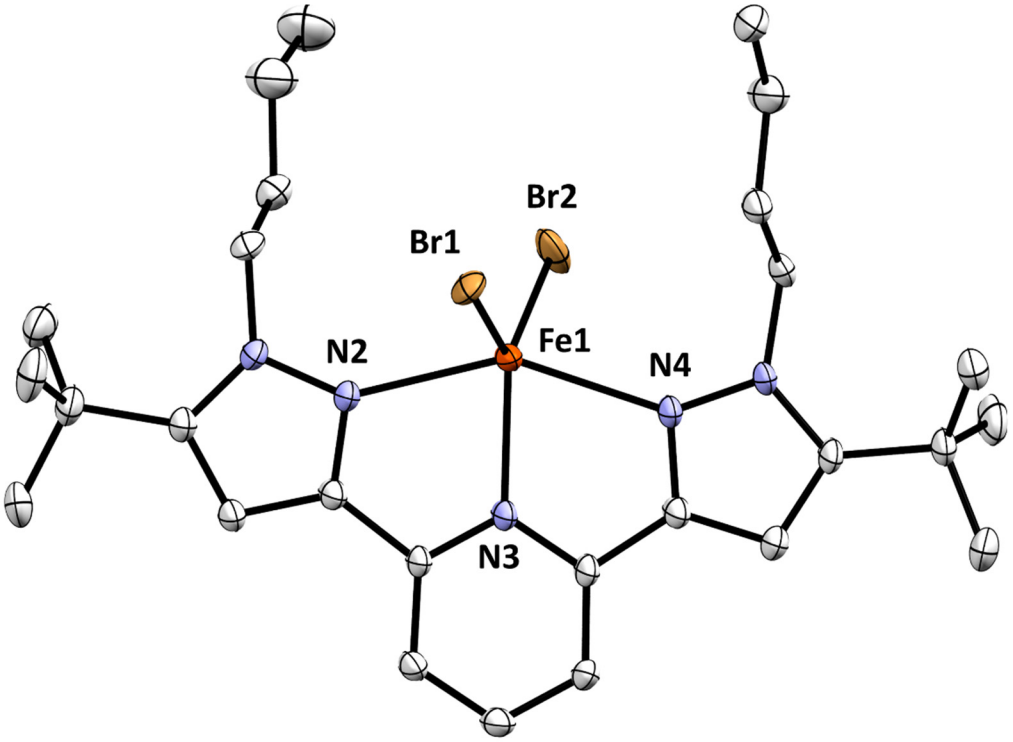

Figure S73 Molecular Structure of **1-Bu** displayed with 50% probability ellipsoids. A second asymmetric molecule in the unit cell and hydrogen atoms have been omitted for clarity.

Crystallographic Details **1-Cl**

Complex: (^{BBN}PDP^{tBu})$FeCl_2$

Local name: jk1191a

Table S3 Experimental parameters of **1-Cl**.

Crystal data	
Chemical formula	$C_{41}H_{63}B_2Cl_2FeN_5$
M_r	774.33
Crystal system, space group	Monoclinic, $P2_1/c$
Temperature (K)	85
a, b, c (Å)	19.8752 (6), 20.4520 (6), 10.2304 (5)
β (°)	96.716 (3)
V (Å^3)	4130.0 (3)
Z	4
Radiation type	Cu $K\alpha$
μ (mm^{-1})	4.37
Crystal size (mm)	0.05 × 0.05 × 0.01
Data collection	
Diffractometer	Abstract diffractometer
Absorption correction	Multi-scan *CrysAlis PRO* 1.171.38.41 (Rigaku Oxford Diffraction, 2015) Empirical absorption correction using spherical harmonics, implemented in SCALE3 ABSPACK scaling algorithm.
T_{min}, T_{max}	0.691, 1.000
No. of measured, independent and observed [$I > 2\sigma(I)$] reflections	63184, 7716, 5482
R_{int}	0.138
$(\sin \theta/\lambda)_{max}$ (Å^{-1})	0.608
Refinement	
$R[F^2 > 2\sigma(F^2)]$, $wR(F^2)$, S	0.069, 0.196, 1.03
No. of reflections	7716
No. of parameters	467
H-atom treatment	H-atom parameters constrained
$\Delta\rho_{max}$, $\Delta\rho_{min}$ (e Å^{-3})	0.65, -0.85

Computer programs: *CrysAlis PRO* 1.171.38.41 (Rigaku OD, 2015), *SHELXS97* (Sheldrick, 2008), *SHELXL2014*/7 (Sheldrick, 2014).

Crystallographic Details ($^{BBN}PDP^{tBu}$)$ZnCl_2$

Complex: ($^{BBN}PDP^{tBu}$)$ZnCl_2$

Local name: jk214

Table S4 Experimental parameters of ($^{BBN}PDP^{tBu}$)$ZnCl_2$.

Crystal data	
Chemical formula	$C_{41}H_{63}B_2Cl_2N_5Zn$
M_r	783.85
Crystal system, space group	Monoclinic, $P2_1/c$
Temperature (K)	150
a, b, c (Å)	19.9291 (8), 20.5205 (8), 10.2091 (4)
β (°)	96.6474 (19)
V (Å^3)	4147.0 (3)
Z	4
Radiation type	Cu $K\alpha$
μ (mm^{-1})	2.26
Crystal size (mm)	0.44 × 0.24 × 0.01
Data collection	
Diffractometer	Bruker AXS D8 Quest CMOS diffractometer
Absorption correction	Multi-scan *SADABS* 2016/2: Krause, L., Herbst-Irmer, R., Sheldrick G.M. & Stalke D., J. Appl. Cryst. 48 (2015) 3-10
T_{min}, T_{max}	0.169, 0.330
No. of measured, independent and observed [$I > 2\sigma(I)$] reflections	25262, 8540, 6206
R_{int}	0.085
$(\sin \theta/\lambda)_{max}$ (Å^{-1})	0.638
Refinement	
$R[F^2 > 2\sigma(F^2)]$, $wR(F^2)$, S	0.075, 0.229, 1.09
No. of reflections	8540
No. of parameters	466
H-atom treatment	H-atom parameters constrained
$\Delta\rho_{max}$, $\Delta\rho_{min}$ (e Å^{-3})	1.10, -0.91

Computer programs: Apex3 v2016.9-0 (Bruker, 2016), *SAINT* V8.37A (Bruker, 2016), *SHELXS97* (Sheldrick, 2008), *SHELXL2016*/6 (Sheldrick, 2015, 2016), SHELXLE Rev714 (Hübschle *et al.*, 2011).

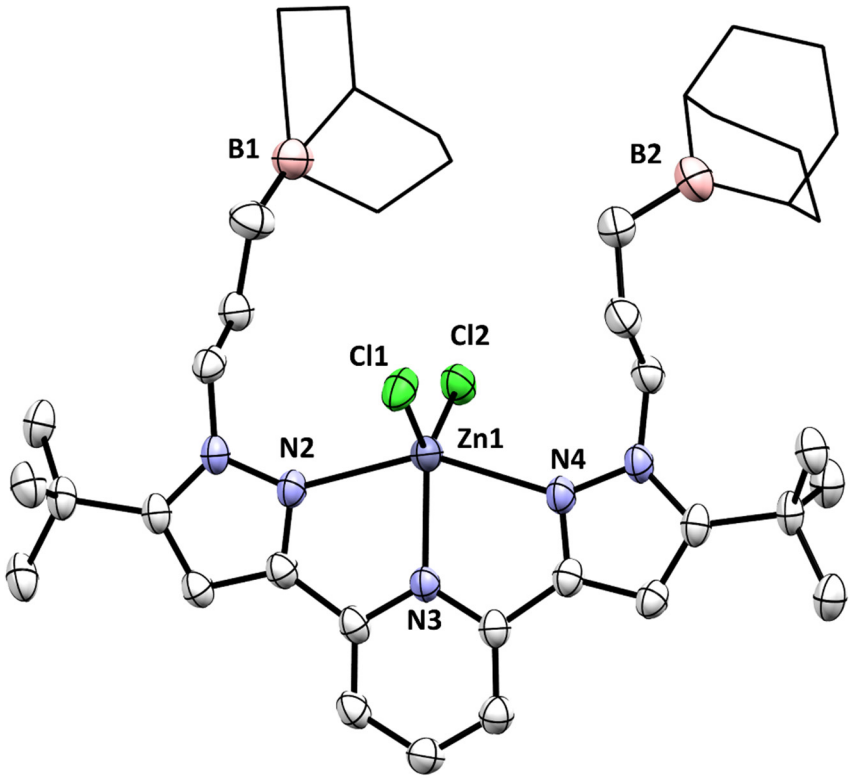

Figure S74 Molecular Structure of (^{BBN}PDP^{tBu})$ZnCl_2$ displayed with 50% probability ellipsoids. Hydrogen atoms have been omitted for clarity.

Crystallographic Details **2-Br**

Complex: (^{BBN}PDP^{tBu})$FeBr_2(N_2H_4)$

Local name: jk2173

Table S5 Experimental parameters of **2-Br**.

Crystal data	
Chemical formula	$C_{41}H_{67}B_2Br_2FeN_7 \cdot CH_2Cl_2$
M_r	980.23
Crystal system, space group	Monoclinic, $P2_1/c$
Temperature (K)	150
a, b, c (Å)	17.4650 (7), 13.1425 (6), 21.1101 (8)
β (°)	107.9851 (15)
V (Å^3)	4608.7 (3)
Z	4
Radiation type	Mo $K\alpha$
μ (mm^{-1})	2.22
Crystal size (mm)	0.57 × 0.40 × 0.14
Data collection	
Diffractometer	Bruker AXS D8 Quest CMOS diffractometer
Absorption correction	Multi-scan *SADABS* 2016/2: Krause, L., Herbst-Irmer, R., Sheldrick G.M. & Stalke D., J. Appl. Cryst. 48 (2015) 3-10
T_{min}, T_{max}	0.576, 0.747
No. of measured, independent and observed [$I > 2\sigma(I)$] reflections	149697, 17565, 13165
R_{int}	0.051
$(\sin \theta/\lambda)_{max}$ (Å^{-1})	0.771
Refinement	
$R[F^2 > 2\sigma(F^2)]$, $wR(F^2)$, S	0.035, 0.092, 1.03
No. of reflections	17565
No. of parameters	539
No. of restraints	63
H-atom treatment	H-atom parameters constrained
$\Delta\rho_{max}$, $\Delta\rho_{min}$ (e Å^{-3})	0.83, -0.78

Computer programs: Apex3 v2016.9-0 (Bruker, 2016), *SAINT* V8.37A (Bruker, 2016), *SHELXS97* (Sheldrick, 2008), *SHELXL2017*/1 (Sheldrick, 2017), SHELXLE Rev859 (Hübschle *et al.*, 2011).

Refinement Details:

A methylene chloride molecule was refined as disordered. The two moieties were restrained to have similar geometries. U^{ij} components of ADPs for disordered atoms closer to each other than 1.7 Å were restrained to be similar. Subject to these conditions the occupancy ratio refined to 0.651(10) to 0.349(10).

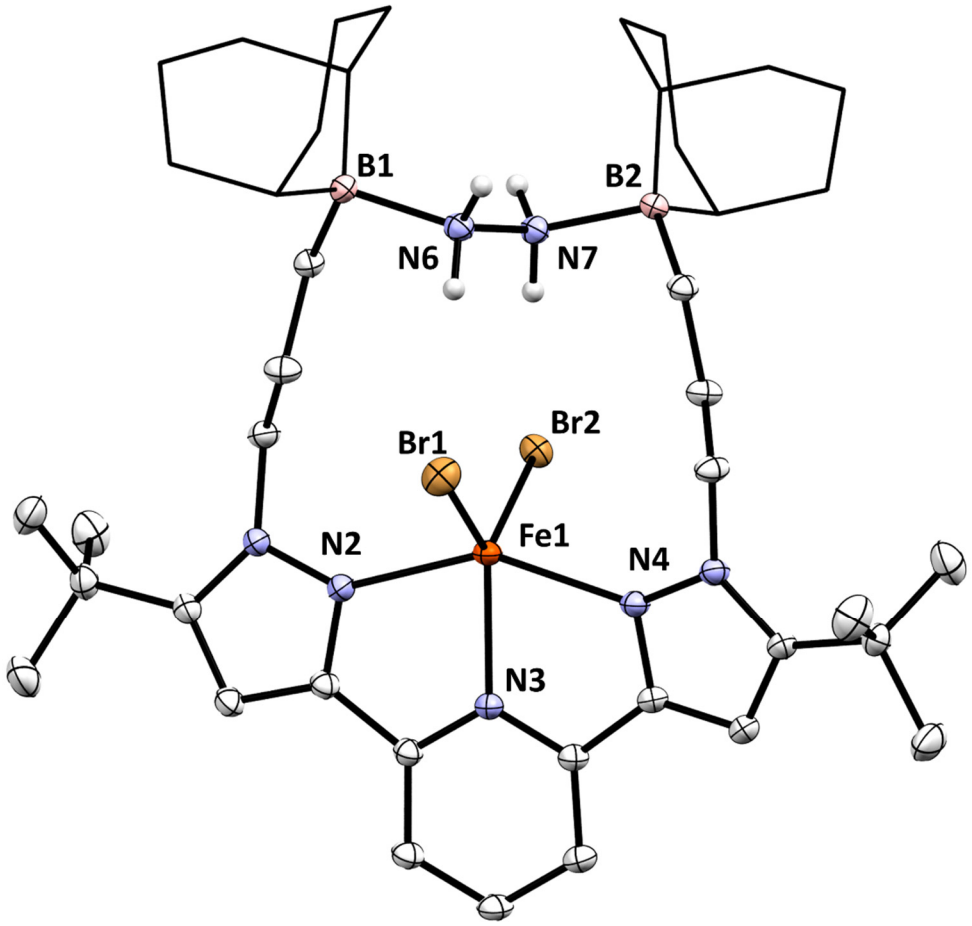

Figure S75 Molecular Structure of **2-Br** displayed with 50% probability ellipsoids. Hydrogen atoms not attached to nitrogen atoms have been omitted for clarity. Cocrystallized solvent molecules have also been omitted.

Crystallographic Details **3-Br**

Complex: (^{BBN}PDP^{tBu})$FeBr_2(N_2H_4)_2$

Local name: jk216

Table S6 Experimental parameters of **3-Br**.

Crystal data	
Chemical formula	$C_{41}H_{71}B_2Br_2FeN_9 \cdot 0.974(CH_2Cl_2)$
M_r	1010.14
Crystal system, space group	Triclinic, $P\overline{1}$
Temperature (K)	150
a, *b*, *c* (Å)	15.9919 (14), 16.2738 (14), 20.0906 (17)
α, β, γ (°)	68.588 (3), 77.949 (3), 84.373 (3)
V (Å^3)	4759.0 (7)
Z	4
Radiation type	Mo $K\alpha$
μ (mm^{-1})	2.15
Crystal size (mm)	0.25 × 0.25 × 0.05
Data collection	
Diffractometer	Bruker AXS D8 Quest CMOS diffractometer
Absorption correction	Multi-scan TWINABS 2012/1: Krause, L., Herbst-Irmer, R., Sheldrick G.M. & Stalke D., J. Appl. Cryst. 48 (2015) 3-10
T_{min}, T_{max}	0.103, 0.155
No. of measured, independent and observed [$I > 2\sigma(I)$] reflections	158482, 29474, 19262
R_{int}	0.100
$(\sin\theta/\lambda)_{max}$ (Å^{-1})	0.706
Refinement	
$R[F^2 > 2\sigma(F^2)]$, $wR(F^2)$, *S*	0.072, 0.144, 1.17
No. of reflections	29474
No. of parameters	1467
No. of restraints	2258
H-atom treatment	H atoms treated by mixture of independent and constrained refinement
	$w = 1/[\sigma^2(F_o^2) + (0.023P)^2 + 13.0649P]$ where $P = (F_o^2 + 2F_c^2)/3$
$\Delta\rho_{max}$, $\Delta\rho_{min}$ (e Å^{-3})	0.91, -0.78

Computer programs: Apex3 v2016.9-0 (Bruker, 2016), *SAINT* V8.37A (Bruker, 2016), *SHELXS97* (Sheldrick, 2008), *SHELXL2016*/6 (Sheldrick, 2015, 2016), SHELXLE Rev714 (Hübschle *et al.*, 2011).

Refinement Details:

The crystal under investigation was found to be non-merohedrally twinned. The orientation matrices for the two components were identified using the program Cell Now, with the two components being related by a 180 ° rotation around the reciprocal b-axis. The two components were integrated using Saint and corrected for absorption using twinabs, resulting in the following statistics:

14502 data (3691 unique) involve domain 1 only, mean I/sigma 14.7

14294 data (3610 unique) involve domain 2 only, mean I/sigma 14.0

134310 data (22396 unique) involve 2 domains, mean I/sigma 8.5

46 data (45 unique) involve 3 domains, mean I/sigma 5.7

The exact twin matrix identified by the integration program was found to be:

-1.00011 0.00040 0.00027

-0.04670 1.00080 -0.58237

-0.00068 0.00271 -1.00069

The structure was solved using direct methods with only the non-overlapping reflections of both components. The structure was refined using the hklf 5 routine with all reflections of both components (including the overlapping ones), resulting in a BASF value of 0.4737(8).

The R_{int} value given is for all reflections and is based on agreement between observed single and composite intensities and those calculated from refined unique intensities and twin fractions (TWINABS (Sheldrick, 2012)).

One of the two crystallographically independent molecules shows close to whole molecule disorder induced by a rotation of one of the hydrazine groups. The rotation induces a slight shift of the ligand, of the connecting propyl arm, and of all atoms of the remainder of the molecule with the exception of the second hydrazine group. The disordered moieties were restrained to have a similar geometry as the same section of the not disordered second molecule. The U^{ij} components of all disordered atoms were restrained to be similar for all atoms closer to each other than 1.7 Å. Disordered hydrazine H atoms were in addition restrained based on hydrogen bonding interactions (with each other and with bromine atoms). Subject to these conditions the occupancy ratio refined to 0.547(4) to 0.453(4). Two methylene chloride molecules were refined as disordered over each two positions. For the second less well-defined molecule, full occupancy for the site as a whole was not enforced. The four moieties were restrained to have similar geometries, and U^{ij} components of all disordered atoms were restrained to be similar for all atoms closer to each other than 1.7 Å. The occupancy ratio for the first solvate molecule refined to 0.663(8) to 0.337(8). The occupancy rates for the second molecule to 0.774(12) and 0.173(12).

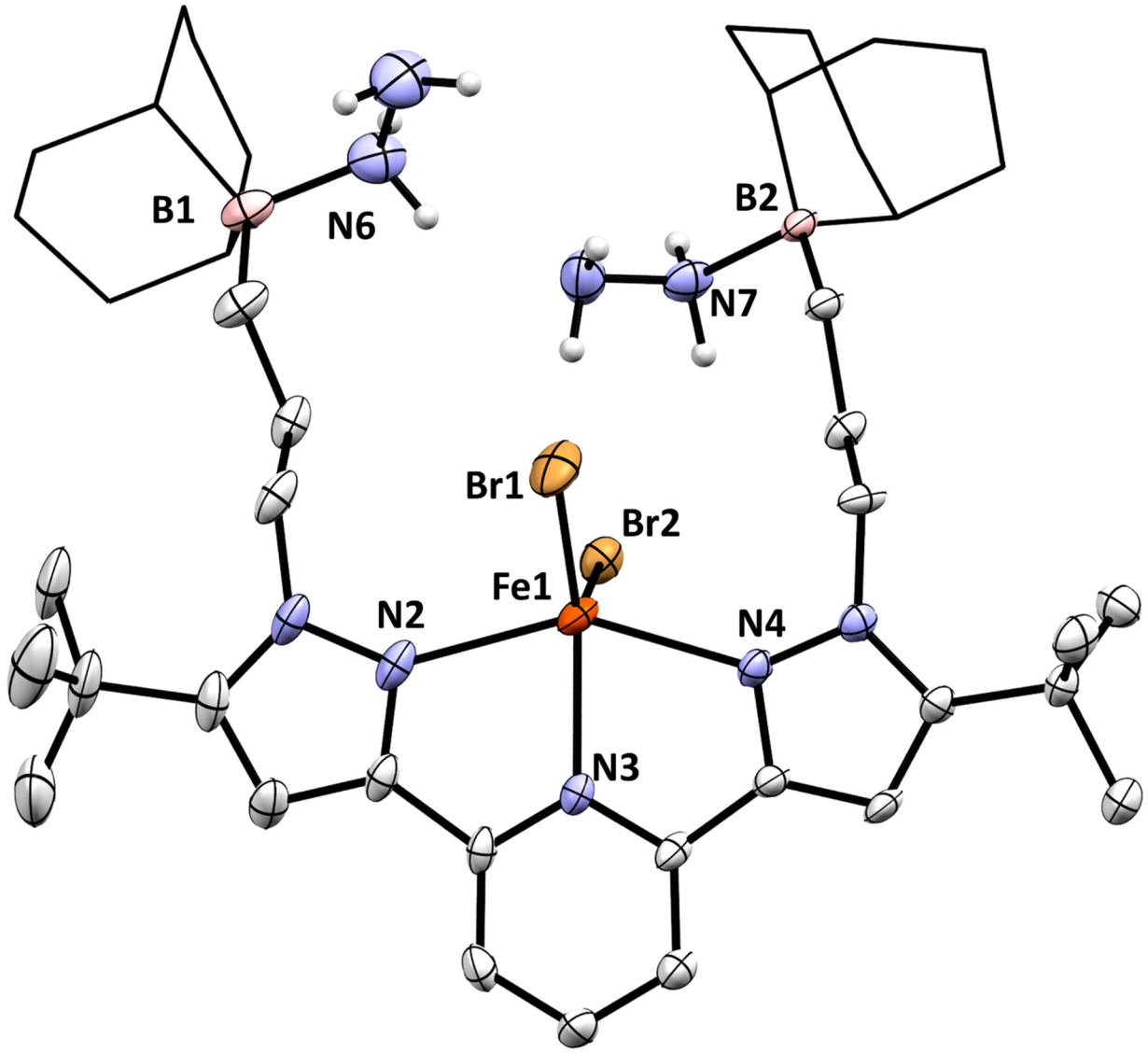

Figure S76 Molecular Structure of **3-Br** displayed with 50% probability ellipsoids. Hydrogen atoms not attached to nitrogen atoms have been omitted for clarity. Cocrystallized solvent molecules and a second asymmetric molecule within the unit cell have also been omitted.

Crystallographic Details **3-Cl**

Complex: (^{BBN}PDP^{tBu})$FeCl_2(N_2H_4)_2$

Local name: jk2133b

Table S7 Experimental parameters of **3-Cl**.

Crystal data	
Chemical formula	$C_{41}H_{71}B_2Cl_2FeN_9 \cdot 0.885(CH_2Cl_2)$
M_r	913.63
Crystal system, space group	Triclinic, $P\overline{1}$
Temperature (K)	150
a, *b*, *c* (Å)	15.8817 (7), 16.2850 (7), 20.1341 (9)
α, β, γ (°)	68.602 (2), 76.235 (3), 84.515 (2)
V (Å^3)	4708.9 (4)
Z	4
Radiation type	Cu *K*α
μ (mm^{-1})	4.84
Crystal size (mm)	0.50 × 0.26 × 0.03
Data collection	
Diffractometer	Bruker AXS D8 Quest CMOS diffractometer
Absorption correction	Multi-scan TWINABS 2012/1: Krause, L., Herbst-Irmer, R., Sheldrick G.M. & Stalke D., J. Appl. Cryst. 48 (2015) 3-10
T_{min}, T_{max}	0.400, 0.754
No. of measured, independent and observed [$I > 2\sigma(I)$] reflections	142709, 18105, 16614
R_{int}	0.141
$(\sin \theta/\lambda)_{max}$ (Å^{-1})	0.641
Refinement	
$R[F^2 > 2\sigma(F^2)]$, $wR(F^2)$, *S*	0.088, 0.238, 1.02
No. of reflections	18105
No. of parameters	1162
No. of restraints	230
H-atom treatment	H atoms treated by a mixture of independent and constrained refinement
$\Delta\rho_{max}$, $\Delta\rho_{min}$ (e Å^{-3})	1.03, -1.28

Computer programs: Apex3 v2016.9-0 (Bruker, 2016), *SAINT* V8.37A (Bruker, 2016), *SHELXS97* (Sheldrick, 2008), *SHELXL2017*/1 (Sheldrick, 2017), SHELXLE Rev859 (Hübschle *et al.*, 2011).

Refinement Details:

The crystal under investigation was found to be non-merohedrally twinned. The orientation matrices for the two components were identified using the program Cell_Now, with the two components being related by a 180 ° rotation around the reciprocal b-axis. The two components were integrated using Saint and corrected for absorption using twinabs, resulting in the following statistics:

48169 data (10435 unique) involve domain 1 only, mean I/sigma 19.4

48019 data (10386 unique) involve domain 2 only, mean I/sigma 12.6

46895 data (11630 unique) involve 2 domains, mean I/sigma 24.2

The exact twin matrix identified by the integration program was found to be

Transforms h1.1(1)->h1.2(2)

-0.99994 0.00009 -0.00023

-0.01984 1.00006 -0.58820

0.00032 0.00021 -1.00012

The structure was solved using direct methods with only the non-overlapping reflections of component 1. The structure was refined using the hklf 5 routine with all reflections of component 1 (including the overlapping ones), resulting in a BASF value of 0.352(2).

The R_{int} value given is for all reflections and is based on agreement between observed single and composite intensities and those calculated from refined unique intensities and twin fractions (TWINABS (Sheldrick, 2012)).

Two dichloromethane molecules were refined as partially occupied and disordered. One site was refined as disordered over two orientations, the second over three. No attempts were made to enforce full occupancy for both sites. The disordered moieties of each site were restrained to have similar geometries. U^{ij} components of ADPs for disordered atoms closer to each other than 1.7 Å were restrained to be similar. ADPs of atoms C42B and C42D were constrained to be identical. A weak anti-bumping restrained was applied to keep solvate H atoms from approaching the main molecule too closely. Subject to these conditions the occupancy rates refined to 0.592(13) and 0.261(12) for the first site, and to 0.594(17), 0.217(17) and 0.106(6) for the second site.

Terminal amine H atoms were assigned from difference densities and N-H distances restrained to 0.91(2) Å. Some H...H distances were restrained to 1.465(20) Å, and some H...Cl distances were restrained based on hydrogen bonding considerations.

Crystallographic Details **4**

Complex: (^{BBN}PDP^{tBu})Fe(NH_2)$_2$

Local name: jk2100

Table S8 Experimental parameters of **4**.

Crystal data	
Chemical formula	$C_{41}H_{67}B_2FeN_7 \cdot CH_2Cl_2$
M_r	820.41
Crystal system, space group	Tetragonal, $P4_32_12$
Temperature (K)	150
a, c (Å)	16.1611 (5), 16.5750 (6)
V (Å^3)	4329.1 (3)
Z	4
Radiation type	Mo $K\alpha$
μ (mm^{-1})	0.51
Crystal size (mm)	0.55 × 0.51 × 0.39
Data collection	
Diffractometer	Bruker AXS D8 Quest CMOS diffractometer
Absorption correction	Multi-scan *SADABS* 2016/2: Krause, L., Herbst-Irmer, R., Sheldrick G.M. & Stalke D., J. Appl. Cryst. 48 (2015) 3-10
T_{min}, T_{max}	0.285, 0.344
No. of measured, independent and observed [$I > 2\sigma(I)$] reflections	48791, 10437, 8195
R_{int}	0.033
$(\sin \theta/\lambda)_{max}$ (Å^{-1})	0.834
Refinement	
$R[F^2 > 2\sigma(F^2)]$, $wR(F^2)$, S	0.052, 0.137, 1.08
No. of reflections	10437
No. of parameters	264
No. of restraints	24
H-atom treatment	H-atom parameters constrained
$\Delta\rho_{max}$, $\Delta\rho_{min}$ (e Å^{-3})	0.51, -0.67
Absolute structure	Flack x determined using 3135 quotients [(I+)-(I-)]/[(I+)+(I-)] (Parsons, Flack and Wagner, Acta Cryst. B69 (2013) 249-259).
Absolute structure parameter	-0.010 (3)

Computer programs: Apex3 v2016.9-0 (Bruker, 2016), *SAINT* V8.37A (Bruker, 2016), *SHELXS97* (Sheldrick, 2008), *SHELXL2016*/6 (Sheldrick, 2015, 2016), SHELXLE Rev714 (Hübschle *et al.*, 2011).

Refinement Details:

A methylene chloride molecule is disordered with the C atom in two alternative positions and Cl atoms moved only insubstantially. All C-Cl distances were restrained to be similar and U^{ij} components of ADPs were restrained to be similar for atoms closer to each other than 1.7 Å. The occupancy ratio refined to 0.413(12) to 0.587(12).

Crystallographic Details **5-OPh**

Complex: (^{BBN}PDP^{tBu})Fe(OPh)$_2$(NH$_3$)$_2$

Local name: jk298

Table S9 Experimental parameters of **5-OPh**.

Crystal data	
Chemical formula	$C_{53}H_{79}B_2FeN_7O_2 \cdot 0.783(C_6H_6O) \cdot 0.217(C_6H_6)$
M_r	1014.33
Crystal system, space group	Triclinic, $P\overline{1}$
Temperature (K)	150
a, b, c (Å)	10.8379 (9), 16.9517 (11), 19.8869 (15)
α, β, γ (°)	105.865 (3), 105.194 (2), 105.175 (2)
V (Å^3)	3165.3 (4)
Z	2
Radiation type	Mo $K\alpha$
μ (mm^{-1})	0.28
Crystal size (mm)	0.52 × 0.38 × 0.14
Data collection	
Diffractometer	Bruker AXS D8 Quest CMOS diffractometer
Absorption correction	Multi-scan *SADABS* 2016/2: Krause, L., Herbst-Irmer, R., Sheldrick G.M. & Stalke D., J. Appl. Cryst. 48 (2015) 3-10
T_{min}, T_{max}	0.357, 0.433
No. of measured, independent and observed [$I > 2\sigma(I)$] reflections	83767, 15586, 12607
R_{int}	0.069
(sin θ/λ)$_{max}$ (Å^{-1})	0.667
Refinement	
$R[F^2 > 2\sigma(F^2)]$, $wR(F^2)$, S	0.067, 0.165, 1.07
No. of reflections	15586
No. of parameters	702
No. of restraints	219
H-atom treatment	H-atom parameters constrained
$\Delta\rho_{max}$, $\Delta\rho_{min}$ (e Å^{-3})	0.86, -0.67

Computer programs: Apex3 v2016.9-0 (Bruker, 2016), *SAINT* V8.37A (Bruker, 2016), *SHELXS97* (Sheldrick, 2008), *SHELXL2016*/6 (Sheldrick, 2015, 2016), SHELXLE Rev714 (Hübschle *et al.*, 2011).

Refinement Details:

A solvent phenol molecule is disordered with a solvent benzene molecule. The benzene molecule was constrained to resemble an ideal hexagon with C-C distances of 1.39 Å. The geometry of the phenol molecule was restrained to be similar to that of a phenolate anion in the structure. U^{ij} Components of ADPs were restrained to be similar for disordered atoms closer to each other than 1.7 Å. Subject to these conditions the occupancy ratio refined to 0.783(6) to 0.217(6) in favor of phenol.

The structure contains additional solvent accessible voids of 486 $Å^3$. The content of the void consists of disordered phenol and benzene molecules with large thermal libration and multiple alternative orientations. Attempts to model disorder with three-plus moieties gave unsatisfactory results and the cif and fcf files were instead corrected for using reverse Fourier transform methods using the SQUEEZE routine (P. van der Sluis & A.L. Spek (1990). Acta Cryst. A46, 194-201) as implemented in the program Platon. The resultant files were used in the further refinement. (The FAB file with details of the Squeeze results is appended to this cif file).

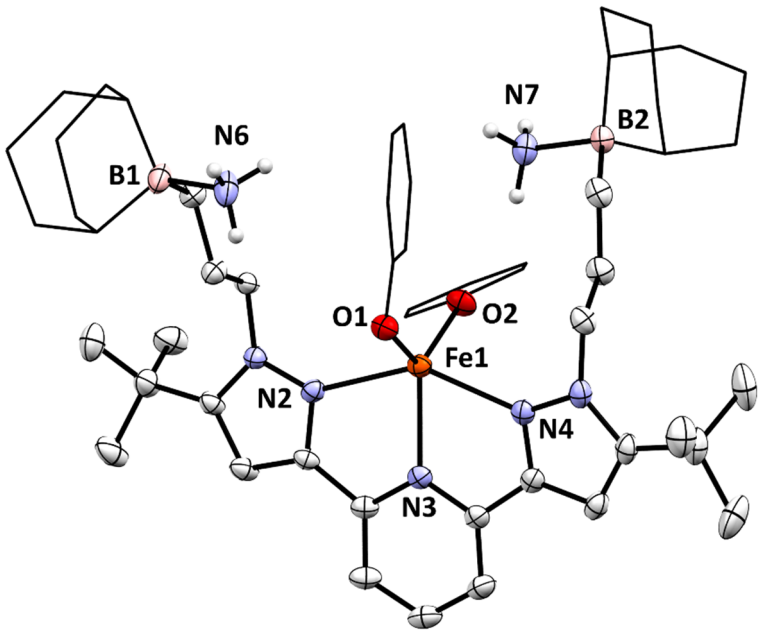

Figure S77 Molecular Structure of **5-OPh** displayed with 50% probability ellipsoids. Hydrogen atoms not attached to nitrogen atoms and cocrystallized solvent molecules have been omitted for clarity.

Crystallographic Details **5-ONO_2**

Complex: ($^{BBN}PDP^{tBu}$)Fe(ONO_2)$_2$(NH_3)$_2$

Local name: jk1285b

Table S10 Experimental parameters of **5-ONO_2**.

Crystal data	
Chemical formula	$C_{41}H_{69}B_2FeN_9O_6$
M_r	861.52
Crystal system, space group	Monoclinic, *P*2/*n*
Temperature (K)	150
a, *b*, *c* (Å)	23.0277 (10), 7.3247 (4), 30.5183 (17)
β (°)	97.474 (3)
V (Å^3)	5103.8 (5)
Z	4
Radiation type	Cu *K*α
μ (mm^{-1})	2.76
Crystal size (mm)	0.50 × 0.07 × 0.04
Data collection	
Diffractometer	Bruker AXS D8 Quest CMOS diffractometer
Absorption correction	Multi-scan *SADABS* 2016/2: Krause, L., Herbst-Irmer, R., Sheldrick G.M. & Stalke D., J. Appl. Cryst. 48 (2015) 3-10
T_{min}, T_{max}	0.166, 0.322
No. of measured, independent and observed [$I > 2\sigma(I)$] reflections	29255, 9375, 5870
R_{int}	0.150
$(\sin \theta/\lambda)_{max}$ (Å^{-1})	0.611
Refinement	
$R[F^2 > 2\sigma(F^2)]$, $wR(F^2)$, *S*	0.088, 0.219, 1.02
No. of reflections	9375
No. of parameters	650
No. of restraints	521
H-atom treatment	H-atom parameters constrained
$\Delta\rho_{max}$, $\Delta\rho_{min}$ (e Å^{-3})	0.44, -0.49

Computer programs: Apex3 v2016.9-0 (Bruker, 2016), *SAINT* V8.37A (Bruker, 2016), *SHELXS97* (Sheldrick, 2008), *SHELXL2016*/6 (Sheldrick, 2015, 2016), SHELXLE Rev714 (Hübschle *et al.*, 2011).

Refinement Details:

One of the ligand sidearms is disordered and was refined as split over two orientations. Both moieties were restrained to have similar geometries as the other, not disordered side arm. U^{ij} components of ADPs of disordered atoms were restrained to be similar for atoms closer to each other than 1.7 Å. Subject to these conditions the occupancy ratio refined to 0.778(5) to 0.222(5).

Large areas beside the disordered side arms are occupied by extensively disordered solvate molecules (most likely disordered pentane). Per unit cell two independent solvent accessible voids of 763 $Å^3$ combined are found. No substantial electron density peaks were found in the solvent accessible voids (less than 1.22 electrons per $Å^3$) and the residual electron density peaks are not arranged in an interpretable pattern. The cif and fcf files were instead corrected for using reverse Fourier transform methods using the SQUEEZE routine (P. van der Sluis & A.L. Spek (1990). Acta Cryst. A46, 194-201) as implemented in the program Platon. The resultant files were used in the further refinement. (The FAB file with details of the Squeeze results is appended to this cif file). The Squeeze procedure corrected for 136 electrons within the solvent accessible voids.

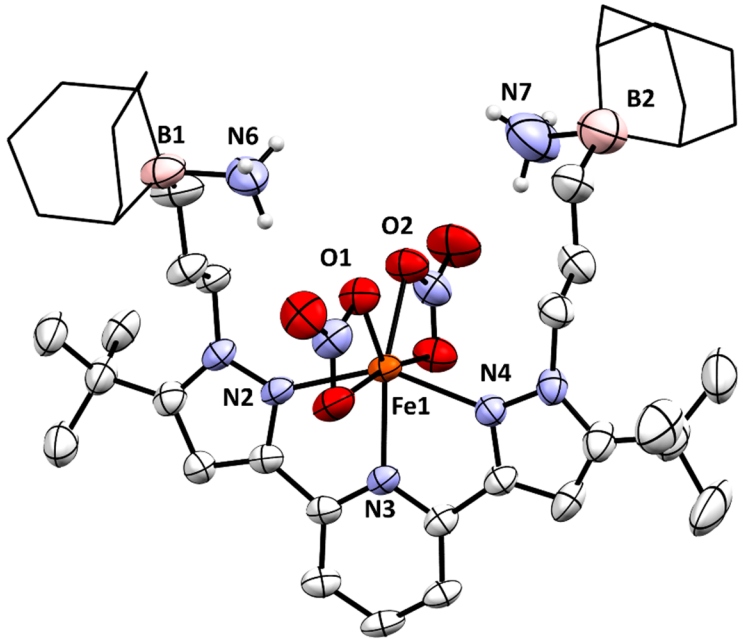

Figure S78 Molecular Structure of **5-ONO$_2$** displayed with 50% probability ellipsoids. Hydrogen atoms not attached to nitrogen atoms have been omitted for clarity.

Crystallographic Details ($^{BBN}PDP^{tBu}$)$ZnCl_2(N_2H_4)$

Complex: ($^{BBN}PDP^{tBu}$)$ZnCl_2(N_2H_4)$

Local name: jk2202

Table S11 Experimental parameters of ($^{BBN}PDP^{tBu}$)$ZnCl_2(N_2H_4)$.

Crystal data	
Chemical formula	$C_{41}H_{67}B_2Cl_2N_7Zn$
M_r	815.90
Crystal system, space group	Triclinic, $P\overline{1}$
Temperature (K)	85
a, *b*, *c* (Å)	11.6502 (4), 14.2465 (5), 15.0298 (5)
α, β, γ (°)	111.319 (3), 107.231 (3), 98.485 (3)
V (Å^3)	2126.27 (14)
Z	2
Radiation type	Cu *K*α
μ (mm^{-1})	2.24
Crystal size (mm)	0.08 × 0.04 × 0.01
Data collection	
Diffractometer	Dtrek-*CrysAlis PRO*-abstract goniometer imported rigaku-*D*TREK* images
Absorption correction	Multi-scan *CrysAlis PRO* 1.171.38.41 (Rigaku Oxford Diffraction, 2015) Empirical absorption correction using spherical harmonics, implemented in SCALE3 ABSPACK scaling algorithm.
T_{min}, T_{max}	0.649, 1.000
No. of measured, independent and observed [$I > 2\sigma(I)$] reflections	32084, 7676, 6899
R_{int}	0.075
$(\sin\theta/\lambda)_{max}$ (Å^{-1})	0.607
Refinement	
$R[F^2 > 2\sigma(F^2)]$, $wR(F^2)$, *S*	0.057, 0.187, 1.06
No. of reflections	7676
No. of parameters	484
H-atom treatment	H-atom parameters constrained
$\Delta\rho_{max}$, $\Delta\rho_{min}$ (e Å^{-3})	1.39, -1.10

Computer programs: *CrysAlis PRO* 1.171.38.41 (Rigaku OD, 2015), *SHELXS97* (Sheldrick, 2008), *SHELXL2014*/7 (Sheldrick, 2014).

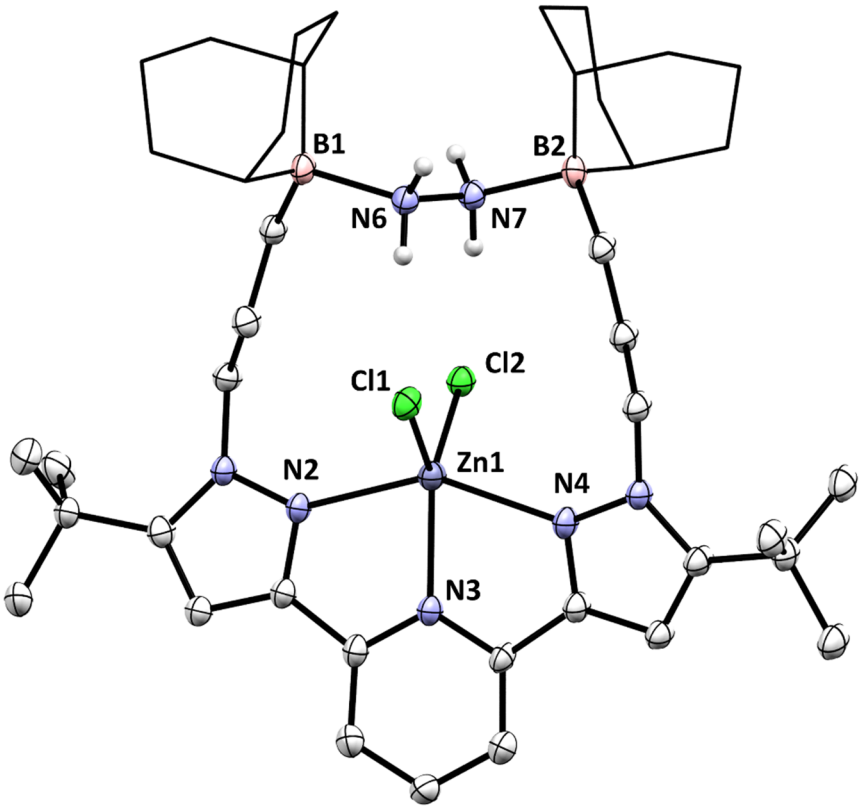

Figure S79 Molecular Structure of (^{BBN}PDP^{tBu})$ZnCl_2(N_2H_4)$ displayed with 50% probability ellipsoids. Hydrogen atoms not attached to nitrogen atoms have been omitted for clarity.

Crystallographic Details **5-Cl**

Complex: (^{BBN}PDP^{tBu})$FeCl_2(NH_3)_2$

Local name: jk2130

Table S12 Experimental parameters of **5-Cl**.

Crystal data	
Chemical formula	$C_{41}H_{69}B_2Cl_2FeN_7 \cdot 3(C_4H_8O)$
M_r	1024.71
Crystal system, space group	Triclinic, $P\overline{1}$
Temperature (K)	150
a, *b*, *c* (Å)	13.3953 (4), 14.2668 (4), 16.5650 (5)
α, β, γ (°)	99.4365 (13), 110.1175 (12), 100.4636 (14)
V (Å^3)	2833.89 (15)
Z	2
Radiation type	Cu *K*α
μ (mm^{-1})	3.35
Crystal size (mm)	0.23 × 0.20 × 0.19
Data collection	
Diffractometer	Bruker AXS D8 Quest CMOS diffractometer
Absorption correction	Multi-scan *SADABS* 2016/2: Krause, L., Herbst-Irmer, R., Sheldrick G.M. & Stalke D., J. Appl. Cryst. 48 (2015) 3-10
T_{min}, T_{max}	0.461, 0.754
No. of measured, independent and observed [$I > 2\sigma(I)$] reflections	27346, 11310, 9899
R_{int}	0.057
$(\sin \theta/\lambda)_{max}$ (Å^{-1})	0.639
Refinement	
$R[F^2 > 2\sigma(F^2)]$, $wR(F^2)$, S	0.050, 0.139, 1.08
No. of reflections	11310
No. of parameters	761
No. of restraints	685
H-atom treatment	H-atom parameters constrained
$\Delta\rho_{max}$, $\Delta\rho_{min}$ (e Å^{-3})	0.73, -0.41

Computer programs: Apex3 v2016.9-0 (Bruker, 2016), *SAINT* V8.37A (Bruker, 2016), *SHELXS97* (Sheldrick, 2008), *SHELXL2017*/1 (Sheldrick, 2017), SHELXLE Rev859 (Hübschle *et al.*, 2011).

Refinement Details:

Two of three THF molecules are disordered. One was refined as disordered over two the other over three domains. The disordered moieties were restrained to have similar geometries as the one not disordered THF molecule. U^{ij} components of ADPs for disordered atoms closer to each other than 1.7 Å were restrained to be similar. Subject to these conditions the occupancy rates refined to 0.137(3), 0.643(3) and 0.220(3), and to 0.430(10) and 0.570(10), respectively.

Crystallographic Details **2-Cl**

Complex: (^{BBN}PDP^{tBu})$FeCl_2(N_2H_4)$

Local name: jk2240

Table S13 Experimental parameters of **2-Cl**.

Crystal data	
Chemical formula	$C_{41}H_{67}B_2Cl_2FeN_7$
M_r	806.38
Crystal system, space group	Triclinic, $P\overline{1}$
Temperature (K)	150
a, b, c (Å)	11.6941 (5), 14.2839 (7), 15.0160 (7)
α, β, γ (°)	111.275 (3), 107.007 (2), 98.892 (3)
V (Å^3)	2137.29 (18)
Z	2
Radiation type	Cu $K\alpha$
μ (mm^{-1})	4.26
Crystal size (mm)	0.21 × 0.16 × 0.08
Data collection	
Diffractometer	Bruker AXS D8 Quest CMOS diffractometer
Absorption correction	Multi-scan *SADABS* 2016/2: Krause, L., Herbst-Irmer, R., Sheldrick G.M. & Stalke D., J. Appl. Cryst. 48 (2015) 3-10
T_{min}, T_{max}	0.426, 0.753
No. of measured, independent and observed [$I > 2\sigma(I)$] reflections	38359, 8071, 6919
R_{int}	0.100
$(\sin\theta/\lambda)_{max}$ (Å^{-1})	0.611
Refinement	
$R[F^2 > 2s(F^2)]$, $wR(F^2)$, S	0.043, 0.111, 1.06
No. of reflections	8071
No. of parameters	484
H-atom treatment	H-atom parameters constrained
$\Delta\rho_{max}$, $\Delta\rho_{min}$ (e Å^{-3})	0.41, -0.35

Computer programs: Apex3 v2016.9-0 (Bruker, 2016), *SAINT* V8.37A (Bruker, 2016), *SHELXS97* (Sheldrick, 2008), *SHELXL2017*/1 (Sheldrick, 2017), SHELXLE Rev859 (Hübschle *et al.*, 2011).

Table S14 Experimentally determined bond distances (Å) and angles (°) for **1-Cl**, **2-Br**, **3-Br**, **3-Cl**, and **4** with numbering scheme depicted below.

Bond (Å) or Angle (°)	(^{BBN}PDP^{tBu})FeCl$_2$ **1-Cl** (X = Cl)	(^{BBN}PDP^{tBu})FeBr$_2$(N$_2$H$_4$) **2-Br** (X = Br)	(^{BBN}PDP^{tBu})FeCl$_2$(N$_2$H$_4$) **2-Cl** (X = Cl)	(^{BBN}PDP^{tBu})FeBr$_2$(N$_2$H$_4$)$_2$ **3-Br** (X = Br)	(^{BBN}PDP^{tBu})FeCl$_2$(N$_2$H$_4$)$_2$ **3-Cl** (X = Cl)	(^{BBN}PDP^{tBu})Fe(NH$_2$)$_2$ **4** (X = NH$_2$)
Fe1-X1	2.3099(12)	2.4879(3)	2.3215(6)	2.4246(11)	2.3001(13)	2.075(2)
Fe1-X2	2.3056(12)	2.4618(3)	2.3335(5)	2.4940(11)	2.3312(12)	--
Fe1-N2	2.243(3)	2.2331(13)	2.2546(14)	2.243(5)	2.239(3)	2.2950(18)
Fe1-N3	2.111(3)	2.0983(13)	2.1184(16)	2.099(4)	2.114(4)	2.124(2)
Fe1-N4	2.245(3)	2.2279(13)	2.2742(15)	2.259(4)	2.255(3)	--
B1-N6	--	1.697(2)	1.694(2)	1.645(9)	1.637(7)	1.633(3)
B2-N7	--	1.698(2)	1.694(2)	1.649(9)	1.646(6)	--
N6-N7	--	1.4681(17)	1.470(2)	--	--	--
ΣB1α	358.9(5)	318.88(12)	320.19(15)	321.2(5)	322.1(4)	325.6(2)
ΣB2α	360.1(6)	319.96(13)	320.38(15)	320.0(5)	320.2(4)	--
τ_5	0.367	0.423	0.375	0.210	0.164	0.017

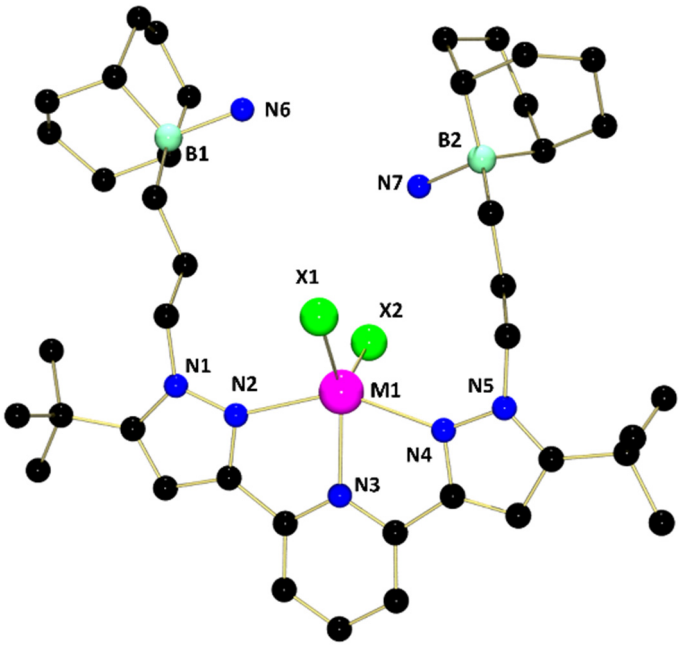

Table S15 Experimentally determined bond distances (Å) and angles (°) for **1-Cl**, **2-Br**, **3-Br**, **3-Cl**, and **4** with numbering scheme depicted below.

Bond (Å) or Angle (°)	(^{BBN}PDP^{tBu})Fe(OPh)$_2$(NH$_3$)$_2$ **5-OPh** (X = OPh)	(^{BBN}PDP^{tBu})Fe(ONO$_2$)$_2$(NH$_3$)$_2$ **5-ONO$_2$** (X = ONO$_2$)	(^{BBN}PDP^{tBu})FeCl$_2$(NH$_3$)$_2$ **5-Cl** (X = Cl)	(^{Bu}PDP^{tBu})FeBr$_2$ **1-Bu** (X =Br)
Fe1-X1	1.9658(17)	2.133(2)	2.3354(5)	2.4511(5)
Fe1-X2	1.9613(17)	2.154(3)	2.2934(6)	2.4537(5)
Fe1-N2	2.2728(19)	2.210(3)	2.2623(16)	2.262(2)
Fe1-N3	2.1429(19)	2.130(3)	2.1253(16)	2.117(2)
Fe1-N4	2.349(2)	2.226(4)	2.2801(16)	2.285(2)
B1-N6	1.651(3)	1.798(12)	1.650(3)	--
B2-N7	1.657(4)	1.699(8)	1.642(3)	--
N6-N7	--	--	--	--
ΣB1α	320.81(2)	309.5(7)	321.42(16)	--
ΣB2α	321.1(2)	312.1(4)	321.90(17)	--
τ_5	0.412	--	0.393	0.437

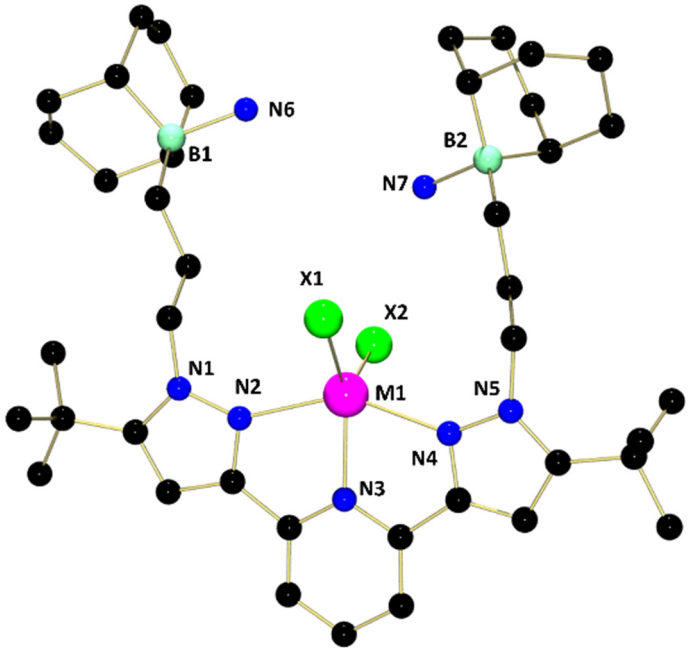

Table S16 Experimentally determined bond distances (Å) and angles (°) for (^{BBN}PDP^{tBu})ZnCl$_2$ and (^{BBN}PDP^{tBu})ZnCl$_2$(N$_2$H$_4$) with numbering scheme depicted below.

Bond (Å) or Angle (°)	(^{BBN}PDP^{tBu})ZnCl$_2$	(^{BBN}PDP^{tBu})ZnCl$_2$(N$_2$H$_4$)
Zn1-Cl1	2.2504(9)	2.2708(7)
Zn1-Cl2	2.2518(9)	2.2815(7)
Zn1-N2	2.273(2)	2.264(2)
Zn1-N3	2.089(3)	2.087(2)
Zn1-N4	2.274(3)	2.304(2)
B1-N6	--	1.696(4)
B2-N7	--	1.682(4)
N6-N7		1.475(3)
ΣB1α	359.0(4)	321.1(2)
ΣB2α	360.0(4)	321.4(2)
τ_5	0.425	0.393

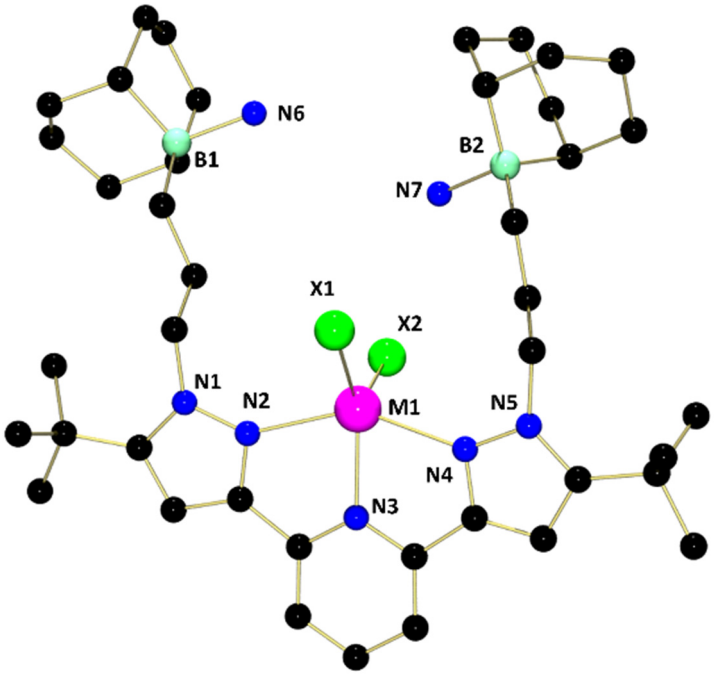

Table S17 Digestion studies for the quantification of NH_x (x = 2-4) produced in various reactions.

			Quantified NH_4^+ (percent)				
Entry		**Reaction**	**Trial 1**	**Trial 2**	**Trial 3**	**Trial 4**	**Average**
1	2-Br	$\xrightarrow[\text{THF, -108 °C}]{2\ KC_8}$	90.62	83.98	86.85	--	87.15 (+/- 1.92)
2	2-Zn	$\xrightarrow[\text{THF, -108 °C}]{2\ KC_8}$	13.76	14.16	14.14	--	14.02 (+/- 0.12)
3	N_2H_4	$\xrightarrow[\text{THF, -108 °C}]{2\ KC_8}$	18.03	22.71	22.27	--	21.00 (+/- 1.35%)
4	1-Cl	$\xrightarrow[\text{THF}]{}$	0	--	--	--	0
5	2-Cl	$\xrightarrow[\text{THF}]{}$	0	--	--	--	0
6	5-Cl	$\xrightarrow[\text{THF}]{}$	101.64	100.89	97.57	93.76	98.47 (+/- 1.97)
7	1-Bu	$\xrightarrow[\text{THF, -108 °C}]{N_2H_4}$	0	0	0	0	0

Details for Entries 1 and 2

The digestion studies described are adapted from the procedure of Schrock et al.[9] General experimental procedure: The metal complex (between 0.021 mmol and 0.017 mmol, sample mass varied for each run) was dissolved in 5 mL THF and frozen in 20 mL scintillation vials. On thaw, KC_8 (2 equiv.) was added an the reaction allowed to stir to room temperature for 60 min. The reactions were then filtered and the solids rinsed with an additional 5 mL THF. HCl (4.0 M in dioxane, 20 equivalents) was then added to the vials and stirred for 30 min. Volatiles were removed in vacuo. The remaining material was dissolved in DMSO-d_6 and a known quantity of $NaBAr^F{}_{24}$ (DMSO-d_6 stock solution) was added and an ^1H NMR spectrum obtained. The quantified percent represents a theoretical production of two equivalents of NH_4^+ per molecule of N_2H_4 in the starting complex.

Details for Entry 3

A known quantity of N_2H_4 (from a THF stock solution, 0.025 mmol in each entry) was dissolved in 4 mL THF and frozen in a 20 mL scintillation vial. While frozen, KC_8 (2 equiv.) was added on top and the vial resealed prior to thawing. The reaction was then warmed to room temperature with stirring for 60 min. The vials were then cooled to -78 °C and HCl (4.0M in dioxane, 20 equiv.) added, the vials sealed, and warmed to room temperature with stirring for 30 min. Volatiles were then removed in vacuo. The resulting solid was extracted into DMSO-d_6 (2 mL), filtered, and the solid rinsed with an additional 1 mL DMSO-d_6. A known quantity of $NaBAr^F{}_{24}$ (DMSO-d_6 stock solution) was added and an ^1H NMR spectrum

obtained. The quantified percent represents a theoretical production of two equivalents of NH_4^+ per molecule of N_2H_4.

Details for Entries 4-6

General experimental procedure: The metal complex (between 0.016 mmol and 0.007 mmol, sample mass varied for each run) was dissolved in 5 mL THF in 20 mL scintillation vials. HCl (4.0 M in dioxane, 20 equivalents) was then added to the vials and stirred for 30 min. Volatiles were removed in vacuo. The remaining material was dissolved in DMSO-d_6 and a known quantity of $NaBAr^F_{24}$ (DMSO-d_6 stock solution) was added and an ^1H NMR spectrum obtained. The quantified percent represents a theoretical production of two equivalents of NH_4^+ per molecule of N_2H_4 or NH_3 in the starting complex.

Details for Entry 7

A known quantity of **1-Bu** (between 0.022 mmol and 0.018 mmol, sample mass varied for each run) was dissolved in 4 mL THF and frozen in a 20 mL scintillation vial. While frozen, N_2H_4 (1 equiv., THF stock solution) was added on top and the vial resealed prior to thawing. The reaction was then warmed to room temperature with stirring for 60 min. The vials were then cooled to -78 °C and HCl (4.0M in dioxane, 20 equiv.) added, the vials sealed, and warmed to room temperature with stirring for 30 min. Volatiles were then removed in vacuo. The resulting solid was dissolved in DMSO-d_6 and a known quantity of $NaBAr^F_{24}$ (DMSO-d_6 stock solution) was added and an ^1H NMR spectrum obtained. The quantified percent represents a theoretical production of two equivalents of NH_4^+ per molecule of N_2H_4 added.

Determination of Activation Numbers

The test substrates $PhCH_2CH_2BPin$,[10] $PhCH_2CH_2BBN$,[11] and $PhCH_2CH_2B(C_6F_5)_2$[12] were prepared according to literature procedures. Acceptor numbers were determined by the Gutmann-Beckett method[13] via the equation:

acceptor number = 2.21 x (δ_{sample} -41.0)

where δ_{sample} is the experimentally determined chemical shift in the ^{31}P NMR spectrum for triethylphosphine oxide.

For each determination, a J-Young NMR tube was charged with 0.005 g (0.037 mmol) of triethylphosphine oxide, an equimolar amount of acceptor substrate, and 1.00 mL C_6D_6. The sample was shaken for 5 min, and the ^{31}P NMR spectrum obtained. The ^{31}P NMR spectra were referenced on a unified scale, where the single primary reference is the frequency of the residual solvent peak in the ^{1}H NMR spectrum. The ^{31}P resonances are referenced vs. phosphoric acid.

Table S18 Acceptor numbers determined for model substrates.

Compound	Acceptor Number
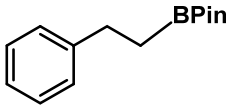	9.99
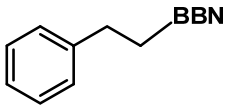	23.40
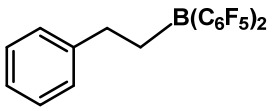	71.80

References

[1] Schrock, R. R.; Liu, A. H.; O'Regan, M. B.; Finch, W. C.; Payack, J. F. *Inorg. Chem.* **1988**, *27*, 3574-3583.

[2] Yoshinari, A.; Tazawa, A.; Kuwata, S.; Ikariya, T. *Chem. Asian J.* **2012**, *7*, 1417-1425.

[3] Yang, Y.; Gao, H.; Zheng, L. *RSC Adv.* **2015**, *5*, 17683-17689.

[4] Chakraborty, S.; Chattopadhyay, J.; Guo, W.; Billups, W. E. *Angew. Chem., Int. Ed.* **2007**, *46*, 4486-4488.

[5] Bruker Advanced X-ray Solutions, Apex3 v2016.9-0, (2016).

[6] P. van der Sluis, A. L. Spek *Acta Crystallogr., Sect. A.* **1990**, *46*, 194-201.

[7] Bruker Advanced X-ray Solutions, Saint v8.34A, (2014).

[8] G. M. Sheldrick *Acta Crystallogr., Sect. A.* **2008**, *64*, 112-122.

[9] Wickramasinghe, L. A.; Ogawa, T.; Schrock, R. R.; Müller, P. *J. Am. Chem. Soc.*, **2017**, *139*, 9132-9135.

[10] Yang, K.; Song, Q. *Green Chem.* **2016**, *18*, 932-936.

[11] Ohmiya, H.; Yokobori, U.; Makida, Y.; Sawamura, M. *J. Am. Chem. Soc.* **2010**, *132*, 2895-2897.

[12] Parks, D. J.; Piers, W. E. *Organometallics* **1998**, *17*, 5492-5503.

[13] Beckett, M. A.; Strickland, G. C.; Holland, J. R.; Sukumar Varma, K. *Polymer* **1996**, *37*, 4629-4631.